LINEAR AND NONLINEAR DRIFT MODES IN INHOMOGENEOUS MULTICOMPONENT PLASMAS

By
Sajad Ali

PhD Thesis
in
Physics

Department of Physics
Faculty of Physical and Numerical Sciences
Abdul Wali Khan University Mardan
Khyber Pakhtunkhawa Pakistan

December 2018

Linear And Nonlinear Drift Modes In Inhomogeneous Multicomponent Plasmas

A Post Graduate Thesis submitted to the Department of Physics, Abdul Wali Khan University Mardan as partial fulfillment of the requirement for the award of Degree of PhD in Physics.

Name	Registration Number
Sajad Ali	Reg No: 12-AU-phD-Phy-S-1

Supervisor
Dr. Mushtaq Ahmad
Adjunct Professor
Department of Physics
Abdul Wali Khan University Mardan (AWKUM)

AUTHOR DECLARATION

I, Sajad Ali hereby state that my PhD thesis titled *Linear and non linear drift modes inhomogeneous multicomponent plasmas* is my own work and has not been submitted previously by me for taking any degree from this university (Abdul Wali Khan University Mardan) or anywhere else in the country/world.

At any time, if my statement is found to be incorrect even after my graduation, the university has the right to withdraw my PhD degree.

_____

Student Signature

Dated:

DEDICATION

I dedicate this thesis to Waseem, Zainab, and Shazil.

ACKNOWLEDGEMENT

First of all I would like to praise and thank GOD almighty, Who put me on this path of getting knowledge, and helped me clear all the hurdles and hardships I faced while getting the education to the Holy prophet Muhammad (peace be upon him) who showed light of knowledge to the humanity as a whole.

I would like to express my heartiest appreciation to my Supervisor Dr. Mushtaq Ahmad, who introduced me to the subject and brought me to this level of research. I am indebted to his continuous support and encouragement not only in the field of plasma physics but also in several other matters in my life. I feel privileged to extend my sincere thanks to one of my closest friend, who always encouraged me and guided me whenever it was required.

I am extremely grateful to Dr. Aurang Zeb, Dean Faculty of Physical and numerical Sciences, AWKUM for providing all the facilities to undertake this research. Last but not the least; I would like to mention mother, wife, kids, brothers and sisters for their sustained love and cooperation. Their prayers always give me strength and courage to move ahead.

SAJAD ALI

ABSTRACT

In the recent decades the physics of multi component plasmas has grown up tremendously. There is hardly any situation in which plasma could be found in simple case consisting of positively charged ion and negatively charged electron only, even if we take an example of electron ion plasma consisting of ionized hydrogen atoms and their detached electrons, In tokomak fusion plasma. The plasma confined is not simple rather than it is contaminated with detached particles of the inner surface of confinement, this makes the parameters very much complex.

Up to certain time the concept of multicomponent plasma was mostly revolving around the concept three particles, plasma ,but with the discovery of Klein concept of metagalaxy , a new class of four component multi component plasma was discovered which set a new mile stone regarding the creation of our universe. Now keeping in view the importance, of the multi component plasma the following thesis consists of the following work

First non-uniform quantum magneto plasma consisting of electron positron ion plasma is explored for Electrostatic Rayleigh-Taylor (ERT) instability. The quantum corrections effects (including Bohm potential and few other parameters) alongside the magnetic field effects on instability mode are also explored. The dispersion relation which is obtained in shape of cubic form is further examined for Different roots of the real along with imaginary root of the RT mode. The obtained dispersion relation along with the growth rates associated with the RT mode are further examined on the analytical, numerical bases. This work is proved to be of great physical importance on the studies of both laboratory as well as to study the magnetized astrophysical entities e,g white dwarfs.

2ndly Electrostatic Gravitational instability is investigated in inhomogeneous pair-ion-electron quantum magneto plasma under drift wave approximation, which consists of positive and negative ions with a electrons. The presence of negative ions with their different streaming velocities turns the dispersion relation into cubic dispersion relation obtained is the instability. It is further shown RT instability varies for magnetic field density.

The drift wave instability was also investigated for four component AMBI plasma both in linear and as well as non linear regimes, following derivation of linear dispersion relation, along with kdv burger equation for evaluation of both shock wave and solitons.

LIST OF PUBLICATIONS

(1). S. Ali, A. Mushtaq, M. Farooq, *Chaos, Solitons and Fractals,* 112, 66–74(2018).

(2). S. Ali, A. Mushtaq, *Journal of Modern Physics*, 8, 636-653(2017).

(3). Z. Ali, S. Ali, I. Ahmad, *Physica B: Condensed Matter*, 420, 2013, 54-57(2013).

(4). A. Mushtaq, S. Ali, *archive. Phy.org.*

Contents

List of Figures

Chapter 1

Introduction

The word plasma for the first time was used by Johannes Purkinje (1787-1869) for the clear fluid of blood after the removal of blood species, The plasma is a Greek word, means some thing that is been moulded . It is a fourth state of matter that posses charged particles(negative and positive), having equal charge densities, with their interactions mostly collective rather than being just binary [1]. Plasma is a fluid form where the potential energies of particles due to their near by particles are lesser than their kinetic energies. Tonks and Langmuir were the pioneers who used the word plasma for an ionized gas, where the ionization was caused by increasing the temperature at low pressure. At laboratory level such mixture of charges could be produced by heating a gas up to a certain extent so that it ionizes [2]. Plasma could be divided into two major categories. Man made plasma and naturally existing plasma. According to an estimate nearly 99 percent of visible universe is made up of plasma. Naturally existing plasmas are believed to exist in upper atmosphere, astronomical bodies such as the stars, white dwarfs, galaxy and our own sun and most of the interstellar medium. Plasma physics is useful in understanding of formation of radiation belts, solar flares, and solar winds. Man made plasma includes confined plasma in fusion reactor, the fluorescent tubes, electric arc produced by welder, the more advanced devices includes generators used for producing electricity from gas jets, magetons and travelling wave tubes [3].

Over the past few decades the research in the field of fusion based reactions has resulted into a new field of plasma physics, that has enabled us to create and incorporate plasmas and associated beams on a very wide range of energies and densities such as in plasma sputtering, plasma

implantation of the ions, plasma etching, plasma microwave based sintering, deposition caused by plasma beam, plasma spray, X-ray sources, super computing fast electronics,Technologies related with plasma fusion are making a fast business in a world market estimating at round about 2hundered billion dollars per annum. Which include markets for coatings of materials ($50B); processing of waste material ($50B); plasma electronics, which includes plasma flat panel displays and high power switches ($40B); high performing semiconductors and IC ($30B); and many more aspects related with ceramics and medical field [4].

A wide range of linear and nonlinear electrostatic along with electromagnetic waves are supported by the plasma state which arises from the collective interaction of the charged particles which can be treated by classical theories as well as quantum mechanically. When the amplitude of perturbation is minute, linear approximations are used where different type of instabilities can be observed. Nonlinearity in plasma can be observed when the waves with larger amplitude are excited by some external sources. Plasma nonlinearities are important to understand the formation and evaluation of nonlinear structures such as vortices and solitons. More over the plasma due to its complicated nature is sub divided into two broad classes as following.

1.1 Classical and Quantum Plasmas

Plasma Physics is usually thought to be a field of classical physics when the inner densities are smaller and the temperature of the plasma species are very high. In classical treatment of plasma, the particles distributions are usually described by Maxwell-Boltzmann (M-B) statistics. However, the quantum effects may exists in plasmas where the particle densities are very large and temperature is very small. In other words quantum effects in plasma become important when λ_{D} the Debye length of the Debye sphere is comparable to the size of the interparticle distance, so that there is an obvious overlap of the analogous wave functions. Under such circumstances, collective behavior of the particles is usually described by the Fermi-Dirac (F-D) distribution function, rather than M-B distribution. The fermionic behavior becomes dominant for lighter plasma particles such as electrons, positrons in case of pair ion plasmas etc. Such plasma systems are found in compact astrophysical entities like white dwarfs , neutron

star inter galactic nuclei [5]. Such plasmas also occur in the interaction experiments of the next generation intense laser-solid density plasma and metal plasma is also an example of quantum plasma. Several appliances operate on the principle of quantum mechanical aspect of plasma for example quantum semiconductor devices, transistors which posses high-electron-mobility, resonant tunneling diodes or superlattices. The procedure of these ultra-small devices depend on the quantum tunneling of the charge carriers through the potential barriers [6]. In the Recently conducted research in spectroscopy based on femto second pump-probe, the effects of quantum plasma have attracted a great deal of attention in the physics of metallic nano structures and in the thin metallic films. Quantum effects have an important role in understanding the Thompson scattering of the X-rays in a high energy dense plasmas provided the experimental procedures for observing the spectral lines of the narrow bandwidth [7].

1.2 Multicomponent Plasma

Textbook plasma is consisting of two charged particles positive ion and negative charges carriers i.e electrons. The mass difference between electrons and ions in typical plasma causes various temporal and spatial variation of collective plasma phenomena. Several plasma phenomena have been diversified and become complicated when the other charged species (negative ion, positive ions, or both negative and positive ions or dust particles) are included in plasma. Such plasma is usually termed as multicomponent plasma [8]. Plasmas containing fine particles besides electrons and positive ions had been the subject of intensive studies in the field of physics along with engineering for instant space astrophysics [9], plasma physics [10], Manufacturing based on plasma technology and the fusion technology [11].

1.2.1 Electron Positron Ion Plasma

The most commonly used plasma is electron-positron EP plasma. It motivated the researchers just because of the fact that electron and positron EP pairs can be created in the magnetospheres of the pulsars. Where the intense radiation creates the EP plasmas is the vicinity of applied magnetic field in the pulsars, therefore, such systems ultimately shows relativistic attitude. The Electron Positron plasmas also existed at the time of creation of the universe and also in

AGN. Various researchers had been studying the propagation of electromagnetic radiation and acceleration of particles in EP plasmas taking into account the relativistic effects. It is also believed that such types of systems might also contain ions concentration as well. The injection of positrons in EI systems also creates EPI plasmas at laboratory level [12].

1.2.2 Pair Ion Plasma

An other tri particle multicomponent plasma is (PI) plasma, it consists of both the Positive ion and the Negative ion along with an electron. The science associated with pair plasma has groomed into the very vast field of the research and innovation as its applications stretches from astrophysics limits to the confined terrestrial plasma in laboratory. One laboratory level the pair ion plasma could be created successfully with a very highly concentrated dense pair-ion (PI) plasma, that consists of the equal amount of both positive and negative charge quantity [13]. PI plasma **posses** both the features of easily accessibility and has a enough lifetime so that collective behavior of this state of plasma could be investigated at laboratory scale under a very stable and controlled conditions[14]. This aspect of Pair Ion plasma motivated the researchers to explore its characteristics.

1.2.3 Ambiplasma

Plasma may occur in four component as well. Such a plasma which consists of protons, electrons, antiprotons and positrons is called Ambi Plasma. This concept of four component ambiplasma had been introduced in the early times of cosmonautics era by Alfven . When Alfven was describing ambiplasma,he also estimated time of the annihilation of this so called ambi plasma (for example, according to his estimates, its lifetime is ˜5×10^6 years at a $1cm^{-3}$ particle number density), he also calculated the losses of energy through the radio emission (As for example, characteristic time of losses of energy through the synchrotron's radiation in a field of ˜$10 - 4G$ is ˜8×10^6 years), and also studied the chances of their separation into matter and antimatter in gravitational and magnetic fields [15].

The mathematical model which explained the theory of ambi plasma is Klein's model of the ambi plasma. It has attracted attention due to its the significance of studying the various properties of this plasma which consists of a mixture of matter and antimatter. Generally, the

ambiplasma might contain a mixture of nearly all the elements and the corresponding anti elements. For study and research purpose the focus is only made on to the case, when it only constitutes the four basic constituents, protons,antiprotons, positrons, and electrons per unit volume [16] .

1.2.4 Dusty Plasma

In some forms a plasma may exists along side with dust particulate. These particles might be so large comparable to size of micron. These are charged, and the nature of their charge depend on their environments. Such mixture of charged particles consisting of electrons, macro-particles, neutrals and ions is termed as 'dusty plasma'. A dusty plasma could be defined as an ordinary electron–ion plasma that contain an extra charged particle/s of micron- or submicron-sized . With the addition of dust particle the complexity of the system is increased to a great extent. That is the reason it is termed as 'complex plasma'. The dusty plasmas normally posses low-temperature, and it is ionized fully or partially. It normally consists of conducting gases(ions, electrons charged dust grains and atoms). Dust particles are massive and with sizes ranging from nanometers to millimeters. These dust particles might be metallic in nature or made from ice. The size and shape of dust particles differs from each other. But when these are viewed from a long distance, they could looks like as point charges. Other name for this specific plasma are 'dust in a plasma'. The dust grain radius is written as (r_{d}), the average inter grain distance is indicated by (a). The situation $d \ll \lambda_{\mathsf{D}} < a$(where the charged particles are considered as an isolated collection of screened particles) is corresponded as 'dust in a plasma', while the situation rd $a < \lambda_{\mathsf{D}}$ (the collective behavior is shown by the charged particles) is corresponded as 'a dusty plasma'. Examples of dusty plasma are nebula and proto-planetary , explosions associated with supernova, explosions of molecular clouds, interplanetary medium, circumlunar rings, and the asteroids. In the planetary rings of the sun , cometary tails , dust clouds around the moon and stream of dust ejected from Jupiter. In a region that are near to earth, there exist noctilucent clouds, tiny (charged) ice particles in shape of clouds which forms during the summer polar mesosphere at height of about 85 km from the earth surface [18].

1.3 Maxwellian Plasma

The EEDF(Electron Energy Distribution Function) performs a vital role in modeling of the plasma. Several methods could be employed to explain EEDF, such as Druyvesteyn, Maxwellian and by the use the Boltzmann equation. EEDF being an very compulsory in plasma modeling phenomena becaus it is required to calculate the reaction rate of reactions of electron collision . Since the transport properties of the electrons may also be derived from the EEDF, the decision to use the EEDF , could influences results of the plasma modeling. If the plasma is in thermodynamic equilibrium, the EEDF tends to be a Maxwellian, If the plasma is in thermodynamic state of equilibrium.

when electrons are in state of the thermodynamic equilibrium with respect to each other, then distribution function tends to be Maxwellian, (meaning that all the electrons are the same temperature) But , it is only valid if the degree of ionization is high. under such a suitable circumstances ,the collision occurring amongst all the electron of the systems drive the distribution towards a Maxwellian shape. An other important effect which occurs inside plasma is the Inelastic collisions which occurs between electrons and heavy particles(ions , dust particulates, impurities), this effect is likely to happen at relatively higher electron energies, this ultimately may causes drop of the EEDF . Hence , the Druyvesteyn distribution function more often will give a precise result for a lower degree of ionization [19].

1.4 Non Maxwellian Plasma

In astrophysical space region and confined plasmas in laboratory , magnetic reconnection is very important process by which magnetic energy is converted into , plasma motion in bulk, thus consequently causing plasma heating. And acceleration of the constituent particles. In the past due to lack of resources only the fluid aspects of the above mentioned process were both theoretically and experimentally analyzed. Apart from fluid description, the cohesionless magnetic reconnection process also posses non-Maxwellian aspects of the velocity space distribution functions (VDF).

Among the different reasons that leads to non M Boltzmann EEDF through the weakly collisional plasma there are:

1. Quick temporal and/or special variation of electrostatic or the electromagnetic fields;

2. The imposition of the boundaries (electrodes, catalytic surfaces);

3. High anisotropy presence ;

4. The collisions(elastic and in elastic), in which the kinetic energy of electron is being exchanged with internal atoms(with their degrees of freedom).

Three types of non-Maxwellian distribution functions are mostly found in plasma confined in laboratory and space. These includes Druyvesteyn, bi-Maxwellian and Lorentzian k-law distributions [20].

1.4.1 Cairns Distribution Function

About 20 years ago (in 1995), the idea of this distribution function was initiated just because of the caviton 's observations (fluctuations associated with number density of ions) with the use of Freja satellite (FS)7 and Viking spacecraft (VS). This is also non thermal distribution function (currently called Cairns Distribution Function) for the electron **species** to illustrate the existence of cavitons first noticed by FS7 and VS.8. The Cairns distribution function is formulated as

$$f_{\mathrm{j}}^{\mathsf{C}}(v_{\mathrm{j}}) = \frac{n_{\mathrm{j}\,0}}{\alpha_1(2\pi)^{\frac{3}{2}}v_{\mathrm{t}}^3}(1+\alpha\frac{v_{\mathrm{j}}^4}{v_{\mathrm{t}}^4})\exp(-\frac{v_{\mathrm{j}}^2}{2v_{\mathrm{t}}^2}) \tag{1.1}$$

In the above equation α is quantity of the high energetic plasma specie in system, which is under consideration, v_{t} being thermal speed associated with jth species ,$n_{\mathrm{j}\,0}$ highlights the number density associated with the plasma [22].

Initially , dynamics associated with ion beam, were explored by Boltzmann distributed electrons using the well known quantum mechanic technique known as reductive perturbation theory. An year after that , Misra et al explored the linear as well as non linear propagation of the DIA mode(in non linear regime) by using the numerical, theoretical techniques. It was later found that there exists the three stable modes , i.e.,the "Slow" and the "Fast" ion-beam modes and the "Ion-acoustic" modes. Among all of those cases leptons possessed MB distribution function.

However, in many cases leptons populations follow the Cairns distribution. These includes

a situation where there are more fast moving particles, it was first used by Cairns *et al* to study the effect of the particles on the solitary structures. It was further shown that when the population of leptons is non thermal, the characteristics of ion sound solitary structures will surely change, and solitons may posses both positive, negative density perturbations . It therefore acts like a basic role model for nearly all non-thermal or non maxwellian, space plasmas, and has been used most often [23].

1.4.2 Kappa Distributed Plasma

Non thermal particle distributions could be found at altitudes such as solar wind along with many space plasmas, the observations confirmed by spacecraft measurements [144] indicated their presence. Such behavior of the non Maxwellian distributions may also exist in Universe with any low-density plasma , where the binary collisions amongst the charges are exceptional. These types of superthermal populations are described very well by the Kappa (k) or generalized Lorentzian velocity distributions functions (VDFs). Such distributions posses high energy tails that deviates from the Maxwellian distribution.

$$f_{\mathsf{i}}\ (\Gamma, v) = \frac{n_{\mathsf{i}}}{2\pi(\kappa w^2{}_{\mathsf{i}})^{\frac{3}{2}}} \frac{\Gamma(\kappa+1)}{\Gamma(\kappa-1)\Gamma(\frac{3}{2})} (1 + \frac{v}{\kappa w^2{}_{\mathsf{i}}})^{-(\ +1)} \tag{1.2}$$

Here w^2_{k} is showing velocity(thermal), m_{i} is the mass of ith of species , n_{i} is the ion density, v represents the velocity of theses particles, and $\Gamma(x)$ is well known Gamma function. The spectral index must posses quite large values $\kappa > 3/2$. The index κ gives the slope of that particular energy spectrum which forms the tail of the suprathermal particles. In the limit $\kappa \rightarrow \infty$ the Kappa function degenerates into a Maxwellian[24].

1.4.3 Q-Non Extensive Distribution

When ever entropy is destroyed then a non-Maxwellian distribution function is resulted, this is normally called q non-extensive distribution function. Nonextensivity is emerged in shape of a difference of entropy with in the entire system, as compared to the sum of the entropies belonging to all respective parts and is known as Tsallis entropy and which is a suitable non extensive generalizaion of the Boltzmann–Gibbs–Shannon (BGS) entropy for statistical equi-

librium. Interparticle forces at long range are performed very accurately by non extensitivity phenomena these includes force of gravity and Newtonian force along with coulomb forces of attraction occurring amongst electric charges in proper fashion with in plasma, which sounds quiet an impossible task with the MB distribution function.

The parameter q (nonextenssive) behaves as a real number while dealing with Tsallis statistics. If q is less than one , then the sum of entropies associated with respective parts is less than the the generalized entropy of the whole system and if q is greater than 1 then reverse situation is observed. Tsallis entropy also gives BGS entropy with in the frame work of q. It has been also observed that velocity distribution of the plasma particles in the space plasmas, also the laboratory plasmas are not purely Maxwellian, and more interestingly the concerned particles obey the distributions that contradicts from Maxwellian distribution[25].

1.5 Drift Wave Instability

So far scientists considered only two kinds of instabilities, which take place in a fluid based model. The first, one is the ideal MHD flute instability , which works upon the plasma thermal energy as it is expanded across a curving magnetic field, and the later is the Resistive Tearing Instability is the second one, which works on the magnetic field energy inside plasma confinement, as it is rearranging toward a configuration of the lower magnetic energy. How ever there is also exists a third classified instability which is arising in fluid plasma, and it is termed as 'Drift-Wave Instability'. it neither requires a curved magnetic field nor magnetic configuration for which the lower state of the magnetic-energy. Drift instabilities are occurring in the most 'universal'form of configurations, i,e the plasma with non-uniform density, which is maintained at equilibrium state by the strong and essentially straight magnetic field. Because of the pervasiveness of this situation, the instabilities of such kind are most of the times termed as 'universal instabilities. Just Like flute instabilities, drift-wave instabilities works on the thermal energy of the plasma as it expands across a magnetic field. Unlike flute instabilities, however, they posses finite wavelengths along the field, and the plasma motion is de coupled, to a significant extent, from that of the magnetic field, so as to avoid energetically unfavorable bending of the field lines. Unlike Rayleigh-Taylor, flute and resistive-tearing instabilities, drift-wave instabilities

are not purely growing, rather it posses complex frequencies , with imaginary part as well , denoted by (the growth rate), which is usually much smaller than the real part. Any such mode of perturbation can be made to grow purely when transformed to a moving frame in which the wave is not moving , but plasma will itself acquire a non-zero velocity in such a frame [26].

1.6 Instabilities in an Inhomogeneous Plasma

A plasma which is in equilibrium condition, is normally characterized by homogeneous Maxwellian particle distributions (rest with respect to each other). When ever the system of plasma deviates from such state of a thermodynamic equilibrium, then it causes free energy, which leads, some times to instabilities, depending on situations. Such plasma deviation can happen in a homogeneous or an in homogeneous system.

In a plasma under homogeneous condition, these deviations from thermodynamic equilibrium are mostly found in the velocity space. Ion-acoustic mode is the best example of such kind of instability which are arised from such deviation of velocity,and in such specific case , is in the form of electrons streaming with respect to ions. The other instability which is Weibel instability results from the anisotropy of electron velocity distribution. These inhomogeneities could only be kept maintained for a very limited duration of time by confining the plasma by some means. Magnetic fields are an obvious choice for achieving this purpose[27]

Plasma Instabilities may also occur in nature. Instabilities arising in the earth ionospheric E-region are made to flow by the currents at E-region altitudes. The instabilities of such type could also be detected at any latitude, but these are very common, and most strongest, at specifically equatorial latitudes and also in a region known as the auroral zone, where these were detected by radar for nearly six decades. These instabilities causes plasma waves, the phase fronts of these waves are highly aligned with the geomagnetic field[29] .

Sometimes for the sake of convenience we divide these into two main categories in accordance with the spatial scale which is involved in the instability. If the scale of instability is of macroscopic size, which are comparable to bulk level of the plasma, these instabilities are termed as macro instabilities. On the other side , if the given size of these instabilities is of microscopic level , these instabilities are termed as micro instabilities. In the latter case it is

natural to assume that kinetic effects will become of greater importance than in the former case. Thus micro instabilities typically some times behaves as kinetic instabilities, while on the other hand macro instabilities could be modelled with in the framework of the plasma fluid model. In some cases, however, it is useful to account for kinetic effects in macro instabilities as well[30] .

Keeping in view the availability of free energy , the plasma instabilities are further divided into the following main categories.

1.6.1 Rayleigh Taylor Instability

In fact Rayleigh Taylor (or 'gravitational') instability is one of the most important MHD instability. In plasma physics this Rayleigh-Taylor instability is created whenever a heavy fluid is supported on top of the light fluid. The interface separating the fluids turned 'rippled', which allows the relatively heavier fluid to fall through the light fluid. Typically in plasmas physics , a Rayleigh-Taylor instability may occur whenever a dense plasma particles are supported against the gravitational field by the pressure of an applied magnetic field. The actual gravitational forces surrounding the plasma are rarely given much importance[30]. The most familiar example of Rayleigh-Taylor Instability is in supernova explosions. Here a shell of concentrated , shocked ejecta is being decelerated gradually by the lower density shocked circumstellar material. This situation creates the well known $R-T$ instability, which results in frinngers of dense ejecta gas ejecting into, and mixing with, the shocked circumstellar material[71]

1.6.2 Universal Instability

In a plasma which is confined , wether there's any electric or magnetic field present or not , it is itself not in the state thermodynamic equilibrium. The confined plasma generates pressure due to its expansion. and consequently plasma expansion energy is generated due to this plasma expansion . This expansion creates instability. In the finite plasma this energy is always present. The waves produced due to this mechanism are called universal instability[30]. When "universal" instability was revived then it was shown that it exists in geometries of plasma possessing straight (sheared) magnetic field lines. Here it is analytically proved that this instability could exist in toroidal geometries that are more sheared. In torus, universal instability is showed to

be closely associated to the electrons in traped mode, although the trapped-electron drive is usually dominant. However, such drive could be weakened or being eliminated, such as in case of stellarators having maximum J property, leaving the parallel Landau resonance to drive a residual mode, which is identified as universal instability[134]

1.7 Fluid Description

The Fluid model describe plasmas in terms of invariable quantities, which are not dependent on the velocity. According to this model, plasma is treated as a fluid which contains charge particles. Under such circumstances we consider the bulk properties rather than that of a single particle. The particles of the fluid always moves randomly due to interparticle collision.

Plasma mostly consists of two types of particles i,e electron and ions. In such a fluid it is not required that each species is to be composed of particles with dissimilar velocities. The fluid model is based on a few equations. The first standard point in the fluid model is that the free particles could neither be destroyed nor be created. This is only applicable if the recombination and ionization effects are neglected . If we assume so then the continuity equation is created which could be derived from the zero velocity moment of the Vlasov equation, and could be written as.

$$\frac{\partial n_{\mathrm{j}}}{\partial t} + \nabla.(n_{\mathrm{j}}\, u_{\mathrm{j}}\,) = 0 \tag{1.3}$$

When ever plasma fluid experiences pressure and also electromagnetic forces, then appropriate evolution equation from the Vlasov equation is obtained . When it is multiplied by mv and integrated over the velocity space, then the required momentum equation is obtained as

$$m_{\mathrm{j}}\, n_{\mathrm{j}}\, [\partial_{\mathrm{t}} v_{\mathrm{j}} + (v_{\mathrm{j}}\, .\nabla) v_{\mathrm{j}}\,] = q_{\mathrm{j}}\, n_{\mathrm{j}}\, (\vec{E} + v_{\mathrm{j}} \times \vec{B}) - \nabla.P_{\mathrm{j}} \tag{1.4}$$

This pressure tensor P is defined as

$$P_{\mathrm{j}}^{\mathrm{i}} = mn\langle (v_{\mathrm{i}} - u_{\mathrm{i}})(v_{\mathrm{j}} - u_{\mathrm{j}}\,)\rangle \tag{1.5}$$

$$P_{\mathrm{j}} = mn(\langle v_{\mathrm{i}} v_{\mathrm{j}} \rangle - u_{\mathrm{i}} u_{\mathrm{j}}) \tag{1.6}$$

Where we are using the definition of mean value of the velocity U, namely $ui = (vi)$. The corresponding flux in the ith direction of $j$directed momentum is given as $Pi + mnu_{\mathrm{i}} u_{\mathrm{j}}$. Surprisingly , this derivation makes this fact very clear that the familiar concept of pressure is, in a more broader sense, a well defined momentum flux. It is further Noted that it is the divergence of this so called flux that give rise to acceleration. In a particular case where the plasma is characterized by various perpendicular and parallel temperatures, relative to the direction of the local magnetic field, then Pi, is always zero for $i\#j$, but when , if $i = j$ and it is $\perp$ to B, then $Pi, = nT \perp$, while if $i = j$ and is parallel then, $Pi, = nT \parallel$[28, 42].

1.8 Solitary Waves and Shocks

Back in the month of August of year 1843, Scott-Russel were the first to see rounded, smooth and well defined and well arranged heap of water which continued to move along the channel apparently without change of their form or their own speed. This solitary wave continued to propagate about distance of one miles at speed of round about eight or nine miles an hour, this shape preserved its original shape of some what thirty feet long and a foot to a foot and a half of height. This observation was the first discovery of soliton. This solitary wave is produced due to cancellation of dispersive effect.

Then In 1895, while analyzing the process of dispersive effect and steepening effect which arises due to nonlinearity present inside the shallow water, The two scientists Korteweg and de Vries were the first one to derive a nonlinear partial differential equation in order to explain the basic properties of these solitary waves. This equation is now called by their names.

Gardner and Morikawa again worked on this phenomena and have found , that the derived equation by Korteweg-de Vries is only valid for the nonlinear magneto-hydrodynamic wave which usually propagates in perpendicular direction to the magnetic field. Theoretical work of Washimi and Taniuti on the propagation of the ion-acoustic solitary wave has been experimentally confirmed by Ikezi, Taylor and Baker. Reinforcement of the marvelous innovation of the inverse scattering method for solution of nonlinear equation of evolution has encouraged

the researchers to disentangle complex nonlinear wave propagation with respect to the strong theoretical ground[33].

1.8.1 Shocks

A shock wave is a phenomena which may occur in a gas or plasma medium in which the discontinuity occurring in the pressure is faster as compared to the speed of sound in that medium. On the laboratory level shock waves could be generated with help of interactions of high intensity laser plasma. Shock posses the characteristic of having sharp electric field in the pressure transition region which is oriented with respect to direction of its propagation and is being able to reflect, under certain conditions, ions to the maximum of twice of the shock velocity.

Classic Example of Shock wave is that it is formed in the air at in front of a supersonic jet . A shock is termed as having no collisions if the free path in between collisions of the particle is much larger than the width of the shock[35] . The situation during which the pulses of large density might turned into sharp wave fronts or "shocks" were investigated in a Q machine by Anderson et al[36]. Cohesionless shocks might exist laboratory level as well as in space.

Because of the fact that transition process of the shocks is irreversible, shock wave could not be termed as a totally steepening nonlinear wave. on the other hand, wave steepening phenomena is a transitory process when it is not stopped, then ultimately it leads to breaking of the wave. Shock waves posses the characteristics of being in the stationary state, while the breaking which is prevented by some other process, for example by dissipation. Any shock with fast, slow, or intermediate , from a macroscopic point of view is a steepened fast, slow, or intermediate magneto sonic wave, with breaking inhibited due to the balance of steepening and dissipation process. so there for nonlinear wave phenomena is applicable to the shock wave process. The steepening process of a fast magneto sonic wave serves as the ignitor to the follow-up microscopic processes,that provides the dissipation effect inside the shock wave front and thus causes the irreversibility process.

Generally , such a situation would be correct for fairly slow shocks , in which the flow speed of the shock leaves quite long time for the steepening process and the subsequent creation of the microscopic processes. Low Mach number shocks would follow up this phenomena. But in

situation where there's high Mach number shocks there will be no long time for the anomalous process that would provide the needed collision frequencies. When we pass across critical Mach number , new effects happens just like particle reflection from the shock front . these kinds of shocks are termed as supercritical. The shock wave phenomena depends strongly on the direction of the applied magnetic field . The behavior of Quasi perpendicular shocks more regular than quasi-parallel shocks[37]. When the concentration of neutral particles is large enough then dissipation effects dominates over the resulting dispersion phenomena , the basic equation which describe the shocks is the following differential equation, which has the similar form as the Burgers equation in the stationary frame.

$$(\Phi - \lambda_{\mathsf{x}})\partial\ \Phi = \mu_{\mathsf{x}}\partial^2\Phi \tag{1.7}$$

The above equation posses the solution of the monotonic shock. Given as

$$\Phi = \lambda_{\mathsf{x}}[1 - \tanh(\frac{\lambda_{\mathsf{x}}}{\mu_{\mathsf{x}}}\xi)] \tag{1.8}$$

Where λ_{x} and $\frac{x}{x}$ both are height and the thickness of shock wave respectively. It is obvious that height along with the thickness of shock is mostly depending on the corresponding concentration of the positrons with in that system. In presence of the neutral particles with in the $e - p - i$ quantum plasma, it is quiet obvious that the electrostatic monotonic and oscillatory shocks might appear inside the quantum plasmas(non uniform)[38].

1.9 Vortical Structures in Plasma

Vortices are Coherent structures that appear in the two-dimensional fluids and in the magnetized plasma. The dynamics of the vortical is totally outrun by so called Navier–Stokes (NS) equations, which corresponds to mono polar vortices. While on other side for a dusty plasma (in magnetized form), one may expect the possible existance of the dipolar or higher chain vortices.

The vortical modes are normally affiliated with the dispersive, non linear structures that

possess a two-dimensional character. Whenever the velocity associated with the plasma particles motion which is associated with the dispersive waves, turns very much larger as compared with phase velocity of waves due to the nonlinear effects, we would encounter a curvature of the propagated wave that leads to the formulation of a bi -dimensional vortex [39]. The theoretical work on vortices starts initially with the work by Hasegawa and Mima , who analyzed and linearlised the work , which was done by Charney , on the vortices formation inside the fluids. This was followed by a flurry of activity in the area of vortices in plasmas. The early work regarding the vortices is the detailed review paper by Horton [40]. On the laboratory level when ever a high density plasma is injected into a magnetic mirror then it creates vortex like structures. Further Observations on this phenomena indicated that these structures always move towards the center of mirror and consequently collide.[41] .

1.10 Outline of Thesis

This thesis comprises of five chapters , the main soul of this thesis is about investigation of various linear and non linear modes of instabilities that occurs in multicomponent plasma, fluid model consisting of equation of motion , continuity equation , with both thermal and non thermal distribution of leptons is utilized for this purpose. Chapter 1st begins with importance of multicomponent plasma. Various types of instabilities occurring in plasma are also discussed,along with various non linear coherent structures (vortices, shocks, solitons). finally fluid model is discussed.

Chapter 2 is about the RT instability in EPI quantum plasma, in which a well known cardando method is applied to the cubic dispersion relation, and both the real and imaginary parts of the RT instability are evaluated.

In **Chapter 3** Electrostatic Gravitational or Rayleigh-Taylor (RT) instability is investigated in an in homogeneous pair-ion-electron quantum magneto plasma consisting of positive and negative ions along with a electrons. A generalized dispersion relation is derived under the drift approximations. The presence of negative ions with their different streaming velocities turns the dispersion relation a cubic equation. Different roots of both the real and the imaginary parts of the RT mode are studied by using the Cardano method of solving the cubic equation, it is

further shown RT instability varies for magnetic field density. In **Chapter 4**, we investigate electro static shock waves and solitons in four component ambi plasma dispersion relation is derived in linear regime and in non linear regime kdv burger equation is derived under wave approximation coupled with ion acoustic mode. A well known tanh method is used to evaluate solitons and shocks, these are further plotted in mathematica.**Chapter 5** gives the concluding statement of the thesis.

Chapter 2

Rayleigh-Taylor (RT) Instability in (EPI) Quantum Plasmas

Cubic Dispersion relation is derived for epi quantum plasma in this chapter. A well known cardano method is used for the evaluation of the real along with imaginary parts of the RT instability. The obtained dispersion relation , and the RT instability growth rate are further examined on analytical , numerical bases with the addition of effects density of laptons, and variations of magnetic field. The current chapter is fabricated to be having resemblance to the studies of laser-produced plasmas at laboratory level and also in study of the compact magnetized astro objects such as the white dwarf.

Classical plasmas usually have low densities and comparatively high temperatures. How ever, modern technologies have developed new techniques which has enabled us to produce low temperature , dense plasma. Moreover it could not be explained correctly by classical mechanics , hence quantum mechanics is applied thereafter. In contrast to the classical plasmas, quantum plasma is dense and is relatively cold , and examples of this quantum plasma are believed to be in many astrophysical phenomenons e.g. in white dwarfs Crust , brown dwarfs, and Magnatar along with Neutron strars *etc* [43, 44] and also within the core of giant planets [45, 46].

Dense Quantum plasma is also expected to occur in the upcoming scheme of the production of laser-based matter compression schemes [47, 49] , where the frequency of the plasmon is shifted. Dense quantum plasmas also have other applications as well , these includes , the

electron hole plasmas inside the quantum wires [50] , thin films and metallic nano structures [51] , quantum diode [52], nanowires and nanophotonics [53], nanoplasmonics (nano scale) [54], quantum lasers with high gain [55] quantum dots(piezo magnetic) and quantum wells [56]

The existence of some unlikely physical phenomenons has been reported, which might be labeled as "quantum", first refers to the particles distinguishability , where the distribution function is changed from the MB to the Fermi-Dirac. For such case λ_{D} is greater than the inter Fermionic distance, accompanied by the degeneracy of temperature and the tunneling effects,thus new the quantum mechanical effects starts [57]. Under such situation the dynamics of the system are also changed. Secondly due to the dispersive effects these particles does not stay in phase space. Thirdly the positron and electron spin may interact with magnetic field via dipoler force thus dynamics are affected [58]. More Recently, the quest in the field of the quantum plasmas has been noticed [57, 67] .

Together all these studies posses effects of the quantum based corrections just like de Broglie potential(Bohm), the spin magnetization and the properties just like zero temperature, Fermi pressure which could significantly enhances the dynamics of plasma. The above literature mainly focuses on the perturbations in the background of the quantum plasma with no in homogenity . However, in some cases, the Quantum type plasma may have the, density features that are not uniform when it is dealt practically, which are often reported to occur in a real (astrophysics) or effective (inertial confinement fusion process) gravitational field.

RT mode is an important effect which is created at the interface plane which separates two fluids of different densities when heavy fluid is accelerating onto the lighter fluid. The instability of such types for fluid in the gravitational field was first discovered by Rayleigh [68] and later on Taylor utilized this to all the accelerated fluids [69]. Since then, this instability mechanism has been explored by several researchers, under various presumptions [70]. Detailed description of RT concept along with other associated parameters and the presumptions has been explored in the [71]. Instabilities(Hydro dynamic) in quantum mechanical plasma have always been a reasonable field of research for the last couple of years. Presuming a QHD(quantum hydrodynamic model) for the Q plasma, so many researchers have highlighted that the interplay occurring between dispersion and dissipation give rise to numerous instabilities just as two stream mode, Kelvin Helmholtz mode and RT mode [72, 74].

Effect of the quantum mechanics on inside waves and plasma RT mode is being studied by the Vitaly in [74]. Effects of quantum mechanics and the magnetic field on the electromagnetic version of the RT Mode has been studied in the incompressible plasmas by deriving its linear growth rate under of the fixed boundary condition [75]. RT mode in horizontal/vertical in homogeneous rotating plasma with the quantum effects was investigated in detail in [77, 78]. Electrostatic RT Mode was investigated in dense Electron Ion quantum magneto plasma in [79] , where ions are supposed to be cold and classical, while on the other hand electrons are more dense. It has also been shown that gradient of density and the quantum speed is also modifying growth rate of RT mode. In contrast to the classical plasma in case of dense quantum magneto plasma, linear growth rate of RT mode is significantly larger, and is fully localized as well. while on the other hand , it has recently been proven that EI plasma appears with in the polar cap of the magnetospheres of pulsars, in early universe, The core regions of accretion disks which are surrounding central black hole in the AGN, in the polar region of the neutron star, in our own galaxy center , the solar flares and more recently has also found in the intense laser pulse that propagates in the plasma [80, 87]. However, it is also suggested [88, 89] that EP plasma still contain a small fraction of the heavy ions. Recently[90, 91, 92], some new and very interesting linear along with nonlinear effects have been shown in EPI plasma.

In the present work electrostatic RT mode is investigated by applying QHD(quantum hydro dynamic) model to quantum EPI plasma. Dispersion relation is calculated under the presumption of drift wave phenomena. Dispersion relation along with the instability growth rate are then studied by Cardano's technique.

2.1 Basic Set of Equations

Consider the $(e-p-i)$ Electron, Positron , Ion plasma with the magnetic field as given by $B_0 = B_0\hat{z}$, where B_0 is the magnitude of the applied magnetic field, which is directed along z axis . Under the equilibrium condition, the gravitational field is supposed to be alighned in along $x-$direction $g = g\hat{x}$. This depicts that both of the density and the gravitational field are directed along x-axis. Electric field and wave is propagating along the y- axis such that

$E = [0, E_y, 0]$ and $K = [0, K_y, 0]$. Considering the momentum equation as

$$m_j\, n_j\, (\frac{\partial}{\partial t} + \vec{U_j} \cdot \nabla)\vec{U_j} = q n_j\, (\vec{E} + \vec{U_j} \times B_0) + m_j\, n_j\, g - \nabla P_{Fj} + (n_j\, \hbar^2)/(2m_j)\nabla(\frac{\nabla^2 \sqrt{n_j}}{\sqrt{n_j}}) = 0 \quad (2.1)$$

The ion continuity equation could be written as

$$\frac{\partial}{\partial t} n_j + \nabla.(n_j\, \vec{U_j}) = 0 \quad (2.2)$$

Where m_j ,q_j , g, n_j and U_j are the mass,electrostatic charge, gravitational acceleration, density, velocity associated with the jth specie on respective bases, here "j" is representing the ,ion ,positron and electron respectively. Condition of quasi-neutrality under equilibrium state is read as $n_{p0} + n_p = n_{e0}$, $\hbar = \frac{h}{2}$ being plank constant and e indicates the charge(electronic). The force term(quantum) i.e. last of the two terms of eq(2.1)are there because of quantum mechanical effects of jth species and is denoting the Q Corr between the fluctuations of the density , and the degeneracy factor of the temperature due to the Fermi-Dirac distribution function. Equation of the state for degenerate positrons and electrons is $P_{Fj} = \hbar^2 n_j^{\frac{5}{3}} \frac{(3\ \ ^2)^{\frac{2}{3}}}{5m_j}$ as Fermi pressure and the pressure gradient force $\nabla P_{Fj} = 2\varepsilon_{Fj}\, \nabla n_j$ with $\varepsilon_{Fj} = (\hbar^2(3\pi^2 n_p)^{\frac{2}{3}} \frac{(\hbar^2(3\ \ ^2 n_{jo})^{\frac{2}{3}}}{2m_j}$ being the jth energy(Fermi) over the Fermi surface. Due to the fact mass of ions is large as compared to positrons and electrons, so therefore it is then presumed that the quantum mechanical effects are kept negligible for the ions. Thus the linearized form of eq(2.1) for cold streaming ions could be written as

$$m_i\, n_i\, (\frac{\partial}{\partial t} + \vec{U_i} \cdot \nabla)\vec{U_i} = q n_i\, (E + \vec{U_i} \times B_0) + m_i\, n_i\, g \quad (2.3)$$

Under the state of equilibrium , we find the drift associated with the ions

$$\vec{U_{i0}} = \frac{-g}{\Omega_c}\hat{y} \quad (2.4)$$

Where $\Omega_c = \frac{B_0}{m_i}$ is the frequency of ion. The equation of motion for Fermionic leptons is

$$m_e n_e (\frac{\partial}{\partial t} + \vec{U_e} \cdot \nabla)\vec{U_e} = -e n_e (E + U_e \times B_0) - 2\varepsilon_{Fe} \nabla n_e + \frac{\hbar^2}{4m_e} \nabla(\nabla^2 n_e) \quad (2.5)$$

$$m_{\mathsf{p}} n_{\mathsf{p}} (\frac{\partial}{\partial t} + \vec{U}_{\mathsf{p}} \cdot \nabla)\vec{U}_{\mathsf{p}} = -e n_{\mathsf{p}} (E + \vec{U}_{\mathsf{p}} \times B_0) - 2\varepsilon_{\mathsf{F}\,\mathsf{p}} \nabla n_{\mathsf{p}} + \frac{\hbar^2}{4m_{\mathsf{p}}} \nabla(\nabla^2 n_{\mathsf{p}}) \tag{2.6}$$

By Following the procedure in low frequency regime ($\partial_{\mathsf{t}} \ll \Omega_{\dot{\mathsf{c}}}$) for electrostatic perturbations, the perpendicular first order components associated with the ion fluid velocity could be expressed as

$$\vec{U}_{\mathsf{i}\perp} = \vec{V}_{\mathsf{E}} + \vec{V}_{\mathsf{p}} \tag{2.7}$$

Further corresponding values of $\vec{V}_{\mathsf{E}}$ ($E \times B$ drift)and $\vec{V}_{\mathsf{P}\mathsf{i}}$ (Polarization Drift) are given as

$$\vec{V}_{\mathsf{E}} = \frac{E_{\mathsf{y}}}{B_0} \hat{x} \tag{2.8}$$

$$\vec{V}_{\mathsf{P}\mathsf{i}} = \frac{1}{\Omega_{\dot{\mathsf{c}}}} (\partial t + U_{\mathsf{b}} \cdot \nabla) \frac{E_{\mathsf{y}}}{B_0} \hat{y} \tag{2.9}$$

In above equations U_{b} depicts the streaming(ion) fluid velocity. As the polarization drift vary with inertia, there fore in comparison to the ions, it could be omitted for both the electrons and the positrons, therefore, from eq(2.5) corresponding perpendicular part corresponding to the velocity vector associated with the quantum mechanical electron(obeying FD statistics) is

$$\vec{U}_{\mathsf{e}\perp} = [\frac{\vec{E}_{\mathsf{y}}}{B_0} + (\frac{2\varepsilon_{\mathsf{F}\,\mathsf{e}}}{eB_0 n_{\mathsf{e}}}) \nabla_\perp n_{\mathsf{e}1} - \hbar^2 \frac{\hbar^2}{4eB_0 n_{\mathsf{e}0} m_{\mathsf{e}}} \nabla_\perp (\nabla^2 n_{\mathsf{e}1})] \hat{x} \tag{2.10}$$

Similarly, perpendicular component associated with the positron, ref eq(2.6) is

$$\vec{U}_{\mathsf{p}\perp} = [\frac{\vec{E}_{\mathsf{y}}}{B_0} + (\frac{2\varepsilon_{\mathsf{F}\,\mathsf{e}}}{eB_0 n_{\mathsf{p}}}) \nabla_\perp n_{\mathsf{p}1} - \hbar^2 \frac{\hbar^2}{4eB_0 n_{\mathsf{p}0} m_{\mathsf{p}}} \nabla_\perp (\nabla^2 n_{\mathsf{p}1})] \hat{x} \tag{2.11}$$

Due to absence of the polarization drift, the streaming term associated with the positron and electron are not omitted in eq(2.10,2.11). In the linearized state, the continuity equations of ions along with that of positrons and electrons are

$$\frac{\partial n_{\mathsf{i}1}}{\partial t} + (\vec{U}_{\mathsf{b}} \nabla)_{\mathsf{h}\ 1} + \partial_{\mathsf{x}} n_{\mathsf{b}}\, \hat{x}.\vec{V}_{\mathsf{E}} + n_{\mathsf{b}}\, \nabla.\vec{V}_{\mathsf{p}} = 0 \tag{2.12}$$

$$\frac{\partial n_{e1}}{\partial t} + \partial_x n_e \left[\frac{\vec{E}_y}{B_0} + \frac{2\varepsilon_{Fe}}{eB_0 n_e}\nabla_\perp n_{e1} - \hbar^2 \frac{\hbar^2}{4eB_0 n_e\ m_e}\nabla_\perp(\nabla^2 n_{e1})\right] = 0 \tag{2.13}$$

$$\frac{\partial n_{p1}}{\partial t} + \partial_x n_p \left[\frac{\vec{E}_y}{B_0} + \frac{2\varepsilon_{Fe}}{eB_0 n_p}\nabla_\perp n_{p1} - \hbar^2 \frac{\hbar^2}{4eB_0 n_p\ m_p}\nabla_\perp(\nabla^2 n_{p1})\right] = 0 \tag{2.14}$$

All the above mentioned equations from (2.7) to (2.13) are reasonable in long wavelength regime, i.e.$k\lambda_{Fj} \ll 1$, where λ_{Fj} being the Fermi length of the positron and electron. We also have presumed that the phase speed associated with RT mode is more than the quantum Bohm potential speed while it is smaller as compared to Fermi speed of positron and electron.. i.e. $\frac{\hbar K}{m_j} \ll \frac{l}{k} \ll V_{(Fp)}$. We have omitted some terms in eq(2.13,2.14) by presuming that constant streaming velocities of positron and electrons are non spatial functions. By supposing the plane wave solution which is of the form $exp(iky - i\omega t)$to all quantities (perturbed)and utilizing drift approximation $\Omega_c^2 \gg (\omega - kU_D)^2$, we then get the the ion number density in the following form

$$n_{i1} = -\frac{in_{i0}}{\omega_D}(\kappa_{En} + \frac{\omega_D k}{\Omega_c})\frac{\vec{E}_y}{B_0} \tag{2.15}$$

In the above equation $\omega_D = \omega - kU_{i0}$is the Doppler shifted frequency and $\kappa_n = \frac{1}{n_{i0}}\partial_x n_{i0}$ being the inverse in homogeneity scale length for ions. Continuity of electron Eq(2.13) is leading to perturbed electron density as

$$n_{e1} = -i\frac{n_{e0}\kappa_e}{(\omega - k\vec{V}_{*e})}\frac{\vec{E}_y}{B_0} \tag{2.16}$$

Where$\kappa_e = \partial_x n_e$ gives the inverse in homogeneity scale length associated with the electrons, and the quantity $Y_q = \sqrt{C_q^2 + \frac{\hbar^2 k^2}{2m_i m_e}}$ illustrates the quantum corrected modified diamagnetic drift velocity which is possesed by the electrons , $C_q = \sqrt{\frac{2"_{Fe}}{m_i}}$ depicts the modified quantum ion acoustic velocity due to electron and is the well-defined quantum ion acoustic speed. Also, if we utilize Eq(2.14) to find the densities of the positron by exercising the same procedure which was previously used to find the electron density we have the following relation

$$n_{p1} = -i\frac{n_{p0}k_p}{(\omega - k\vec{V}_{*e})}\frac{\vec{E}_y}{B_0} \tag{2.17}$$

With $k_{p} = \frac{@n_{p0}}{@x}$ is the inverse in homogeneity scale length of positrons, while $\vec{V}_{*P} = \frac{U_{qp}^2 k_{np}}{\Omega_{ci}}$ is quantum corrected modified diamagnetic drift velocity for positron with Y_{q} is modified ion acoustic speed(quantum), which is due to the positron.

2.2 Evaluation Of Dispersion Relation Using RT Instability

Using the condition $k\lambda_{Fp} \ll 1$,the condition of Quasi Neutrality could be written as

$$n_{p1} + n_{i1} = n_{e1} \tag{2.18}$$

Using2.15-2.17 in 2.38 a generalized dispersion relation is obtained as

$$(1-p)(\frac{\Omega_c\, k_n}{\omega_D} + k) + \frac{p\Omega_c\, k_p}{\omega + k.\vec{V}_{*p}} - \frac{\Omega_c\, k_e}{\omega - k.\vec{V}_{*e}} = 0 \tag{2.19}$$

Here the quantity $p = n_{p0}/n_{e0}$ is representing the electron and positron ratio. When the concentration of positron is ignored i.e. $p = 0$,then the dispersion relation of RT mode in E I Quantum Magnetoplasma is given [80] i.e.

$$\omega_D\omega = -\kappa_e\ \Omega_c\, U_{i0} + \kappa_e\ Y_q^2\,(\kappa_e\ + \frac{k\omega_{_D}}{\Omega_c}) \tag{2.20}$$

In order to manipulate analysis of the instability by consolidating ions streaming we then get the dispersion relation of eq(2.19) in the following form

$$(1-p)k\omega^2 - \omega^2[k^2(\vec{V}_{*e} - U_{i0} - \vec{V}_{*p}) - (1-p)\Omega_c\ \kappa_n\ - p\kappa_p\ \Omega_c\ + \kappa_e\ \Omega_c\ ] - \omega[(1-p)\Omega_c\ \kappa_n\ k(\vec{V}_{*e} - \vec{V}_{*p}) + \tag{2.21}$$
$$(1-p)k^3(\vec{V}_{*p}\vec{V}_{*e} + \vec{V}_{*e}U_{i0} - U_{i0}\vec{V}_{*p} + p\kappa_p\ \Omega_c\ k(\vec{V}_{*e} + U_{i0}) - \kappa_e\ \Omega_c\ (U_{i0} - \vec{V}_{*e})] - (1-p)\Omega_c\ \kappa_e\ k^2\vec{V}_{*e}\vec{V}_{*p} +$$

$$(1-p)k^4U_{i0}\vec{V}_{*e}\vec{V}_{*p} + p\Omega_c\ \kappa_p\ k^2\vec{V}_{*e}U_{i0} + \Omega_c\ \kappa_e\ k^2\vec{V}_{*p}U_{i0} = 0$$

By instigating the gravitational field , cubic form of the equation could be formulated as

$$\omega^3 + A\omega^2 + B\omega + C = 0 \tag{2.22}$$

All the constants i,e, A, B along with C are all real and are being defined

$$A = k(\vec{V}_{*\mathsf{D}} - \vec{V}_{*\mathsf{e}} - \frac{g}{\Omega_{\mathfrak{c}}})$$

$$\begin{aligned} B &= -\frac{\Omega_{\mathfrak{c}}\ \vec{V}_{*\mathsf{e}}\kappa_{\mathfrak{e}}}{(1-p)} - (\frac{p}{1-p})\kappa_{\mathfrak{p}}\ \Omega_{\mathfrak{c}}\ \vec{V}_{*\mathsf{p}} - g\kappa_{\mathfrak{n}}\ + k^2(\frac{\vec{V}_{*\mathsf{e}}g}{\Omega_{\mathfrak{c}}} - \frac{g\vec{V}_{*\mathsf{p}}}{\Omega_{\mathfrak{c}}} - \vec{V}_{*\mathsf{e}}\vec{V}_{*\mathsf{e}} \\ C &= -\frac{V_{*\mathsf{e}}\vec{V}_{*\mathsf{p}}k}{\Omega_{\mathfrak{c}}}(gk^2 + \Omega_{\mathfrak{c}}^2\ \kappa_{\mathfrak{n}}\ ) - gk(\frac{p\vec{V}_{*\mathsf{e}}\kappa_{\mathfrak{p}}}{1-p} + \frac{\vec{V}_{*\mathsf{p}}\kappa_{\mathfrak{e}}}{1-p}) \end{aligned} \tag{2.23}$$

The eq(2.22,2.23) could be written in normalized form as

$$\tilde{\omega}^3 + A\tilde{\omega}^2 + B\tilde{\omega} + C = 0 \tag{2.24a}$$

$$A = \tilde{k}[\alpha\beta\tilde{\rho}_{\mathsf{s}}^2(1 + \frac{H_{\mathsf{e}}^2\tilde{\lambda}_{\mathsf{Fe}}^2\tilde{k}^2}{4\alpha}) - \tilde{\rho}_{\mathsf{s}}^2(1 + \frac{H_{\mathsf{e}}^2\tilde{\lambda}_{\mathsf{Fe}}^2\tilde{k}^2}{4}) - \tilde{g}$$

$$B = -(\frac{\tilde{\rho}_{\mathsf{s}}^2}{1-p})(1 + \frac{H_{\mathsf{e}}^2\tilde{\lambda}_{\mathsf{Fe}}^2\tilde{k}^2}{4}) - \alpha\beta^2\tilde{\rho}_{\mathsf{s}}^2(\frac{p}{1-p})(1 + \frac{H_{\mathsf{e}}^2\tilde{\lambda}_{\mathsf{Fe}}^2\tilde{k}^2}{4}) - \tilde{g}\Gamma + \tilde{k}^2$$

$$\tilde{g}\tilde{\rho}_{\mathsf{s}}^2(1 + \frac{H_{\mathsf{e}}^2\tilde{\lambda}_{\mathsf{Fe}}^2\tilde{k}^2}{4}) - \alpha\tilde{g}\tilde{\rho}_{\mathsf{s}}^2(1 + \frac{H_{\mathsf{e}}^2\tilde{\lambda}_{\mathsf{Fe}}^2\tilde{k}^2}{4\alpha}) - \alpha\beta^2\tilde{\rho}_{\mathsf{s}}^4(1 + \frac{H_{\mathsf{e}}^2\tilde{\lambda}_{\mathsf{Fe}}^2\tilde{k}^2}{4})(1 + \frac{H_{\mathsf{e}}^2\tilde{\lambda}_{\mathsf{Fe}}^2\tilde{k}^2}{4})$$

$$C = -\tilde{k}(\Gamma + \tilde{g}\tilde{k}^2)\alpha\beta^2\tilde{\rho}_{\mathsf{s}}^4(1 + \frac{H_{\mathsf{e}}^2\tilde{\lambda}_{\mathsf{Fe}}^2\tilde{k}^2}{4\alpha})(1 + \frac{H_{\mathsf{e}}^2\tilde{\lambda}_{\mathsf{Fe}}^2\tilde{k}^2}{4}) - \frac{\tilde{g}\tilde{k}^2\tilde{\rho}_{\mathsf{s}}^2\beta}{1-p}[(1+p)(1 + \frac{H_{\mathsf{e}}^2\tilde{\lambda}_{\mathsf{Fe}}^2\tilde{k}^2}{4}) + \alpha + p$$

Normalized Bohm parameters are given below as

$\tilde{k} = \frac{}{_{ne}}$, $\tilde{g} = \frac{\mathsf{g}_{\ ne}}{\Omega_{ci}^2}, \tilde{\omega}_{\mathsf{r}} = \frac{!_{\ r}}{\Omega_{ci}}, \tilde{\gamma} = \frac{}{\Omega_{ci}}, \tilde{\rho}_{\mathsf{s}} = \frac{_{ne}\Upsilon_{sq}}{\Omega_{ci}}, \tilde{\lambda}_{\mathsf{Fe}} = \lambda_{\mathsf{Fe}}\kappa_{\mathfrak{e}}\ , \alpha = \frac{"_{Fe}}{"_{Fp}}, \beta = \frac{_{np}}{_{ne}}, \Gamma = \frac{_{ni}}{_{ne}}$.

The Bohm parameters(normalized) is representing ratio of the plasmon energy and the Fermi

energy and the λ_{Fe} is the electron Fermi length whileρ_{s} is representing the ion-sound gyro-radius.2.24a is normalized cubic dispersion relation. Now consider the simple case $\tilde{\omega}^3 <<< 1$ where we make term $\tilde{\omega}^3$ to be negligible in 2.24a and so

$$A\tilde{\omega}^2 + B\tilde{\omega} + C = 0 \tag{2.25}$$

The equation(2.25) is the quadratic equation. The instability is created when $B^2 - 4AC < 0$. We use $\omega = \omega_{\mathsf{r}} + i\gamma$ (where ω_{r} is representing real frequency of the wave and γ being the growth rate) in eq(2.25) also solving it we then obtain

$$\omega_{\mathsf{r}} = -\frac{B}{2A}, \gamma = \sqrt{-\frac{B^2}{4A^2} + \frac{C}{A}} \tag{2.26}$$

It is obvious that particle number density is dependent on quantum mechanical effects , The data used was observed from magnetars, neutron stars and the white dwarfs. Fig.2.1 is showing the ω_{r} (real frequency in normalized state) versus k (wave number in normalised form) for different positron concentration values i.e.$p = 1/6$ (solid line) , $p = 1/8$ (dashed line). It is clearly observed that electrostatic $R - T$ instability is well separated. Fig.2.2 is depicting the growth rate γ associated the wave for various values of concentration of positrons i.e. $p = 1/6$ (solid line) , $p = 1/8$ (dashed line). It is very clear that γ is increasing for smaller k, until the threshold $k \equiv k_{\mathsf{c}}$ is achieved , then the γ starts decreasing and instability with in system starts to reduce. Positron concentration is strongly affecting the growth rate γ and, in fact, is decreasing with the increase in value of p. hence , the positrons number would tend to lower $R - T$ mode in the EPI system.

2.3 Analysis of Instability By The Cardano's Method

For cubic equation we are using Cardano's method , we shall be discussing the RT instability analysis by using the 2.24a . In order to manipulate the process of instability , again put

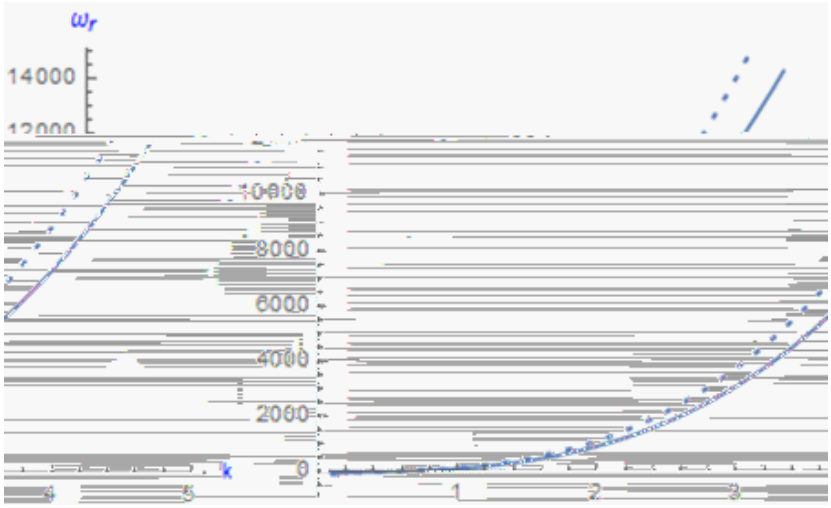

Figure 2-1: Fig 2.1 Solution to Eq. (2.25), the normalized real wave frequencyω_r , versus the scaled wave number $\frac{k}{ne}$ in EPI quantum magnetoplasma for different values of positron concentration i.e. $p = \frac{1}{6}$ (solid line) and $p = \frac{1}{8}$ (dashed line). Other Physical parameters are taken as $n_{e0} = 6 \times 10^{27}, \kappa_e = \frac{k}{10}, \Gamma = 20$, $g_{WD} = 1000000$ and $B_0 = 10^6$.

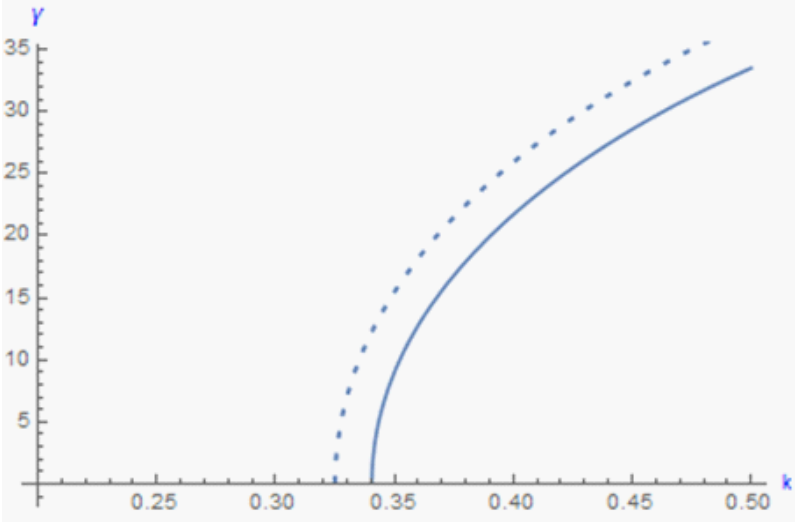

Figure 2-2: Solution to Eq(2.25) , the normalized growth rate $\frac{\gamma}{\Omega_{ci}}$, versus the scaled wave number$\frac{k}{ne}$ in EPI quantum magnetoplasma for different values of positron concentration i.e. $p = 1/6$ (solid line) and $p = \frac{1}{8}$ (dashed line). Other Physical parameters are taken as $n_{e0} = 6 \times 10^{27}$,$\kappa_e = \frac{k}{10}$, $\Gamma = 20$, $g_{WD} = 1000000$ and $B_0 = 10^6$.

$\omega = \omega_r + i\gamma$(where ω_r is the real frequency associated with the waves , and γ being growth rate) in 2.25 then solving it for $\gamma^2 \ll \omega_r^2$we obtain the real as well as imaginary parts.

$$\tilde{\omega}_r^3 + A\tilde{\omega}_r^2 + B\tilde{\omega}_r + C = 0 \tag{2.27}$$

$$\gamma = \sqrt{3\omega^2 + 2\omega A + B} \tag{2.28}$$

Introducing$\tilde{\omega}_r = z - \frac{A}{3}$ also by assuming the term $p$and q as, $p = \frac{3B^2 - A^2}{3}, q = \frac{2A^2 - 9AB + 27C}{27}$ and the eq(2.27) is then formulated to the cubic equation with no term with 2nd degree i.e

$$z^3 + zp + q = 0 \tag{2.29}$$

If $p = q = 0$, then $z = 0$. Else, we assume case where the value of p or q tends to zero and also when both are non zero. We shall assume those cases where both of them are non zero. imagine , this , for both of the two numbers i,e u and v respectively .

$$(u - v)^2 + 3uv(u - v) = u^2 - v^2 \tag{2.30}$$

We could solve the cubic equation , when we find the values of u, v

$$\begin{aligned} u^2 &= -\frac{q}{2} + \sqrt{\Delta} \\ v^2 &= \frac{q}{2} + \sqrt{\Delta} \\ \Delta &= \frac{q^2}{4} + \frac{p^2}{27} \end{aligned} \tag{2.31}$$

The type of the Cardano roots could be determined by the discriminant Δ as given below.

1.If Δ is zero, then all of the roots are being real in nature, with two being equal(at least).

2.If the Δ being greater than zero, then $\sqrt{\Delta}$ is a real , and one root is real, and the other two roots are complex numbers.

3.If Δ is less than zero , then $\sqrt{\Delta}$ is imaginary, so all the roots are real, and u and v will be complex numbers. it is termed as irreducible case. We shall only consider case (2) and (3) .

2.4 One Real Root and Two Complex Root

Here, Δ is $+ve$, there fore square root would be the real one. For such a case, the real root could be obtained as follows

$$\omega_{r1} = \sqrt[3]{-\frac{q}{2} + \sqrt{\Delta}} - \sqrt[3]{\frac{q}{2} + \sqrt{\Delta}} - \frac{A}{3} \tag{2.32}$$

Other two roots are complex in nature and not to be included. In Regards for this real root the following growth rate of RT mode is obtained as under .

$$\gamma_{11} = \sqrt{3\omega_{r1}^2 + 2\omega_{r1}A + B} \tag{2.33}$$

2.5 All Roots Real and Different

As $u = \sqrt[3]{-\frac{q}{2} + \sqrt{\Delta}}$ and , so for this particular case $\sqrt{\Delta}$ is purely imaginary i.e. $\Delta < 0$ which implies

$$u = -\frac{q}{2} + i\sqrt{-\Delta}$$

$$v = \frac{q}{2} + i\sqrt{-\Delta}$$

By incorporating the trigonometric concept of analysis we get the normalized three real roots of RT mode as .

$$\omega_{r21} = 2r^{\frac{1}{3}} \cos(\frac{\phi}{3}) - \frac{A}{3} \tag{2.34}$$

$$\omega_{r22} = 2r^{\frac{1}{3}} \cos(\frac{\phi + 2\pi}{3}) - \frac{A}{3} \tag{2.35}$$

$$\omega_{r23} = 2r^{\frac{1}{3}} \cos(\frac{\phi + 4\pi}{3}) - \frac{A}{3} \tag{2.36}$$

Where $r = \sqrt{(-\frac{p}{3})^3}$ and $\cos\phi = [-\frac{q}{2\sqrt{(-\frac{p}{3})^3}}]$. The three normalized growth rates for the $R-T$ instability are given as follow

$$\gamma_{21} \approx \sqrt{3\omega_{r21}^2 + 2\acute{a}\omega_{r\,21} + B} \tag{2.37}$$

$$\gamma_{22} \approx \sqrt{3\omega_{r22}^2 + 2\acute{a}\omega_{r\,22} + B} \tag{2.38}$$

$$\gamma_{23} \approx \sqrt{3\omega_{r23}^2 + 2\acute{a}\omega_{r\,23} + B} \tag{2.39}$$

One out of these three modes will show a growing trend , which would ultimately be determining the growth rate of R-T instability.

2.6 Results and Discussions

In order to see the detail view of the quantum effects which includes , the Pauli-exclusion principle and tunneling across the Bohm potential on the growth rate of the R-T mode . eq(2.31) - (2.38) along with coefficients are analyzed numerically . The typical parameters of interiors of neutrons stars, white dwarfs and magnetars in the *cgs* system of units are given [96]$c = 3 \times 10^6 m/\sec$, $m_{ep} = 9.11 \times 10^{-28} kg, m_i = 1.67 \times 10^{-27} kg, e = 4.8 \times 10^{10} C, h = 1.05 \times 10^{-27}, k_B = 1.38 \times 10^{-16}, n_0 = 10^{23} - 10^{25}, p < 1$. It should further be noted that equations used in this chapter are in the dimensionless form.

2.6.1 Analysis of R-T Mode of Eq. (2.33)

For this specific case, the growth rate of 2.38)is been based on the real frequency 2.38) which is explicating the RT instability in quantum EPI plasma. By utilizing the above mentioned data in the normalized coefficients of the 2.38) growth rate of (2.33) has been plotted for the electrostatic RT mode including the effects of density, and the variation of the ambient magnetic field (Figs.2.3., and 2.4). Moreover it is also observed from the above figures that growth rate tends to damp, which indicates that the in homogeneity in the plasma is acting like

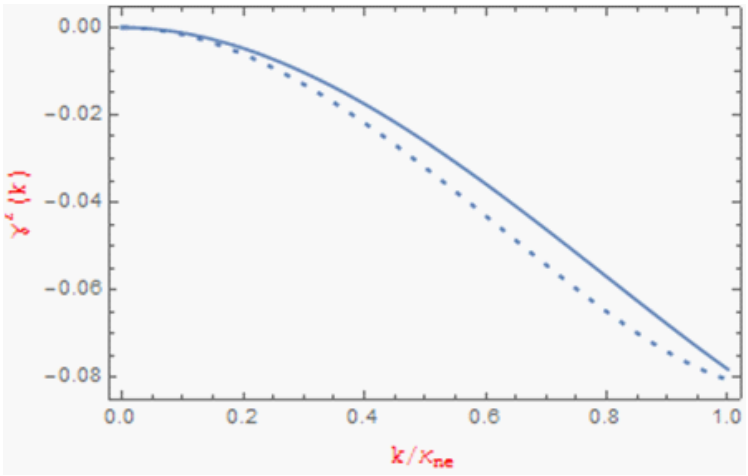

Figure 2-3: Solution to Eq(2.33), the normalized growth rate$\frac{\gamma}{\Omega_{ci}}$, versus the scaled wave number$\frac{k}{\kappa_{ne}}$ in EPI quantum magnetoplasma with electron density variation i.e. $n_{e0} = 5 \times 10^{27}$ (solid curve) and $n_{e0} = 6 \times 10^{27}$ (dashed curve). Other Physical parameters are taken as n_{p0}=10^{27}, $\kappa_{\theta} = \frac{k}{10}$, $\Gamma = 0.6$, $g_{WD} = 1000000$ and $B_0 = 10^6$.

a sink. Further more its energy is taken from the perturbation. The out come of this analysis (i.e. damping phenomenas), in the nonlinear regime gave rise to shocks with in such a system which are way beyond the prescribed scope of the present work. It has also been shown in the Fig.2.3, and in the Fig.2.4 that damping rate is increasing with the increase in density, and is decreasing with the magnetic field B_0.

2.7

2.8 Analysis of R-T Mode of Eqs. (2.37-2.39)

By using the Cardano method for the solution of eq 2.27 under the assumption that all roots are completely different and real , consequently we obtain the real form of the **??**) and also three growth rates to that Eqs(2.37-2.39) , for this mode. By utilizing above mentioned data , normalized growth rate eq 2.27 is being plotted for the *RT* mode, under the effects of the

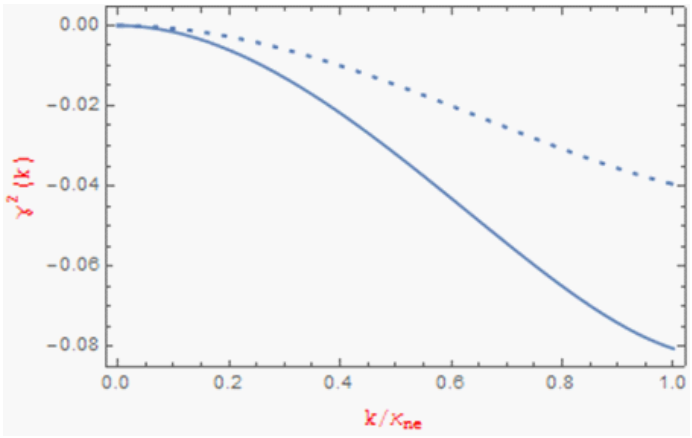

Figure 2-4: Damping curves of normalized growth rate $\frac{\gamma}{\Omega_{ci}}$ versus normalized wavenumber $\frac{k}{\kappa_{ne}}$ (given by Eq. (233))in EPI quantum magnetoplasma for different values of magnetic field variation i.e.$\Omega_c = 10^8$ (solid curve) and $\Omega_c = 1.5 \times 10^8$ (dashed curve). Other Physical parameters are taken as $n_{p0} = 10^{27}$, $\kappa_e = \frac{k}{10}$,$\Gamma = 0.6$, $g_{WD} = 1000000$ and $n_e = 6 \times 10^{27}$.

density of electron, and applied magnetic field as shown in Figs 2.5 and 2.6. Fig 2.5 (Fig2.6) illustrates that the growth rate is increasing (decreasing) with the increase in the number density (Magnetic field B_0).

Thus magnetic field B_0 press down the instability as it keeps the particles to be confined in centre rather than being on boundary for localized wave . Further more Ω_c is greater than frequency of wave mode , so if we increase B_0then this comparison turns more clear. And growth rate is decreased. If electron number density is increased then consequently a plasma turns out to be more denser and shrunk that makes more particlates available and hence give energy to the wave to perturbate as $\frac{1}{k} < V_{Fe}$. This in turn increases growth rates and turns RT mode more unstable. Fig.2.7 is demonstrating the stabilizing effect of the positron concentration effects upon the variation of growth rate eq(2.37). It shows that RT mode growth rate is decreasing with the variation of p. It further makes it clear that concentration of positrons acts a stabilizing agent in analysis of instability. It also depicts that the growth rate is decreasing with increase in the values of p.

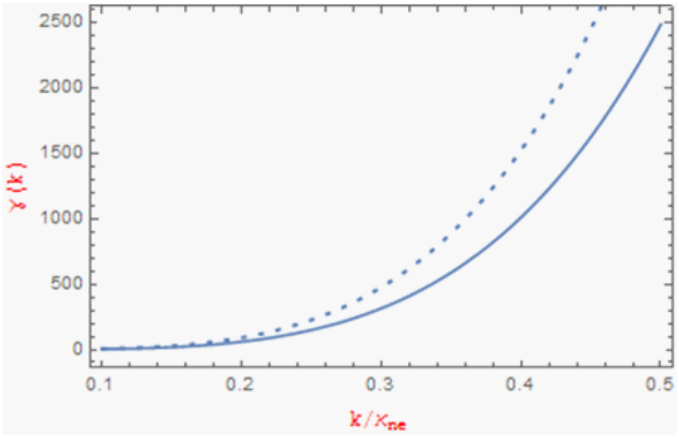

Figure 2-5: Normalized growth rate $\frac{\gamma}{\Omega_{ci}}$ versus normalized wavenumber $\frac{k}{\kappa_{ne}}$ (given by Eq(2.37)in EPI quantum magnetoplasma for different values of electron density i.e. $n_{e0} = 6 \times 10^{27}$ (solid curve) and $n_{e0} = 6.5 \times 10^{27}$ (dashed curve). Other Physical parameters are taken as $n_{p0} = 10^{27}$, $\kappa_{e} = \frac{k}{10}, \Gamma = 20, g_{WD} = 1000000$ and $B_0 = 10^6$.

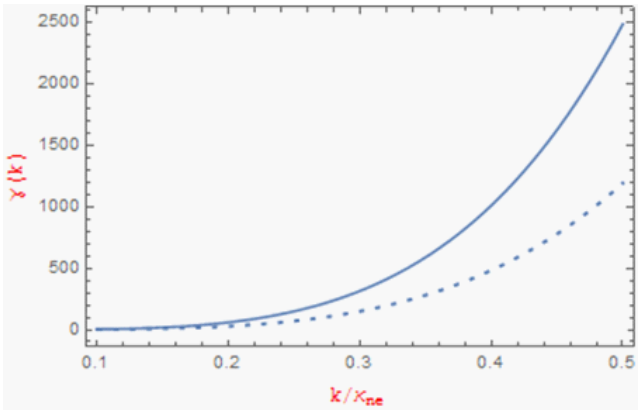

Figure 2-6: Normalized growth rate,eq 2.37, versus normalized wavenumber $\frac{k}{\kappa_{ne}}$ (given by Eq.2.37 in EPI quantum magnetoplasma for different values of magnetic field variation i.e. $\Omega_{c} = 10^8$ (solid curve) and $\Omega_{c} = 1.2 \times 10^8$ (dashed curve). Other Physical parameters are taken as $n_{p0} = 10^{27}, \kappa_{e} = \frac{k}{10}, \Gamma = 20, g_{WD} = 1000000$**and**$n_{e} = 6 \times 10^{27}$**.**

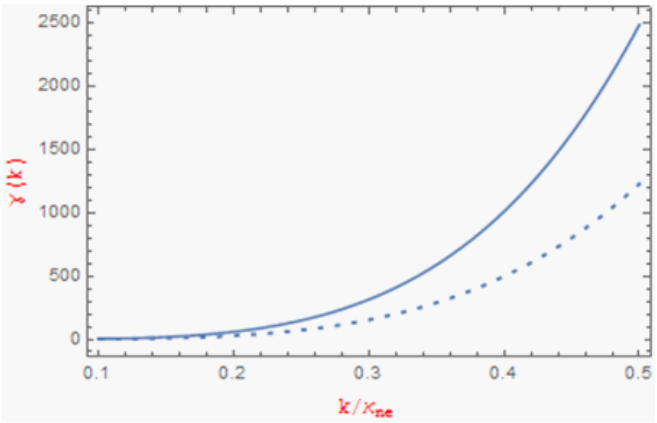

Figure 2-7: Normalized growth rate$\frac{\gamma}{\Omega_{ci}}$ versus normalized wavenumber$\frac{k}{\kappa_{ne}}$ (given by Eq. 2.37)in EPI quantum magnetoplasma for different values of positron concentration i.e. $n_{p0} = 10^{27}(solidcurve)andn_{p0} = 1.2 \times 10^{27}$ (dashed curve). Other Physical parameters are taken as $n_{e0} = 6 \times 10^{27}, \kappa_{e} = \frac{k}{10}, \Gamma = 20, g_{WD} = 1000000\text{and}B_0 = 10^6$.

Similarly the same growth rate which is that of the Fig.2.7 is depicted in the Fig.2. 8 for the second root eq(2.38) with positron concentration variation. This implies that the growth rate is decreasing when we increase in the values of p. Fig2. 9 along with Fig 2.10 unveil that variation of growth rate of the second root (2.38) for various values of the density of electron and the magnetic field B_0 respectively. These two figures manifest that growth rate is increasing (decreasing) with increase in number density (magnetic field B_0). The variation of the growth rate for second root is of the standard form and is depicting the similar attitude which is illustrated in various other literature. The third root(2.39)exhibits the damping trend.

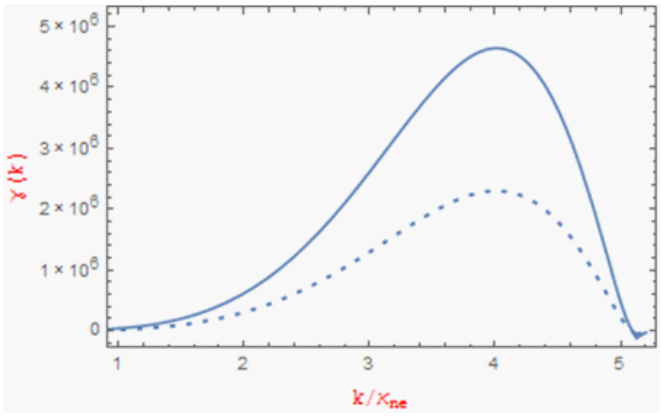

Figure 2-8: Normalized growth rate$\frac{\gamma}{\Omega_{ci}}$ versus normalized wavenumber$\frac{k}{\kappa_{ne}}$ (given by .2.38)in EPI quantum magnetoplasma for different values of positron concentration i.e. $n_{p0} = 10^{27}$ (solid curve) and $n_{p0} = 1.2 \times 10^{27}$ (dashed curve). Other Physical parameters are taken as $n_{e0} = 6 \times 10^{27}, \kappa_{e} = \frac{k}{10}$, $\Gamma = 20, g_{WD} = 1000000 \text{and} B_0 = 10^6$.

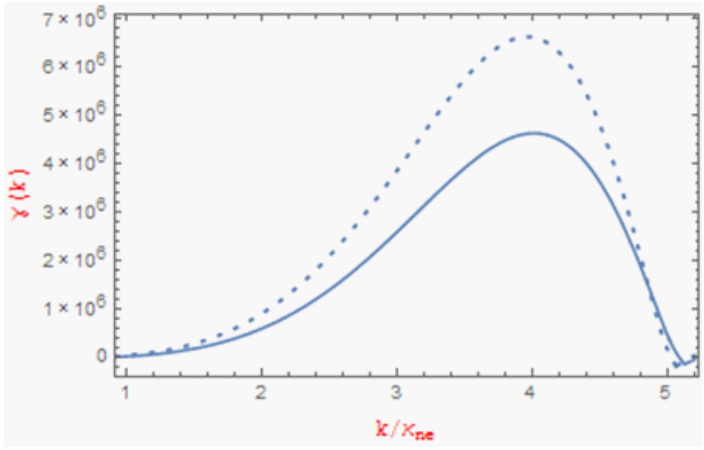

Figure 2-9: Normalized growth rate$\frac{\gamma}{\Omega_{ci}}$ versus normalized wavenumber$\frac{k}{\kappa_{ne}}$ (given by 2.38)in EPI quantum magnetoplasma for different values of electron concentration i.e. $n_{e0} = 6 \times 10^{27}$ (solid curve) and $n_{e0} = 6.5 \times 10^{27}$ (dashed curve). Other Physical parameters are taken as, $n_{p0} = 10^{27}, \kappa_{e} = \frac{k}{10}, \Gamma = 20, g_{WD} = 1000000$ and$B_0 = 10^6$.

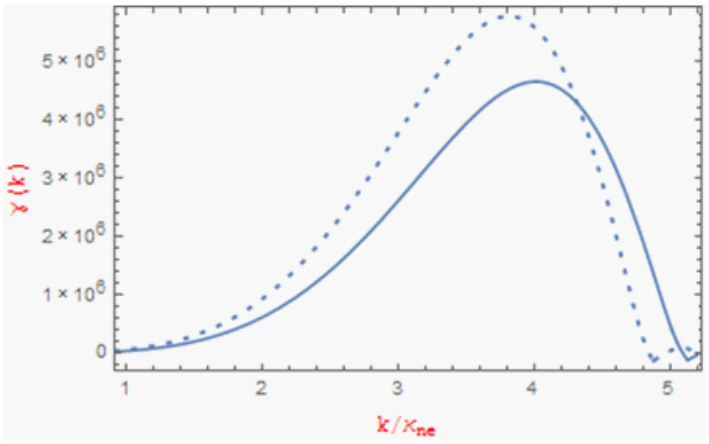

Figure 2-10: Normalized growth rate $\frac{\gamma}{\Omega_{ci}}$ *versus normalized wavenumber* $\frac{k}{\kappa_{ne}}$ *(given by.2.38) in EPI quantum magnetoplasma for different values of magnetic field i.e.* $\Omega_c = 10^8$ *(solid curve) and* $\Omega_c = 0.9 \times 10^8$ *(dashed curve). Other Physical parameters are taken as* $n_{p0} = 10^{27}, \kappa_e = \frac{k}{10}, \Gamma = 20, g_{WD} = 1000000$ *and* $n_e = 6 \times 10^{27}$.

2.9

2.10 Summary and Conclusion

To sum up, we studied the *RT* mode in EPI quantum magneto plasma which consisted of electron, positron and ion particles, both on analytical and numerical bases. We used the well known quantum hydrodynamic model where ions are dealt as being cold and classical while on the other hand positron and electrons are deemed quantum mechanical and inertialless with respect to their corresponding Fermi temperatures. A Generalized dispersion relation was derived, with in the frame work of the drift wave phenomena. The existence of positron turns this equation into the cubic form. In the clarified form , the real growth rate associated with the RT mode was examined with the effect of the concentration of positron. The well known Cardano's method was used to solve the cubic equation for the evaluation of real along with the imaginary roots of RT mode. It was unveiled that the growth rates , which are derived by Cardano's method for RT mode is increasing with the increase in electron density while it decreased with the increase of the magnetic field (Bo) and the concentration of the positrons

. In this chapter the examples of celestial body (like white dwarf) are also discussed , which clearly demonstrates the presence of RT mode in EPI quantum magnetoplasma.

Chapter 3

Electrostatic Gravitational Instability in Multi-Ion Dense Quantum Magnetised Plasma

In this chapter we investigate Electrostatic Gravitational or Rayleigh-Taylor (RT) instability in an in homogeneous pair-ion-electron quantum magnetised plasma consisting of negative and positive ions with electrons. A well defined Dispersion relation is derived obeying approximation of drift wave. The presence of negative ions with their different streaming velocities turns dispersion relation into a cubic. Different roots associated with the real and the imaginary parts of the RT mode are studied by using the Cardano method it is further shown RT instability varies for magnetic field density.

Classical plasma usually have low densities and are very hot. But modern technology has made us able to create a comparatively dense plasma, such type of plasma could not be illustrated thoroughly by the classical mechanic laws and hence quantum mechanics laws will be employed. As compared to the classical plasma, Quantum plasma posses the characteristics of having the high number density with low temperature, there are numerous examples in the nature in which both the plasma and quantum effects exists all together, like in the astrophysical environment (neutron stars, white dwarfs, magnatars etc.)[97] , in plasmas which are produced in intense laser beam [98], in nonlinear quantum optics [99, 100], in the microelectronic

devices[101] and many others. In the quantum regimes, the thermal de-Broglie wave length ($\lambda_{\mathtt{B}} = \frac{\hbar}{\mathtt{m}\ _{T}}$) asses the quantum degeneracy effects and illustrates the spatial extension associated with the wave function assigned to charged particles due to the quantum uncertainty[102, 103]. Such parameter should be of the order or more than average interferometric distance. In such a situation, the thermal energy turns out to be smaller as compared to the Fermi energy. consequently the electron Fermi pressure subjugates the thermal pressure at high number densities reinforcing the compact objects against the gravitational burst.

Two models, Wigner-Poisson and Schrödinger-Maxwell and are used for the manifestation of plasma quantum hydrodynamic along with its statistical behavior. Wigner-Poisson model is utilized for the interpretation of momentum, energy and transportation of charge while on the other hand Schrödinger-Poisson model is retained to manipulate other issues just like negative differential resistances and resonant tunneling in the semiconductor physics etc.[104]. There recently has been an escalation in the fascination of dense Q plasma see the Refs.[103, 104, 105, 106, 107, 108, 109, 110, 111]. Together all these studies incorporate the effects of quantum corrections like,spin magnetizationm, Fermi pressure,Bohm–de Broglie potential, the zero temperature and relativistic temperature degeneracy like properties which can remarkably improve the dynamics of the plasma. On the other side, dense pair-ion or multi-ions plasma at laboratory level has just recently been created [112, 113] and various kinds of the nonlinear waves in such plasma has also been verified experimentally. However, the inclusion of other charged particles like dust particulates into pair-ion plasma in order to produce multi component plasmas obliging different types of nonlinear wave phenomena may also be predicted. Similarly the nonlinear spreading of dust ion-acoustic waves in multi-ion dense plasma system comprising of degenerate electrons, both positive and negative ions, arbitrary charged dust grains have been explored with effect of cosmology environments [114].

By using the QHD model the transmission of small and finite-amplitude quantum electrostatic shock wave in a symmetric pair (ion) inertialess plasma with immobile background were studied by[115]. The ion-acoustic waves in a degenerate multi-ion magnetoplasma with requisition of astrophysical plasmas of the white dwarf have been explored by[116], by manipulating the hydrodynamic equations of negative and positive ions, and the Poisson equation, along with degenerate electrons. Hydrodynamic equations along with the Poisson equation are used to

investigate the Dust-ion-acoustic solitary waves in a cohesionless pair ion dense plasma which contain positive and negative ions, fraction of stationary charged (positive or negative) dust grains and degenerate electrons[117].

The above literatures mostly emphasis on perturbations in the background of quantum plasma. However, quantum plasmas could often involve nonuniform density outline, when dealt on practical bases, which normally happens in a real (e.g. in astrophysics) or effective (e.g. in inertial confined fusion) external gravitational field. In classical regime, a stratified plasma in a gravitational field definitely presents either internal waves or the Rayleigh-Taylor (RT) instability relying on whether the stratification is stable or un stable [118]. Rayleigh-Taylor instability is the surface instability which occurs between two fluids when their mutual densities are dissimilar and accelerates toward each other. This is the instability in which heavy fluid is supported by light fluid layer .

In early stage it was concluded that for RT instability amplitude, perturbations develops exponentially with time at the interface[119]. Goldston along with Rutherford studied linear growth rate of the RT instability for limited equilibrium flow [120], while Wu et al. [121] studied it in the presence of horizontal magnetic field. Bhatia and Sharma [122] described RT mode with horizontal magnetic field along with spinning. The RT instability and dispersion relation is defined in non uniform magnetic quantum plasma[123], which displays that RT mode is stabilized by quantum correction . For an ideal incompressible plasma the effects of quantum pressure along with magnetic field on RT instability were also investigated[124], with the clear cut appearance of linear growth rate in the presence of fixed boundary conditions. The electrostatic RT mode produced in the dense EI quantum magnetoplasma was studied[125] , where ions are Considered to be cold and classical while electrons being dense and quantum mechanical. It is displayed that the gradient of density along with quantum speed vary remarkably for the of RT mode instability growth rate. in contrast to the classical case , the RT instability growth rate is outstandingly higher and highly confined in Q plasma .

The inspiration of the present work is based on a few of the observation and predictions of dense muti-ions plasma in the environment of dense astrophysical objects, like it is observed and assumed that the electron–positron or proton and anti proton pairs in the white dwarfs can be created during the crumble of white dwarf into neutron stars [126, 127]. The surplus of

antiproton and positron fluxes are also estimated[128, 129] and then reported with observations [130]by supernova in the white dwarf environment .

Now keeping in view the importance of above literature on dense multi-ions plasmas we explore the electrostatic RT instability by utilizing the QHD model of quantum multi-ion-electron plasma. Our this work might be helpful in exploring various features of analysis of electrostatic instability on laboratory level and also in dense astrophysical plasmas where two well defined groups of ions and Fermi distributed electrons are there [114].

3.1 Basic Formulation and Instability Analysis

For the present calculations, Consider multi-ion dense quantum magnetized plasma with the in homogeneity gradient. A very high electron number density is possessed by Astrophysical entity(e,i, white dwarfs . $n \simeq 10^{29} cm^{-3}$)and consequently, the average distance between the particles is much smaller and posses large momentum exhibiting a degenerated Fermi gas. In such a vicinity the degenerate inertialess electrons are well described by Thomas fermi approximation[117]. The ion component could be treated as a classical gas [116]. The background quasi neutrality conditions is given as

$$n_{+0} = n_{\mathsf{e}0} + n_{-0}, \tag{3.1}$$

Where $n_{\pm 0}$ denotes the positive/negative ions density, while $n_{\mathsf{e}0}$ is the background number density of electron. The applied magnetic field is projected along the z-axis i.e. $\mathbf{B}_0 = B_0 \hat{z}$, where B_0 **denotes** the strength of applied magnetic field. Let for this problem we assume that equilibrium, the density gradient and the gravitational field are alighned in opposite direction, i.e. $\partial_{\mathsf{x}} n_{0\mathsf{j}} = -|\nabla n_{0\mathsf{j}}|\,\hat{x}$ and $\mathbf{g} = g\hat{x}$ with $j = +,-$, e is denoting the positive, negative ions and electrons respectively. The wave propagation vector and electric field are assumed to be directed in $y$direction i.e. $\tilde{\mathbf{k}} = k\hat{y}$ and $\tilde{\mathbf{E}} = E\hat{y}$. To look into the problem of RT mode of instability in a dense pair-ion-electron quantum plasma, we consider the following QHD model i.e. the continuity and momentum equations

$$\partial_{\mathsf{t}} n_{\mathsf{j}} + \boldsymbol{\nabla} \cdot (n_{\mathsf{j}}\, \tilde{\mathbf{V}}_{\mathsf{j}}) = 0 \tag{3.2}$$

$$m_{\mathsf{j}}\, n_{\mathsf{j}}\, (\partial\frac{\partial}{\partial t} + \tilde{\mathbf{V}}_{\mathsf{j}}\, \cdot \nabla)\tilde{\mathbf{V}}_{\mathsf{j}} = q_{\mathsf{j}}\, n_{\mathsf{j}}\, (\tilde{\mathbf{E}} + \tilde{\mathbf{V}}_{\mathsf{j}}\, \times \mathbf{B}_0) + m_{\mathsf{j}}\, n_{\mathsf{j}}\, \mathbf{g} - \boldsymbol{\nabla}\vec{P}_{\mathsf{j}} + Q, \tag{3.3}$$

Where m_{j} , $\mathbf{g}$,q_{j} , n_{j} and $\tilde{\mathbf{V}}_{\mathsf{j}}$ are denoting the mass of particle, acceleration due to gravity, charge ,density and velocity of the jth species respectively, and $\hbar$ is the Planck's constant divided by 2π, here $Q = \frac{\mathsf{n}_j\hbar^2}{2\mathsf{m}_j}\boldsymbol{\nabla}\left(\frac{\nabla^2\sqrt{n_{\mathsf{j}}}}{\sqrt{n_{\mathsf{j}}}}\right)$ represents the Bohm Potential . The quantum force term i.e. the last two terms of (3.3) appear due to quantum mechanical effects of the jth specie and denote the quantum correlation between fluctuations of density and quantum Fermi statistics. Equation of state for The degenerate electrons is given as $P_{\mathsf{Fe}} = \frac{(3\ \ ^2)^{\frac{2}{3}}}{5\mathsf{m}_e}\hbar^2 n_{\mathsf{e}}^{\frac{5}{3}}$ [3.3]. and the pressure gradient force $\nabla P_{\mathsf{Fe}} = 2\epsilon_{_{Fe}}\nabla n_{\mathsf{e}}$ with $\epsilon_{_{Fe}} = (3\pi^2 n_{\mathsf{e0}})^{\frac{2}{3}}\hbar^2/2m_{\mathsf{e}}$ is basically the electron Fermi energy on Fermi surface. Furthermore due to lighter mass of electrons compared to ions we presume that the quantum mechanical effects are skipped for both the positive and negative ions so Eq. (3.3) for cold $\pm$ ions could be written as

$$m_{\pm}n_{\pm}(\frac{\partial}{\partial t} + \tilde{\mathbf{V}}_{\pm}\cdot\nabla)\tilde{\mathbf{V}}_{\pm} = \pm en_{\pm}\left(\tilde{\mathbf{E}} + \tilde{\mathbf{V}}_{\pm}\times\mathbf{B}_0\right) + m_{\pm}n_{\pm}\mathbf{g}, \tag{3.4}$$

Under the equilibrium condition the $\pm$ ions drift is given as

$$\tilde{\mathbf{V}}_{\pm 0} = \mp\frac{g}{\omega_{\mathsf{c}\pm}}\hat{y} \tag{3.5}$$

In above equation $\omega_{\mathsf{c}\pm} = eB_0/m_{\pm}$ represents the cyclotron frequency for both positive and negative ions. Similarly for electrons at zero order we have two drifts i.e. the gravitational drift

$$\tilde{\mathbf{V}}_{\mathsf{e0}} = \frac{g}{\omega_{\mathsf{e}}}\hat{y},$$

And the modified diamagnetic drift due to Fermi pressure and Bohm potential

$$\tilde{\mathbf{V}}_{\mathsf{De0}} = \left(-\frac{2\epsilon_{_{Fe}}}{eB_0}\kappa_{\mathsf{e}} + \frac{\hbar^2}{4eB_0m_{\mathsf{e}}}\frac{1}{n_{\mathsf{e0}}}\partial_{\mathsf{x}}^3 n_{\mathsf{e0}}\right)\hat{y} \tag{3.6}$$

Gravitational drift at zero order could be skipped in the limit $\dfrac{m_{\mathsf{e}}}{m_{\pm}} \to 0$. In diamagnetic drift , term due to the Bohm potential is excluded by the presumption that the in homogeneity scale

length is formidable than the Larmor radius, which reduces Eq.3.6 to

$$\tilde{\mathbf{V}}_{\mathsf{De0}} = -\frac{2\epsilon_{_{Fe}}}{eB_0}\kappa_{\mathsf{e}}\ \hat{y}$$

Here $\kappa_{\mathsf{e}} = \frac{1}{\mathsf{n}_{e0}}\frac{@}{@\mathsf{x}}n_{\mathsf{e0}}$ is an in homogeneity scale length of the density for electron and $\omega_{\mathsf{e}} = eB_0/m_{\mathsf{e}}$ being the electron gyrofrequency. By Following the strategy for low frequency ($\partial_{\mathsf{t}} << \omega_{\mathsf{c}\pm}$) electrostatic perturbations, the perpendicular first order components of the positive and negative ion fluid velocity are

$$\tilde{\mathbf{V}}_{\pm\perp} = \tilde{\mathbf{V}}_{\mathsf{E}} + \tilde{\mathbf{V}}_{\pm\mathsf{p}}, \tag{3.7}$$

where $\tilde{\mathbf{V}}_{\mathsf{E}}(= -\frac{1}{\mathsf{B}_0}\vec{E}\times\hat{z})$ represents the $E\times B$ drift while $\tilde{\mathbf{V}}_{\pm\mathsf{p}}(= \mp\frac{1}{!_{c\pm}}(\partial_{\mathsf{t}} + \tilde{\mathbf{V}}_{\pm0}\cdot\boldsymbol{\nabla})(\tilde{\mathbf{V}}_{\pm1}\times\hat{z}))$ depicts the appropriate polarization drifts of both the positive and negative ions. The $\tilde{\mathbf{V}}_{\mathsf{E}}$ and $\tilde{\mathbf{V}}_{\pm\mathsf{p}}$ drifts can be further be simplified

$$\tilde{\mathbf{V}}_{\mathsf{E}} = -\frac{\vec{E}_{\mathsf{y}}}{B_0}\hat{x}, \tilde{\mathbf{V}}_{\pm\mathsf{p}} = \pm\frac{1}{\omega_{\mathsf{c}\pm}}\left(\partial_{\mathsf{t}} + \mathbf{V}_{\pm0}\cdot\boldsymbol{\nabla}\right)\left(\frac{\vec{E}_{\mathsf{y}}}{B_0}\right)\hat{y} \tag{3.8}$$

In the above equations $\vec{V}_{\pm0}$ stands for drift velocity of both the positive and negative ions . The equation of motion for Fermionic electrons in linearized form is given is

$$m_{\mathsf{e}}n_{\mathsf{e0}}(\partial_{\mathsf{t}}\frac{\partial}{\partial t} + \tilde{\mathbf{V}}_{\mathsf{e0}}\cdot\nabla)\tilde{\mathbf{V}}_{\mathsf{e}} = -en_{\mathsf{e0}}(\tilde{\mathbf{E}} + \tilde{\mathbf{V}}_{\mathsf{e}}\times\mathbf{B}_0) - 2\epsilon_{_{Fe}}\boldsymbol{\nabla}n_{\mathsf{e1}} + Q_1 \tag{3.9}$$

Where the exact manifestation of the first order of the Bohm term in Eq. (3.9) could be interpreted as

$$P_1 = \frac{\hbar^2}{2}\frac{1}{m_{\mathsf{e}}}\left[\begin{array}{c} \frac{1}{2}\nabla.\left(\nabla^2 n_{\mathsf{e1}}\right) - \frac{\boldsymbol{\nabla}n_{\mathsf{e0}}\left(\nabla^2 n_{\mathsf{e1}}\right)}{2n_{\mathsf{e}}} - \frac{\boldsymbol{\nabla}n_{\mathsf{e1}}\left(\nabla^2 n_{\mathsf{e0}}\right)}{2n_{\mathsf{e}}} + \frac{n_{\mathsf{e1}}\boldsymbol{\nabla}n_{\mathsf{e}}\left(\nabla^2 n_{\mathsf{e0}}\right)}{2n_{\mathsf{e}}^2} - \frac{\boldsymbol{\nabla}\left(\boldsymbol{\nabla}n_{\mathsf{e}}\cdot\boldsymbol{\nabla}n_{\mathsf{e1}}\right)}{2n_{\mathsf{e}}} \\ + \frac{n_{\mathsf{e1}}\boldsymbol{\nabla}\left(\nabla n_{\mathsf{e0}}\right)^2}{4n_{\mathsf{e}}^2} + \frac{\left(\nabla n_{\mathsf{e0}}\right)^2\boldsymbol{\nabla}n_{\mathsf{e1}}}{2n_{\mathsf{e}}^2} - \frac{\left(\boldsymbol{\nabla}n_{\mathsf{e}}\right)^3}{n_{\mathsf{e}}^3}n_{\mathsf{e1}} + \frac{\left(\boldsymbol{\nabla}n_{\mathsf{e}}\cdot\boldsymbol{\nabla}n_{\mathsf{e1}}\right)}{n_{\mathsf{e}}^2}\boldsymbol{\nabla}n_{\mathsf{e}} \end{array}\right] \tag{3.10}$$

In Eq.3.10 only the first and the second terms could be able to contribute, while all the others are abandoned due to our geometry selection and by supposition that Larmour radius is less than in homogeneity scale length. Because of this deduction all the higher order derivatives for in homogeneity terms are omitted. Also since polarization drift vary directly with inertia,

it could be omitted for electrons i.e. $\vec{V}_{\mathsf{e}} = 0$. So by applying the approximation of the drift wave $\omega << \omega_{\mathsf{e}}$, the momentum equation for electrons along with the magnetic field could be simplified by omitting the inertial term appearing on the left-hand side of Eq3.9. Thus from 3.9, the linear perpendicular component of velocity for the Fermionic electron is

$$\tilde{\mathbf{V}}_{\mathsf{e}\perp} = \frac{1}{B_0}(\vec{E}\times\hat{z}) + \frac{2\epsilon_{_{Fe}}}{eB_0}\frac{1}{n_{\mathsf{e}}}\boldsymbol{\nabla} n_{\mathsf{e}1}\times\hat{z} - \frac{P_1}{eB_0 n_{\mathsf{e}}}\times\hat{z} = \left(\frac{\vec{E}_{\mathsf{y}}}{B_0} + \frac{2\epsilon_{_{Fe}}}{eB_0}\frac{\nabla_\perp n_{\mathsf{e}1}}{n_{\mathsf{e}}} - \frac{\hbar^2}{4eB_0}\frac{1}{n_{\mathsf{e}}\, m_{\mathsf{e}}}\nabla_\perp(\nabla^2 n_{\mathsf{e}1})\right)\hat{x} + \left(\frac{2\epsilon_{_{Fe}}\kappa_{\mathsf{e}}}{eB_0}\frac{\nabla_\perp n_{\mathsf{e}1}}{n_{\mathsf{e}}} - \frac{\hbar^2\kappa_{\mathsf{e}}}{4eB_0 m_{\mathsf{e}}}\frac{\nabla^2 n_{\mathsf{e}1}}{n_{\mathsf{e}}}\right)\hat{y} \tag{3.11}$$

The linearized electron continuity equation is

$$\partial_{\mathsf{t}} n_{\mathsf{e}1} + \boldsymbol{\nabla}\cdot(n_{\mathsf{e}}\tilde{\mathbf{V}}_{\mathsf{e}}) = 0 \tag{3.12}$$

Where linearized $\boldsymbol{\nabla}\cdot(n_{\mathsf{e}}\tilde{\mathbf{V}}_{\mathsf{e}})_1$ can be written as

$$\boldsymbol{\nabla}\cdot(n_{\mathsf{e}}\tilde{\mathbf{V}}_{\mathsf{e}})_1 = \boldsymbol{\nabla}_\perp n_{\mathsf{e}1}\cdot\tilde{\mathbf{V}}_{\mathsf{D}\mathsf{e}0} + \boldsymbol{\nabla}_\perp n_{\mathsf{e}0}\cdot\tilde{\mathbf{V}}_{\mathsf{e}\perp} + n_{\mathsf{e}0}\boldsymbol{\nabla}_\perp\cdot\tilde{\mathbf{V}}_{\mathsf{e}\perp} = \frac{2\epsilon_{_{Fe}}\kappa_{\mathsf{e}}}{eB_0}\nabla_\perp n_{\mathsf{e}1} - \frac{\hbar^2\kappa_{\mathsf{e}}}{2eB_0 m_{\mathsf{e}}}\nabla^2 n_{\mathsf{e}1} + \partial_{\mathsf{x}} n_{\mathsf{e}0}\hat{x}\cdot\frac{\vec{E}_{\mathsf{y}}}{B_0} \tag{3.13}$$

Due to the presence of diamagnetic drift, electron background drifting term is appearing in Eq. (3.13). We have neglected the term $n_{\mathsf{e}1}(\boldsymbol{\nabla}\cdot\mathbf{V}_{\mathsf{e}0})$ in Eq. (3.13) by assuming that a constant electron-streaming velocity is not a function of space. Similarly for $\pm$ ions the linearized continuity equation can be written as

$$\partial_{\mathsf{t}} n_{\pm1} + \left(\tilde{\mathbf{V}}_{\pm0}\cdot\boldsymbol{\nabla}\right) n_{\pm1} + \partial_{\mathsf{x}} n_{\pm0}\hat{x}\cdot\tilde{\mathbf{V}}_{\mathsf{E}} + n_{\pm0}\boldsymbol{\nabla}\cdot\tilde{\mathbf{V}}_{\pm\mathsf{p}} = 0 \tag{3.14}$$

Presuming a plane wave solution , which is of the form $\exp(iky - i\omega t)$ to all perturbed quantities, and also by using the drift approximation $(\omega - kV_{\pm0}) < \omega_{\mathsf{c}\pm}$ in the Eqs. (3.7)-(3.14), we then get the number density for both the positive and negative ions as

$$n_{\pm1} = \frac{-in_{\pm0}}{\omega_{\pm\mathsf{D}}}\left(\kappa_{\mathsf{n}\pm} \pm \frac{k\omega_{\pm\mathsf{D}}}{\omega_{\mathsf{c}\pm}}\right)\left(\frac{\vec{E}_{\mathsf{y}}}{B_0}\right) \tag{3.15}$$

Where $\omega_{\pm\mathsf{D}} = \omega - k\vec{V}_{.\pm0}$ is Doppler shifted frequency and $\kappa_{\mathsf{n}\pm} = \frac{1}{\mathsf{n}_{\pm0}}\partial_{\mathsf{x}} n_{\pm0}$ denotes the inverse in homogeneity scale length associated with the negative and positive ions. The electron

continuity Eq. (3.12) leads to the density of perturbed electron as

$$n_{e1} = -i\frac{n_{e0}\kappa_B}{\left(\omega - \frac{k\kappa_B\ \vec{V}_q^2}{\omega_{c+}}\right)}\left(\frac{\vec{E}_y}{B_0}\right) \tag{3.16}$$

The existence of quantum Bohm potential and quantum Fermi pressure creates a modified quantum speed $\vec{V}_q = \left(Y_q^2\ + \frac{\hbar^2 k^2}{2m_e m_j}\right)^{1=2}$ with the definition of well known quantum acoustic speed $Y_q\ = \left(\frac{2\epsilon_{Fe}}{m_+}\right)^{1=2}$ [66]. **Under the assumption $k\lambda_{Fe} \ll 1$ we may formulate the perturbed quasi neutrality condition as**

$$n_{+1} \simeq n_{e1} + n_{-1}, \tag{3.17}$$

Avoiding the Poisson equation [124]. This is possible because the unstable waves posses low frequencies. Let $\omega_c = \omega_{c-} = \omega_{c+}$ because of the same mass of $\pm$ ions. Using Eqs.(3.15) and (3.16) in Eq.(3.17) we get a generalized dispersion relation as

$$\frac{n_{+0}}{\omega_{+D}}\frac{k\omega_{+D} + \omega_c\kappa_{n+}}{\omega_c} = \frac{n_{-0}}{\omega_{-D}}\frac{\omega_c\kappa_{n-} - k\omega_{-D}}{\omega_c} + \frac{n_{e0}\kappa_B}{(\omega - k\vec{V}_*)}, \tag{3.18}$$

Where $V_* = \frac{\kappa_B\ \vec{V}_q^2}{\omega_c}$ denotes the quantum corrected modified diamagnetic drift velocity. Relation (3.13) narrates that the streaming of both the positive and negative ions , along with their densities, and the quantum nature of electrons have streamlined the relation quite outstandingly. In the absence of negative ions we have

$$\omega\left(\omega - k.\vec{V}_{+0}\right) = -\kappa_B\ \omega_c\vec{V}_{+0} + \kappa_B\ \vec{V}_q^2\left(\kappa_B\ + \frac{k\left(\omega - k.\vec{V}_{+0}\right)}{\omega_c}\right), \tag{3.19}$$

Which is identically the same as eq3.10 of [124], for RT Mode in the electron-ion quantum plasma.

Now Let us consider the case where positive and negative ions are being drifted with constant speed comparative to electrons. This scenario is identical to the case of electron beam , which propagates in a pair-ion plasma. Let $\vec{V}_{+0} = \vec{V}_{-0} = \vec{V}_0$, then for this particular condition the

Eq. (3.18) turns into the following quadratic equation

$$\omega^2+\omega k\left(\frac{g}{\omega_{\mathsf{c}}}-\frac{\kappa_{\mathsf{B}}\ \vec{V}_{\mathsf{q}}^2}{\omega_{\mathsf{c}}}\right)-\frac{g\kappa_{\mathsf{B}}}{1+N_{-0}}\left[N_{\mathsf{e}0}\left(1+\frac{\kappa_{\mathsf{B}}\ \vec{V}_{\mathsf{q}}^2}{g}\right)+\frac{k^2\vec{V}_{\mathsf{q}}^2}{\omega_{\mathsf{c}}^2}\left(1+N_{-0}\right)\right]=0, \tag{3.20}$$

With $N_{-0}=\frac{\mathsf{n}_{-0}}{\mathsf{n}_{+0}}$, and $V_0=-\frac{\mathsf{g}}{!_c}$, $N_{\mathsf{e}0}=\frac{\mathsf{n}_{e0}}{\mathsf{n}_{+0}}$Eq. (3.20) Being the desired enhanced dispersion relation for the electrostatic RT instability in a dense quantum pair-ion-electron magnetized plasma. By omitting the quantum effects ($\hbar\to 0$) , $N_{-0}\to 0$, one can get the earlier result of [65]. Instability is most likely to happen when ω is complicated(complex) i.e. by using $\omega=\omega_{\mathsf{r}}+i\gamma$ in Eq. (3.20) then for both the real and imaginary parts we get

$$\omega_{\mathsf{r}}=-\frac{k}{2}\left(\frac{g}{\omega_{\mathsf{c}}}-\frac{\kappa_{\mathsf{B}}\ \vec{V}_{\mathsf{q}}^2}{\omega_{\mathsf{c}}}\right) \tag{3.21}$$

$$\gamma=\left[-\frac{g\kappa_{\mathsf{B}}}{1+N_{-0}}\left\{N_{\mathsf{e}0}\left(1+\frac{\kappa_{\mathsf{B}}\ \vec{V}_{\mathsf{q}}^2}{g}\right)+\frac{\left(1+N_{-0}\right)k^2\vec{V}_{\mathsf{q}}^2}{\omega_{\mathsf{c}}^2}\right\}+\frac{k^2}{4}\left(\frac{\kappa_{\mathsf{B}}\ \vec{V}_{\mathsf{q}}^2}{\omega_{\mathsf{c}}}-\frac{g}{\omega_{\mathsf{c}}}\right)^2\right]^{\frac{1}{2}} \tag{3.22}$$

It depicts that RT mode would evolve if g and κ_{B} posses opposite signs , means both should be in the opposite directions. This indicates that the light fluid is holding the heavy fluid; otherwise, ω is not imaginary but real and the plasma is stabilized. Since the magnetic field supports the heavy plasma against the gravitational force, so the effects of magnetic field curvature could be modeled by the use of g. The gravitational force here is acting like centrifugal force which rotates the particle in curvature. Therefore it is observed here that the instability is depending on the sign of curvature. This sets a stabilizing trend in plasma , and vice versa [124].

By using the small k or long wavelength approximation the second term in Eq. (3.22) is ignored and the growth rate for RT mode of instability can be obtained as

$$\gamma=\left[-\frac{g\kappa_{\mathsf{B}}}{1+N_{-0}}\left\{N_{\mathsf{e}0}+\left(1+N_{-0}\right)k^2\rho_{\mathsf{s}}^2\left(1+\frac{k^2H_{\mathsf{e}}^2\lambda_{\mathsf{F}\,\mathsf{e}}^2}{4}\right)\right\}+\frac{N_{\mathsf{e}0}\kappa_{\mathsf{B}}^2\ Y_{\mathsf{q}}^2}{1+N_{-0}}\left(1+\frac{k^2H_{\mathsf{e}}^2\lambda_{\mathsf{F}\,\mathsf{e}}^2}{4}\right)\right]^{\frac{1}{2}} \tag{3.23}$$

Similarly the real part of the wave frequency can be obtained as

$$\omega_{r} = -\frac{k}{2}\left[\frac{g}{\omega_{c}} - \frac{\kappa_{B}\ Y_{q}^{2}}{\omega_{c}}\left(1 + \frac{k^{2}H_{e}^{2}\lambda_{Fe}^{2}}{4}\right)\right] \tag{3.24}$$

During the derivation of Eqs. (3.23) and (3.24) we have expressed the quantum speed U_{q} in terms of the quantum parameter (H_{e}) and Fermi length (λ_{Fe}) of electron as $U_{q} = Y_{q}\ \left(1 + \frac{k^{2}H_{e}^{2}\ {}^{2}_{Fe}}{4}\right)^{1=2}$, where $H_{e} = \dfrac{\hbar\omega_{p}}{2\epsilon_{_{Fe}}}$ shows the effect of density interaction and gives the ratio between plasmon energy and the Fermi energy while $\lambda_{Fe} = \sqrt{\frac{2\ _{Fe}}{4\ n_{e0}e^{2}}}$ sketches the Fermi screening length. Also $\rho_{s}(= Y_{q}\ /\omega_{c})$ exemplify the ion-sound gyro radius. By using the normalized parameters such as $\acute{\gamma} = \dfrac{\gamma}{\omega_{c}}$, $\acute{\omega}_{r} = \dfrac{\omega_{r}}{\omega_{c}}$, $\acute{g} = \dfrac{g\kappa_{B}}{\omega_{c}^{2}}$, $\acute{k} = \dfrac{k}{\kappa_{B}}$, $\acute{\rho}_{s} = \dfrac{\kappa_{B}\ Y_{q}}{\omega_{c}}$, and $\tilde{\lambda}_{Fe} = \kappa_{B}\ \lambda_{Fe}$, we can express Eqs. (3.23) and (3.24) in normalized form as

$$\acute{\gamma}\left(\acute{k}\right) = \left[-\frac{\acute{g}}{1+N_{-0}}\left\{N_{e0} + (1+N_{-0})\,\acute{k}^{2}\acute{\rho}_{s}^{2}\left(1 + \frac{\acute{k}^{2}H_{e}^{2}\acute{\lambda}_{Fe}^{2}}{4}\right)\right\} + \frac{N_{e0}\acute{\rho}_{s}^{2}}{1+N_{-0}}\left(1 + \frac{\acute{k}^{2}H_{e}^{2}\acute{\lambda}_{Fe}^{2}}{4}\right)\right]^{\frac{1}{2}} \tag{3.25}$$

$$\acute{\omega}_{r} = -\frac{\acute{k}}{2}\left[\acute{g} - \acute{\rho}_{s}^{2}\left(1 + \frac{\acute{k}^{2}H_{e}^{2}\acute{\lambda}_{Fe}^{2}}{4}\right)\right] \tag{3.26}$$

3.2 RT Instability Analysis

In order to discuss the instability analysis by manipulating both the positive and negative ions (drifting), we are introducing the phase velocity defined $\vec{V}_{\cdot} = \dfrac{\omega}{k}$ which makes the Eq. (3.18) as

$$\frac{\omega_{c}}{1+N_{-0}}\left(\frac{N_{-0}\kappa_{n-}}{\vec{V}_{\cdot} - \vec{V}_{+0}} - \frac{\kappa_{n+}}{\vec{V}_{\cdot} - \vec{V}_{-0}} + \frac{N_{e0}\kappa_{B}}{\vec{V}_{\cdot} - \vec{V}_{*}}\right) = k^{2}$$

This may be expressed as

$$G\left(\vec{V}_{\cdot}\right) = \frac{\omega_{c}}{1+N_{-0}}\left(\frac{N_{-0}\kappa_{n-}}{\vec{V}_{\cdot} - \vec{V}_{-0}} - \frac{\kappa_{n+}}{\vec{V}_{\cdot} - \vec{V}_{+0}} + \frac{N_{e0}\kappa_{B}}{\vec{V}_{\cdot} - \vec{V}_{*}}\right) = k^{2} \tag{3.27}$$

Since this equation is of third order and carry real coefficients, there would be three solutions for $\vec{V}_{\cdot}$ with complex nature. It is perceived that k has some real value, which is labeled as k_{c}. For $k_{c}^{2} < k^{2}$ Eq. (3.27) has three real roots so that the system reinforce three waves which

disseminate without decay or growth. On the other hand, if $k_c^2 > k^2$, Eq. (3.27) has two complex roots and one real. The two complex roots complementary to complex frequencies. Since these frequencies are complex conjugates, one of them will be referred to a mode that grows exponentially with time. Hence even a tiny perturbation of the system will result into arbitrarily large values. One can find the value of k_c by finding the value of $\vec{V}_p$ for which $\frac{dG}{dV_p} = 0$. If the drifts have the same magnitude with opposite sense, we may adopt

$$G\left(V_p\right) = \frac{\omega_c}{1+N_{-0}}\left(\frac{N_{-0}\kappa_{n-} - \kappa_{n+}}{\vec{V}_p - \vec{V}_0} + \frac{N_{e0}\kappa_e}{\vec{V}_p - \vec{V}_*}\right) = k^2 \tag{3.28}$$

And $\frac{dG}{dV_p} = 0$ gives critical phase speed as

$$\vec{V}_{p,c} = \frac{\vec{V}_*\sqrt{\kappa_{n+} - N_{-0}\kappa_{n-}} - \vec{V}_0\sqrt{N_{e0}\kappa_e}}{\sqrt{\kappa_{n+} - N_{-0}\kappa_{n-}} - \sqrt{N_{e0}\kappa_e}} \tag{3.29}$$

Hence we find that

$$k_c^2 = \frac{\omega_c}{1+N_{-0}}\frac{\left(\sqrt{\kappa_{n+} - N_{-0}\kappa_{n-}} - \sqrt{N_{e0}\kappa_e}\right)^2}{\vec{V}_0 - \vec{V}_*} \tag{3.30}$$

We see that (3.30) has a peculiar significance. Our physical intuition tells us that as $(\vec{V}_0 - \vec{V}_*)$ becomes arbitrarily small,and k_c becomes arbitrarily large. This shows that the system becomes unstable for a larger range of wave number. Also k_c depends on N_{-0}, κ_n and ω_c which effectuate the system to be stable or unstable.

Further simplification of (3.30) with the definitions of Eq. (3.5) i.e. $V_{+0} = -\frac{g}{!_c}$ and $V_{-0} = \frac{g}{!_c}$ gives the following form of cubic equation

$$\vec{V}_p^3 - \vec{V}_p^2\vec{V}_* - \vec{V}_p\left(\frac{g^2}{\omega_c^2} + \frac{N_{e0}\kappa_e}{1+N_{-0}}\frac{\omega_c\vec{V}_*}{k^2} + \frac{\kappa_{n+}+N_{-0}\kappa_{n-}}{1+N_{-0}}\frac{g}{k^2}\right) + \frac{\vec{V}_* g^2}{\omega_c^2} + \frac{\kappa_{n+}+N_{-0}\kappa_{n-}}{1+N_{-0}}\frac{\vec{V}_* g}{k^2} + \frac{N_{e0}\kappa_e}{1+N_{-0}}\frac{g^2}{k^2\omega_c} = 0$$

In terms of ω we arrive to the following form of normalized cubic equation

$$\acute{\omega}^3 + A\acute{\omega}^2 + B\,\acute{\omega} + C = 0 \tag{3.31}$$

Where the normalized constants $\tilde{a}$, $\tilde{b}$ and $\tilde{c}$ all are real and are defined as

$$A = -\acute{k}.\acute{\rho}_{\mathsf{s}}^2\left(1+\frac{\acute{k}^2 H_{\mathsf{e}}^2 \acute{\lambda}_{\mathsf{Fe}}^2}{4}\right) \tag{3.32}$$

$$B = -\left(\acute{k}\acute{g}\right)^2 - \acute{\rho}_{\mathsf{s}}^2\left(\frac{N_{\mathsf{e}0}}{1+N_{-0}}\right)\left(1+\frac{\acute{k}^2 H_{\mathsf{e}}^2 \acute{\lambda}_{\mathsf{Fe}}^2}{4}\right) - \acute{g}.\eta \tag{3.33}$$

$$C = \acute{k}\acute{g}^2\left[\frac{N_{\mathsf{e}0}}{1+N_{-0}} + \frac{\acute{\rho}_{\mathsf{s}}^2}{\acute{g}}\eta\left(1+\frac{\acute{k}^2 H_{\mathsf{e}}^2 \acute{\lambda}_{\mathsf{Fe}}^2}{4}\right) + \acute{k}^2\acute{\rho}_{\mathsf{s}}^2\left(1+\frac{\acute{k}^2 H_{\mathsf{e}}^2 \acute{\lambda}_{\mathsf{Fe}}^2}{4}\right)\right] \tag{3.34}$$

Where $\eta = \dfrac{\kappa_{\mathsf{n}+} + N_{-0}\kappa_{\mathsf{n}-}}{\kappa_{\mathsf{e}}\ (1+N_{-0})}$.

By using Cardano method we shall discuss the analysis of the RT mode by using Eq. (3.31). In order to address the instability process let $\omega = \omega_{\mathsf{r}} + i\gamma$ (omit the tilt sign). This is possible if some of the roots are complex, where $\omega_{\mathsf{r}} = \mathrm{Re}\,(\omega)$ and $\gamma = \mathrm{Im}\,(\omega)$. Positive $\mathrm{Im}\,(\omega)$ shows a wave (with exponential growth rate) ,while negative $\mathrm{Im}\,(\omega)$ illustrates a damped wave. Since roots ω are occurring in the conjugate pairs, one shall always be unstable unless all roots are real. Damped roots are not self-excited and are of no use. With this manipulation and assumption that $\gamma^2 << \omega_{\mathsf{r}}^2$ Eq. (3.31) is decomposed to real and imaginary parts as

$$\omega_{\mathsf{r}1}^3 + A\omega_{\mathsf{r}}^2 + B\omega_{\mathsf{r}} + C \simeq 0 \tag{3.35}$$

$$\gamma \approx \sqrt{3\omega_{\mathsf{r}}^2 + 2A\omega_{\mathsf{r}} + B} \tag{3.36}$$

From Eqs. (3.35) and (3.36), it is evident that for three real roots of ω_{r}, we have three growth rates; two shows damping trend while one shows growth. In order To find that root of ω_{r} for which γ shows a growing trend we solve (3.35) with the help of Cardano method. Let $\omega_{\mathsf{r}} = \dot{z} - \dfrac{\dot{a}}{3}$ $\Rightarrow \dot{z} = \omega_{\mathsf{r}} + \dfrac{\dot{a}}{3}$, the equation then reduces to reduced cubic equation having no second degree term i.e.

$$\dot{z}^3 + X\dot{z} + Y = 0, \tag{3.37}$$

Where $P = \frac{1}{3}(3.\dot{b}^2 - \dot{a}^2)$, $Q = \frac{1}{27}(2.\dot{a}^3 - 9.\dot{a}.\dot{b} + 27.\dot{c})$. By using the Cardano's rule as given in [134], the root of Eq. 3.37 can be written by following the procedure

$$\dot{z} = [\sqrt{X^2+Y^2} - Y]^{\frac{1}{3}} - [\sqrt{X^3+Y^2} + Y]^{\frac{1}{3}} \tag{3.38}$$

If we assume the numerical values of constants in such a way that $X^3 + Y^2 < 0$, the solution for z is then

$$\dot{z} = -2\sqrt{-X}\cos\left[\frac{1}{3}\arctan\left(\frac{\sqrt{-X^3 - Y^2}}{Y}\right)\right] \tag{3.39}$$

Using P, Q and $\dot{z} = \omega_{\mathsf{a}} + \frac{\mathsf{A}}{3}$ in (3.39) we then determine the root of ω_{r} as

$$\omega_{\mathsf{r}} = -\frac{A}{3} - 2\sqrt{\frac{1}{3}(A^2 - 3B^2)}\cos\left[\frac{1}{3}\arctan\left(\frac{\sqrt{-\frac{1}{27}(3B^2 - A^2)^3 - \frac{1}{729}(2A^3 - 9.AB + 27C)^2}}{\frac{1}{27}(2A^3 - 9AB + 27C)}\right)\right] \tag{3.40}$$

We could obtain other roots but this is giving the growing rate root so we reckon only this root. For this ω_{r} we can get the required growth rate as given in (3.36).

3.3 Results and Discussion

In order to contemplate the complete scenario of the quantum effects that comprises of the Pauli exclusion and the Bohm potential tunneling across , Fermi pressure upon RT mode growth rate. The Eqs. (3.25), (3.26) and (3.36) are resolved numerically. For the numerical analysis we use the values as given [47, 68]. white dwarf, having number density,$\sim 10^{28}$ cm^{-3} and $B_0 = \left(10^8 - 10^{14}\right)$G [136]. Such an astrophysical domain, has a very high number density of the electrons, and as a result degenerate inertialess electrons should be described and one can hypothesized the existence of multi-ions, as classical gas. Although this choice is evidently counterintuitive, but is persuaded by the above astrophysical objects environment, and are being suggested by [114, 116].

When both of the ions have same drifting magnitude of velocity, the growth rate as given in (3.25) is then explaining the RT instability in muti-ions quantum plasma. In order to explore the impact of Bohm potential along with the Fermi degenerate pressure on the RT instability we analyzed numerically the (3.25). In Fig 3.1. the vertical axis (horizontal axis) illustrates

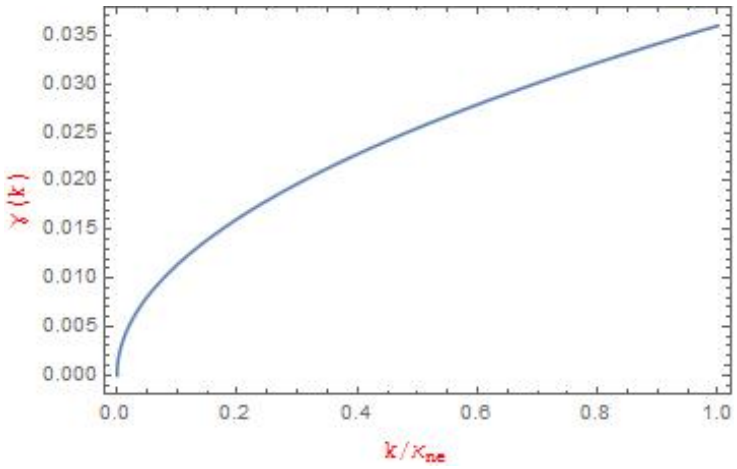

Figure 3-1: (Color online): Variation of the normalized growth rate γ/ω_c versus the scaled wave number k/κ_e (Eq. (3.25)) in muti-ions magnetoplasma with classical limit ($H_e = 0$). Other parameters are taken as $n_e = 10^{28}$ cm^{-3}, $n_{+0} = 1.01 \times 10^{28}$ cm^{-3} and $B_0 = 10^8$G.

the normalized growth rate $\gamma = 10^{-28}\gamma$ (normalized wave number k) of the RT mode in pair-ion-electron quantum plasma and manifest the classical counterpart of quantum plasma. It demonstrates that the growth rate of RT mode enhances with the normalized k. The effects of density discrepancy and magnetic field strength on the growth rate of RT mode are shown respectivley in Fig.?? and ??. The instability shows increasing (decreasing) trend with the variation of density (magnetic field).

When positive and negative ions are drifting with different velocity $\vec{V}_{\pm 0} = \mp \frac{g}{\omega_{c\pm}} \hat{y}$, the real frequency ω_r as a function of k is numerically examined from Eq. (3.16) for various values of the electron number density and magnetic fields, which are shown in Figs3.3, and 3.4 respectively. Fig 3.3 shows that when values of n_e are increased real frequency ω_r decreases, showing decreasing trend against k. While on the other hand, ω_r is increased depicting increasing trend, when B_0 are gradually been increased as shown in Fig3.4.

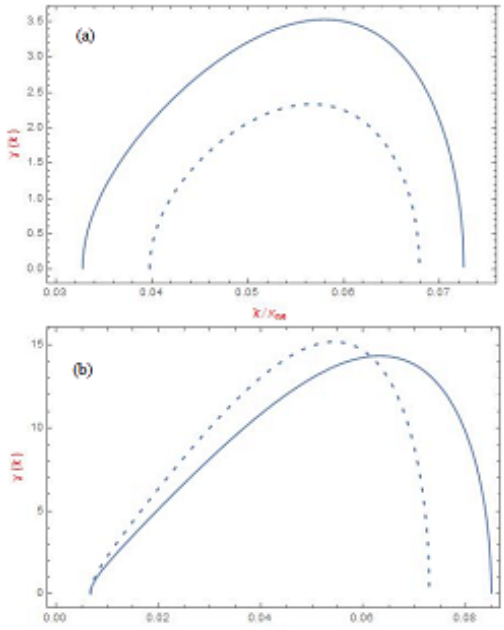

Figure 3-2: (Color online): Plot of the normalized growth rate (γ/ω_c) (Eq. (**??**)) as a function of wavenumber (k/κ_e) in a PIE quantum magnetoplasma with (a) density variation i.e. $n_e = 10^{28}$ (solid curve) and $n_e = 0.8 \times 10^{28}$ (dashed curve) (b) magnetic field variation i.e. $\omega_c = 10$ (solid curve) and $\omega_c = 8$ (dashed curve). Other Physical parameters are the same as in Fig. 3.1

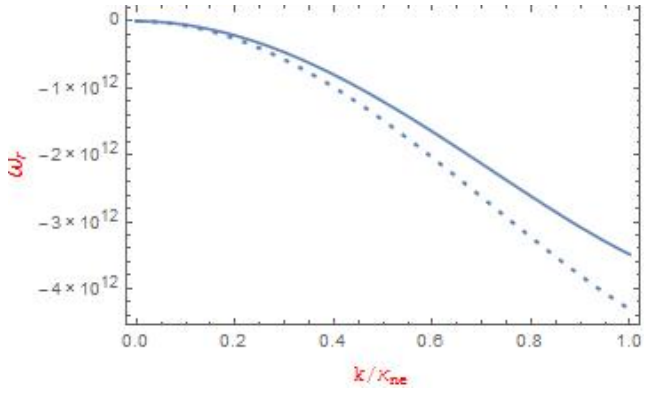

Figure 3-3: (Color online): Sketches of ω_r as a function of wave vector k for different values of n_e using Eq. 3.40 such that $n_e = 10^{28}$ (solid curve) and $n_e = 0.5 \times 10^{28}$ (dashed curve). Other Physical parameters are taken as $\kappa_e = \frac{k}{10}$, $\eta = 0.8$, $g_{WD} = 1000000$ and normalized $\omega_c = 10$.

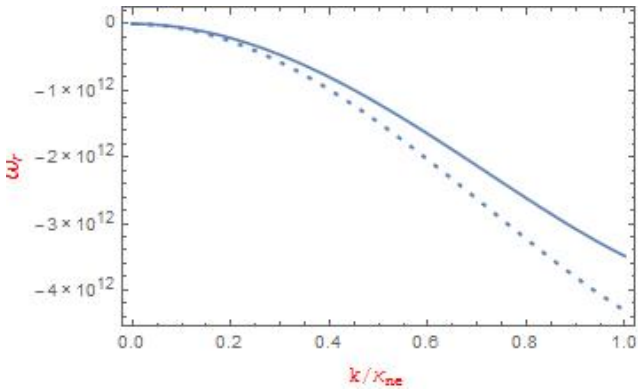

Figure 3-4: (Color online): Variation of real frequency 3.40as a function of k for different values of of magnetic field, such that $\omega_{\mathsf{c}} = 10$ (solid curve) and $\omega_{\mathsf{c}} = 9$ (dashed curve). Other Physical parameters are the same as in Fig. 3 with $n_{\mathsf{e}} = 10^{28}$.

RT mode is explicated by the growth rate with in multi-ion-electron quantum plasma. By utilizing coefficients(normalized) (3.32)- (3.34) the growth rate(normalized) (3.16) is being plotted for the electrostatic RT mode with the variation of magnetic field along with density and ambient magnetic field. Fig. 3.5 (Fig.3.6) depicts that the growth rate is increasing (decreasing) by increase in the number density (magnetic field B_0). So the instability is suppressed by magnetic field, the particles are confined more in at center than at corners. Also the ω_{c} is greater than the wave frequency so by increasing B_0 makes this comparison more clear and ultimately the growth rate is decreased. On the other side when the number density is increased, the plasma turns more dense and is shrunked which marks the availability of more particles also, wave perturbation is given more energy as $\frac{\mathsf{I}}{\mathsf{k}} < V_{\mathsf{Fe}}$. And consequently the growth rates are increased , and the RT mode is made more unstable.

3.4 Conclusion

To summarize, we had studied numerous growth rates of R–T mode in the nonuniform PI quantum plasma. Which fragments are positive , negative ions, with a hint of electrons. Quantum hydrodynamic equations are being engaged with presumptions that both the ions are classical and cold. While the electrons have no inertia and are being treated as quantum mechanical. A optimized dispersion relation has been obtained with in the frame work os the drift wave

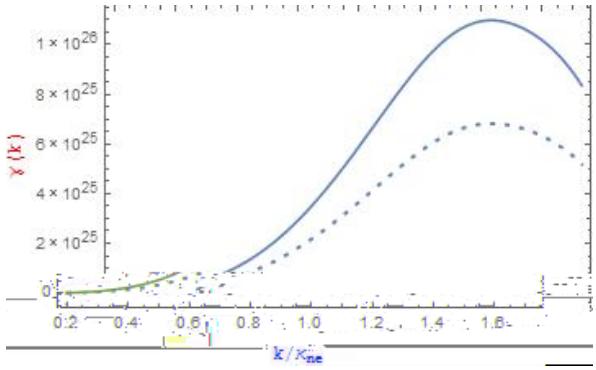

Figure 3-5: (Color online): Normalized growth rate (γ/ω_c) versus normalized wavenumber (k/κ_e) [given by (3.36)] for different values of electron density variation i.e. $n_e = 10^{28}$ (solid curve) and $n_e = 0.7 \times 10^{28}$ (dashed curve). Other Physical parameters are the same as in Fig.3.3.

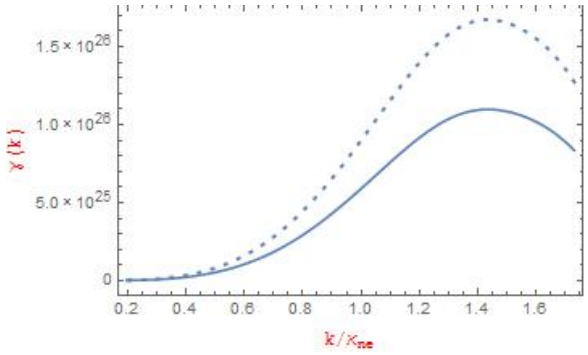

Figure 3-6: (Colour online): Normalized growth rate (γ/ω_c) versus normalized wavenumber (k/κ_e) [given by (3.36)] for different values of magnetic field variation i.e. $\omega_c = 10$ (solid curve) and $\omega_c = 9$ (dashed curve). Other Physical parameters are the same as in Fig. 3 with $n_e = 10^{28}$.

approximation and are explored both on analytical and numerical bases. With presumption that, when both ions have same drift velocity, the growth rate (3.23) is derived with effects of both classical and quantum phenomenons. The existence of negative ions with their different drift velocities turn the dispersion relation into a cubic equation. Using the Cardano method for the solution of cubic equation, we obtain a root for both the real and imaginary modes of the wave associated with RT mode. Dispersion relation is obtained from the real part and the growth rate of the RT mode is obtained from the imaginay part. The growth rate of RT instability is explored in detail with the variation of density and the magnetic field. It is deduced that quantum speed and density gradient are improving due to density variation and hence RT mode is modified significantly. It is shown that growth rate of the R–T mode in a nonuniform multi-ions quantum plasma increases (decreases) with density (magnetic field B_0). Our findings are general and could be helpful in understanding the RT imode in the celestial objects or future laboratory experiments. It is anticipated that in future a highly magnetized dense multicomponent plasmas will be produced at laboratory level . Thus the the findings mentioned in this chapter could be helpful to study dense magneto plasmas on both astrophysical and laboratory level.

Chapter 4

Drift Instabilities In an In Homogeneous Kappa Distributed Ambiplasma

In the present chapter, four component ambiplasma which consists of the positive , negative ion along with the electron and the positron is evaluated using fluid model. Coupled with drift modes produced as a result of applied magnetic field are explored by deriving its dispersion relation, in the first case. And in 2nd case coupled drift solitons are explored using a well known kdv burger equation in non linear regime neglecting dissipation effect. The results are further plotted using one of the most effective hyperbolic trigonometric function in Wolfram Mathematica™. Also considering non thermality of ambi plasma in the space, kappa distributed function was utilized in such type of problems.

Most of the times when we talk about plasma we say that plasma might consist of the two components, that is completely ionized(most of the time) is assumed to carry out experimental and more specifically theoretical research [138, 139]. Any way actual plasma ,that is produced in various experiments, also which is assumed for the theoretical calculations, and naturally occuring plasma that exist in the earth ionosphere is not simple in practical sense but rather multicomponent. Even if we consider the simple case of generation of the hydrogen for the fusion process, the plasma contained with in the chamber is not 100 percent real hydrogen

gas in ionic form along side the electrons but it is accompanied by the impurities which are emitted the radiation chamber. This ultimately changes the plasma prameters to a greater extent [140]. Ambiplasma is relatively new type of multicomponent plasma that consists of positive(negative ions) with electrons and positrons, the interest in this field was motivated by Metagalaxy concept introduced in early 60s by klein[141]. This theory of multicomponent plasma is also an outstanding contendant to understand the creation of universe along side big bang theory, the reason being that it could be traced in early universe that is suppose to be containing matter and antimatter equally. it is still believed that both of the regions , that contained matter(anti matter) were separated widely , more interestingly at boundary line , matter is mixed with anti-matter regions thus a kind of buffer zone is created , such a region is termed as the ambiplasma [142]. with the passage of time new and new advancement were made in this Ambi plasma theory and the introduction of asymmetry principle of the universe of matter and antimatter set a new mile stone in understanding the symmetry of the cosmic ambi plasma. So according to this theory the universe is made up of cloud of the ambiplasma, which posses an extremely asymmetric nature, more over the portion of anti matter is very less [143].

The data obtained from spacecraft has attributed the non thermal particle behavior particularly at very high regions in the solar wind. It also exists in many other plasma occurring space [144]. Most often such distribution function exists those regions of space where density is low density, in mathematical terminology kappa distribution is used to deal with particles having such velocity distribution functions [145]. This mathematical technique usually used to highlight such type of plasmas where there are more particles are at high energy as that of lower energy particles at equilibrium state [146].

Much of the attention has been paid to area, and many as many scientist made remarkable achievements in this field. these include Summers and Thorne [147, 148, 149], Helberg and Mace [150, 151] also characterized electrostatic waves that are emerging in the anisotropic Kappa/Maxwellian plasma. Zaheer and Murtaza [152] had also investigated the (anistropic)Non-Maxwellian distribution functions.

Many particles plasma can also have transport properties, transport properties are due to drift. Sagdeev and rudakov were the irst one to have predicted these type of waves [153] D

'Angelo and Motley varified these drift waves on Expermental bases just a few years back [154]. Literally speaking inhomogenious slots in magnetised plasma are responsible for the generation of these perturbations.

In inhomogenious linearised plasma transport phenomena mostly occurs due to coupled drift perturbations (specifically in low frequencey regime) [155]. The type of waves are most oftenly termed as ion drift instabilities, and these exist in a low pressure inhomogenious plasma which is ,inside an in a homogenious magnetic field [156, 157].

In inhomogenious multicomponent plasma certein nonlinear structures just like shocks , solitons and vortics may also occur depending on the type of perturbation produced [158]. It is also very well clear that the plasma with density inhomogenety and temperature gradient may also give rise to drift solitons having finite amplitude. The Main charatesitic of the drift solitons is that solitons are structures that could sustain its shape while moving , these expands in a space due to the dispersion, therefore these solitons are also termed as the non spreading structures [159]. The most important drift soliton is rossby(soliton). The shocks were for first time noticed in the laboratory by [160]. These shocks were been viewed in the thin layer of liquid that rotates, more over it constitutes long living un spreading anti cyclone. The shock may exists in the astrophysical field as well. Shocks are mostly occurring in collissional plasma e,g in our atmosphere and also in interstellar space, which is collisionless media . In daily life on observatory bases these are also being observed in sky around covering supersonic aircrafts, and in the supernovae in interstellular environment , planetary,cometary and galactic bow shocks, the events termed as (IP) events[161]

Now owing to the significance of ambiplasmas, current work emphasises on investigating both linear coupled drift modes along with non linear structures just like shock along with the soliton in non thermal and anti Maxwellian collisional ambi plasma. Now in order to get into the accessibility of the ambiplasma for the transport properties, coupled drift solitons are further explored.

4.1 Mathematical Formulation

For this problem we pressume , four component inhomogeneous magnetised Ambi plasma which consist of the positive along negative ions, and non-thermal distributed laptons with non-thermal distribution function. Such kind of particles obeys the kappa distribution function, this kind of distribution function is used for both the linear calculation as well as the nonlinear transmission of the coupled drift ion waves. The magnetic field $\mathbf{B_0}$ is always uniformally kept and is normall along z-direction $\mathbf{B_0} = B_0\hat{z}$. We further pressumed that the density gradient to be alighned along on x-axis i.e. $n_{j\,0} = n_{j\,0}(x)$. Resultant electrostatic mode Usually propagates around both of the y , z-axes i.e. wave vector posses the following shape (0, k_y, k_z). In low frequency regime becaus, of the inhomogenity in density, and obliqueness inside plasma, two kinds of modes (drift and acoustic) that usually are in coupling state, propagates. We explore the same coupled modes obying the condition *(i,e)* $k_y > k_z$ in first portion, and non linear structures (solitons and shock) second part of our work. The set of equations could be written as

$$\partial_t \mathbf{v_j} + (\mathbf{v_j} \cdot \boldsymbol{\nabla})\mathbf{v_j} = -\frac{e\boldsymbol{\nabla}\phi}{m_j} \pm \Omega_j\,(\mathbf{v_j} \times \hat{z}) - \nu_{jn}\ \mathbf{v_j} \tag{4.1}$$

$$\partial_t n_j + \boldsymbol{\nabla} \cdot (n_j\,\mathbf{v_j}) = 0, \tag{4.2}$$

In the above equation subscript j is used particularly for $+(-)$ ion. Quantities , $\mathbf{v_j}$, n_j , m_j represent respectively fluid velocity, number density and the mass associated with jth species of ions and the ϕ being wave function associated with the potential. The collisional oscillations associated with jth specie of the ions along with the neutrals is illustrated through the variable ν_{jn} . here $\Omega_j = \dfrac{eB_0}{m_j\,c}$ is the cyclotron frequency of the positive(negative) ion(s). We will solve this problem with quazi neutrality condition.

$$n_{+0} + n_{p0} = n_{-0} + n_{e0}, \tag{4.3}$$

In the above equation n_{p0} , n_{+0}, n_{-0}, n_{e0} being the corresponding densities of , positron,

positive ions, negative ions and the number densities of electrons(positron) respectively. Neutrality condition for various charges can be reformulated as , $\mu_p = 1-\mu_+ +\mu_-$, where $\mu_p = \frac{n_{p0}}{n_{e0}}$, $\mu_+ = \frac{n_{+0}}{n_{e0}}$ and $\mu_- = \frac{n_{-0}}{n_{e0}}$. When we applly the magnetic field along z-direction in perpendicular direction, the polarization drift and $\vec{E}\times\vec{B}$ are generated along x and y- axis respectively. The Perpendicular part associated with the velocity of Eq. (4.1) in the low frequency regime $\frac{d}{dt} << \Omega_\pm$ are $v_{j\perp} = v_E + v_p + v_c$,here first term indicates the $E\times B$ drift , while 2nd term is indicating the polarization drift similarly the last one indicates the collisional drift with their values are given as $\frac{1}{B_0}(z\times\nabla\phi)$, $-\frac{1}{B_0\Omega_j}\frac{d}{dt}(\boldsymbol{\nabla}_\perp\phi)$, $\frac{v_j}{B_0\Omega_j}\boldsymbol{\nabla}_\perp\phi$ respectively. We have used the electrostatic field approximation i.e. $\tilde{\mathbf{E}} = -\boldsymbol{\nabla}\phi$. For perturbations, under low the frequencey (in contrast to the ion gyro frequency Ω_j) parallel components of the fluid velocities of the beyons are described by

$$\left(\frac{\partial}{\partial t} + \mathbf{v}_z \cdot \boldsymbol{\nabla} + \nu_n\right)\mathbf{v}_z = \mp\frac{e}{m}\frac{\partial\phi}{\partial z} \tag{4.4}$$

The continuity equation (4.2) along with using of the values of the v_E, v_p and v_c could be narrated in following form.

$$\frac{\partial n_j}{\partial t} = \frac{n_{j0}}{B_0}k_n\ \boldsymbol{\nabla}_\perp\phi \pm \frac{n_{j0}}{B_0\Omega_j}\frac{d}{dt}(\boldsymbol{\nabla}_\perp^2\phi) \pm \frac{n_{j0}v_c}{B_0\Omega_j}\boldsymbol{\nabla}_\perp^2\phi - n_{j0}\frac{\partial}{\partial z}v_z \ , \tag{4.5}$$

Where $k_n = \frac{1}{n_{j0}}\frac{@}{@x}(n_{j0})$ is density scale(inverse inhomogenety) length. When the Poisson's equation is differentiated with the time and , by using charge neutrality condition, could be arranged in the following form

$$\partial_t\nabla^2\phi = -4\pi e n_{e0}\left[\mu_+\partial_t\left(\frac{n_+}{n_{+0}}\right) - \mu_-\partial_t\left(\frac{n_-}{n_{-0}}\right) + \mu_p\partial_t\left(\frac{n_p}{n_{p0}}\right) - \partial_t\left(\frac{n_e}{n_{e0}}\right)\right] \tag{4.6}$$

The natural co-existence of the ambiplasma can be linked through astro physics. The theory says that there is a region which is separating the matter from the anti matter it is like a buffer zone. Data which is Observed from space craft also confirmed non thermal behavior with in the space and the outer regions. Literature belonging to astrophysics and the space physics ,

well known kappa distribution function could be narrated as

$$f_0(v) = \frac{n_{\mathrm{e,p}\ 0}}{(\kappa\pi)^{3=2}\,\theta_{\mathrm{e,p}}^3}\,\frac{\Gamma\left[\kappa_{\mathrm{e,p}}\ +1\right]}{\Gamma\left[\kappa_{\mathrm{e,p}}\ -1/2\right]}\left[1+\left(1+\frac{v_{\mathrm{e,\ p}}^2}{\kappa_{\mathrm{e,p}}\ \theta^2}\pm\frac{2e\phi}{m\theta_{\mathrm{e,p}}^2}\right)\right]^{-(\ +1)} \tag{4.7}$$

Where $\theta = \left[(2\kappa-3)/2\kappa\right]^{1=2} v_{\mathrm{T\,e,p}}$ illustrate effective thermal(thermal) speed which have spectral index i,e $\kappa > 3/2$, $v_{\mathrm{T\,e,p}} = \sqrt{\frac{2\mathrm{k}_B\mathrm{T}_{e,p}}{\mathrm{m}}}$ is thermal speed,$n_{\mathrm{e,p}\ 0}$ is particles number density in equilibrium, $\Gamma(x)$ highlights the gamma function, $T_{\mathrm{e,p}}$ being the temperature associated with positron and electron similarly m being the mass associated with concerned particles. If the spectral index κ tends to ∞, then above distribution is reduced the pure to Maxwellian form. We have pressumed the similar sinario in here, which is adopted for amiplasma with the non-thermal distributions of the electrons along with the positrons. By Integrating the kappa distribution function of (4.7) . Then it further gives number density of the electrons along with the positrons as following

$$n_{\mathrm{e}} = n_{\mathrm{e0}}\left[1-\frac{e\phi}{K_{\mathrm{B}}T_{\mathrm{e}}(\kappa_{\mathrm{e}}-\frac{3}{2})}\right]^{-\ _e+\frac{1}{2}} \tag{4.8}$$

$$n_{\mathrm{p}} = n_{\mathrm{p0}}\left[1+\frac{e\phi}{K_{\mathrm{B}}T_{\mathrm{p}}(\kappa_{\mathrm{p}}-\frac{3}{2})}\right]^{-\ _p+\frac{1}{2}} \tag{4.9}$$

Eqs. (4.8) and (4.9) under the assumption $\frac{\mathrm{e}}{\mathrm{k}_B\mathrm{T}_e} << 1$ and $\frac{\mathrm{e}}{\mathrm{k}_B\mathrm{T}_p} << 1$ can be expanded as

$$n_{\mathrm{e}} = n_{\mathrm{e0}}\left[1+c_1\left(\frac{e\phi}{k_{\mathrm{B}}T_{\mathrm{e}}}\right)+c_2\left(\frac{e^2\phi^2}{k_{\mathrm{B}}^2T_{\mathrm{e}}^2}\right)\right] \tag{4.10}$$

$$n_{\mathrm{p}} = n_{\mathrm{p0}}\left[1+c_1\left(\frac{e\phi}{k_{\mathrm{B}}T_{\mathrm{e}}}\right)+c_2\left(\frac{e^2\phi^2}{k_{\mathrm{B}}^2T_{\mathrm{e}}^2}\right)\right], \tag{4.11}$$

In the above equations the nonlinearities are retained upto the second order. More over the terms of higher order are being ignored. In here $c_1 = \frac{_e+\frac{1}{2}}{_e-\frac{3}{2}}$, $c_2 = \frac{(\ _e+\frac{1}{2})(\ _e-\frac{1}{2})}{(\ _e-\frac{3}{2})^2}$, $c_3 = \frac{_p+\frac{1}{2}}{_p-\frac{3}{2}}$and $c_4 = \frac{(\ _p+\frac{1}{2})(\ _p-\frac{1}{2})}{(\ _p-\frac{3}{2})^2}$. Using . (4.5), (4.10) and (4.11) in Eq. (4.6), we obtain nonlinear equation in the following form.

$$A\frac{\partial\phi}{\partial t}+\frac{e\ D}{2k_{\mathsf{B}}T_{\mathsf{e}}}\frac{\partial\phi^2}{\partial t}-\lambda_{\mathsf{De}}^2\frac{\partial}{\partial t}\nabla^2\phi-\rho_{\mathsf{i}}^2\left(\mu_+\frac{d}{dt}+\mu_-\frac{d}{dt}\right)\nabla_\perp^2\phi-V_{*\mathsf{m}}\nabla_\perp\phi-\rho_{\mathsf{i}}^2\nu_{\mathsf{n}}\nabla_\perp^2\phi$$

$$+4\pi e\lambda_{\mathsf{De}}^2\frac{\partial}{\partial z}\left(n_{+0}v_{\mathsf{z}+}-n_{-0}v_{\mathsf{z}-}\right)=0, \tag{4.12}$$

Where $A=\left(c_1+c_3\mu_{\mathsf{p}}\frac{\mathsf{T}_e}{\mathsf{T}_p}\right)$, $D=\left(c_2-c_4\mu_{\mathsf{p}}\frac{\mathsf{T}_e^2}{\mathsf{T}_p^2}\right)$, $\rho_{\mathsf{i}}=\frac{\mathsf{C}_{si}}{\Omega_j}$ is larmor radius of jth ion species. C_{s} $(=\sqrt{\frac{\mathsf{K}_B\mathsf{T}_e}{\mathsf{m}_i}})$ is the acoustic speed associated with both the positive, negative ions, $\lambda_{\mathsf{De}}=\sqrt{\frac{\mathsf{K}_B\mathsf{T}_e}{4\ \mathsf{n}_{e0}\mathsf{e}^2}}$is the debye length associated with the electron. $\nu_{\mathsf{n}}=\nu_{+\mathsf{n}}\mu_++\nu_{-\mathsf{n}}\mu_-$ is the collisional frequencies(densities weighted) and $V_{*\mathsf{m}}=V_{+*}\mu_++V_{-*}\mu_-$ (with $V_{\mathsf{j}*}=\pm\frac{\mathsf{K}_B\mathsf{T}_e}{\mathsf{e}\ \ 0}k_{\mathsf{j}}$) is the diamagnetic drift velocity(combined) associated with the both of the positive along with the negative ions(in combined form). Parallel components associated with the velocity from the Eq. (4.4) in the weak nonlinearity limit and weak dispersion could be narrated as

$$\frac{\partial v_{\mathsf{j}}}{\partial t}+v_{\mathsf{j}}\ \frac{\partial}{\partial z}v_{\mathsf{j}}\ =\mp\frac{e}{m_{\mathsf{i}}}\frac{\partial\phi}{\partial z} \tag{4.13}$$

The linear along with the nonlinear profiles of the coupled drift (electrostatic) modes in the non uniform plasma having inertial effects of the negative and positive ions accompanied by (kappa) distributions of the positrons and electrons , are being illustrated by the Eqs. (4.12) , (4.13). In order to expand the properties of the plasma in linear regime, lets consider , perturbations that propagates in the yz plane and having ω frequencey which is form of the $\exp[i(k_{\mathsf{y}}y+k_{\mathsf{z}}z-\omega t)$ by linearizing Eqs. (4.12) and (4.13), we then get linear dispersion relation of the following form

$$\omega^2\left[A+\lambda_{\mathsf{De}}^2k^2+(\mu_++\mu_-)\rho_{\mathsf{i}}^2k_{\mathsf{y}}^2\right]-\omega\omega_*+i\omega\rho_{\mathsf{i}}^2v_{\mathsf{n}}k_{\mathsf{y}}^2-c_{\mathsf{s}}^2\left(\mu_++\mu_-\right)k_{\mathsf{z}}^2=0, \tag{4.14}$$

Where $\omega_*=-k_{\mathsf{y}}V_{*\mathsf{m}}$. In the absence of the collisional term, the dispersion relation could be formulated as

$$\omega^2\left[A+\lambda_{\mathsf{De}}^2k^2+(\mu_++\mu_-)\rho_{\mathsf{i}}^2k_{\mathsf{y}}^2\right]-\omega\omega_*-c_{\mathsf{s}}^2\left(\mu_++\mu_-\right)k_{\mathsf{z}}^2=0 \tag{4.15}$$

The term containing k_z^2 in (4.15) arise becaus of the parallel motion to the magnetic field, and term which contains $\rho_i^2 k_y^2$ is originating from polarization drift of the ions. In absence of the concentration of the positron (i.e., $n_{p0} \to 0$) and Maxwellian distributed electrons (i.e., $c_1 \to 1$), then the A in (4.15) is equal to unity.

Further more when we omit the concentration of negative ion. (i.e., $\mu_- \to 0$), it reduces to $\omega^2(1 + \lambda_{De}^2 k^2 + \rho_i^2 k_y^2) - \omega\omega_* - c_s^2\, k_z^2 = 0$, which is showing the dispersion relation associated with the low frequency longitudinal drift modes in an Ion electron plasma.

In order to evaluate generation of the nonlinear structures(coherent) which are in shape of shocks and the solitons, We are introducing the stationary frame which is of the form $\chi = y + \theta z - ut$, that moves with the velocity u along the $yz-$plane. The angle of the wave front θ which is directing from the $z-$axis is coupling with both of the ion acoustic waves and the ion drift waves. We extend the order of nonlinearities upto the second. Eq. (4.13) after the transformation with application of the stationary frame of reference , results in

$$v_{iz} = \pm\frac{e\theta}{mu}\phi + \frac{\alpha}{2u}\left(\frac{e\theta}{mu}\right)^2 \phi^2 \tag{4.16}$$

Also by the transformation of the Eq. (4.12) through the χ and utilising values of v_{iz} from Eq. (4.16), we obtain nonlinear equation , when we ignore the third order nonlinearities(4.17-4.19)

$$\left(\lambda_{De}^2 + \rho_m^2\right)\frac{d^3\phi}{d\chi^3} + \left[C_s^2\,\frac{e\theta}{2um_i}\left(\frac{\theta}{u}\right)^3(\mu_+ - \mu_-) - \frac{eD}{2k_B T_e}\right]\frac{d\phi^2}{d\chi} - \left(\frac{\rho_m^2}{u}\nu_n\right)\frac{d^2\phi}{d\chi^2}$$

$$- \left(A + \frac{V_{*m}}{u} - C_m^2\,\frac{\alpha^2}{u^2}\right)\frac{d\phi}{d\chi} + \left[\rho_i^2(\mu_+ - \mu_-)\frac{e\theta}{m_i u^2}\right]\phi\frac{d^3\phi}{d\chi^3} = 0, \tag{4.17}$$

Where $\rho_m^2 = \rho_i^2(\mu_+ + \mu_-)$ and $C_m^2 = C_s^2\,(\mu_+ + \mu_-)$. The second along with the last term are the nonlinear terms having the different differential order in the eq (4.17). The last term could be ignored as compared to second term, becaus of the following reasons. Let suppose that ratio between the nonlinear and the characteristic length for low frequency wave is $\phi^2/l \backsim \varepsilon$. where $\varepsilon < 1$, then $\left(\phi^2/l^3\right) << 1$. Similarly for the long wavelength (weak dispersion) regime we have supposed that $\rho_i k << 1 \Rightarrow \rho_i << l$, then under this approximation $\left(\rho_i^2\phi^2/l^3\right) <<< 1$. Hence Eq. (4.17) could be written in following form

$$\left(\lambda_{\mathsf{De}}^2+\rho_{\mathsf{m}}^2\right)\frac{d^3\phi}{d\chi^3}+\left[C_{\mathsf{s}}^2\,\frac{e\theta}{2um_{\mathsf{i}}}\left(\frac{\theta}{u}\right)^3(\mu_+-\mu_-)-\frac{eD}{2k_{\mathsf{B}}T_{\mathsf{e}}}\right]\frac{d\phi^2}{d\chi}-\left(\frac{\rho_{\mathsf{m}}^2}{u}\nu_{\mathsf{n}}\right)\frac{d^2\phi}{d\chi^2}$$

$$-\left(A+\frac{V_{*\mathsf{m}}}{u}-C_{\mathsf{m}}^2\,\frac{\alpha^2}{u^2}\right)\frac{d\phi}{d\chi}=0 \tag{4.18}$$

Integrating (4.18) with for χ and then by using boundry conditions i.e., $\phi=0$ as $\chi\to\pm\infty$, we then obtaind equation of the following form.

$$\frac{d^2\phi}{d\eta^2}-F\frac{d\phi}{d\eta}+H\phi^2-L\phi=0, \tag{4.19}$$

with

$$F=\frac{\rho_{\mathsf{m}}^2\;\nu_{\mathsf{n}}}{u(\lambda_{\mathsf{De}}^2+\rho_{\mathsf{m}}^2\;)}$$

$$H=\frac{C_{\mathsf{s}}^2\,\frac{\mathsf{e}}{2\mathsf{m}}\left(-\right)^4(\mu_+-\mu_-)-\frac{\mathsf{D}}{2\mathsf{k}_B\mathsf{T}_e}}{\lambda_{\mathsf{De}}^2+\rho_{\mathsf{m}}^2}$$

$$L=\frac{A+\frac{\mathsf{V}_{*m}}{\mathsf{u}}-C_{\mathsf{m}}^2\quad\left(\frac{}{\mathsf{u}}\right)^2}{(\lambda_{\mathsf{De}}^2+\rho_{\mathsf{m}}^2\;)}$$

Using normalized quantities such as $\psi=\frac{\mathsf{e}}{\mathsf{K}_B\mathsf{T}_e}$ and $\xi=\frac{\mathsf{K}}{\;im}$,here K is a constant, which we would determine later, then Eq. (4.19) could be further be expressed in normalized form as follows

$$-\gamma\psi+\frac{1}{2}\psi^2-qK\frac{d\psi}{d\xi}+pK^2\frac{d^2\psi}{d\xi^2}=0 \tag{4.20}$$

With γ, q and p having the following values

$$\gamma=\frac{A+\delta-(\theta f\delta)^2(\mu_+-\mu_-)}{(\alpha f\delta)^4(1-\mu_{\mathsf{p}})-D}$$

$$q=\frac{\theta f\sigma(\mu_++\mu_-)}{(\theta f\delta)^4(1-\mu_{\mathsf{p}})-D}$$

$$p = \frac{\frac{2}{\frac{De}{2}} + 1}{(\theta f \delta)^4 (1 - \mu_p) - D}$$

Where $\delta = \frac{V_{*m}}{u}$, $f = \frac{C_{si}}{V_{*m}}$, and $\sigma = \frac{n}{\Omega_{ci}}$. Equation (4.20) being the transformed KdVBurger equation that represents nonlinear profiles of the obliquely propagating electr drift modes (here ion acoustic modes are being coupled with the drift modes) in magnetized plasma(collissional) having both of the positive along the negative ions, and nonthermal (kappa) distributions of positrons and electrons.

4.2 Shock Wave Solution

Equation (4.20) is the transformed KdVBurger equation having $C = 0$. We have followed Tanh-method [W. Malfleit and W. Hereman, Phys. Scr. 54, 563 (1996)] to find the shock solutions of Eq. (4.20) and also defining electrostatic potential $\psi(\xi)$(normalised) as under

$$\psi(\xi) = S(Y) = \sum_{n=0}^{N} a_n Y^n \tag{4.21}$$

With

$$Y = \tanh(\xi)$$

Then Eq. (4.20) could be narrated in terms of Y as

$-\gamma S(Y) + \frac{1}{2} S^2(Y) + pk^2(1 - Y^2) \left[-2Y \frac{\partial S(Y)}{\partial Y} + (1 - Y^2) \frac{\partial^2 S(Y)}{\partial Y^2} \right] - qk(1 - Y^2) \frac{\partial S(Y)}{\partial Y} = 0$

By substituting the Eq. (4.21) into the Eq. (**??**) and balancing highest power of Y, gives $N = 2$. Considering the possible solution $S(Y) = (1 - Y)T(Y)$ with $T(Y) = b_0(1 + b_1 Y)$ and substituting it in equation(**??**) with the limit $Y \to 1$(as $\xi \to \infty$), we then obtain value of γ in terms of the parameters p and q as

$$\gamma = 4pK^2 + 2qK \tag{4.22}$$

Using equation (4.22) and possible solution of $S(Y) = (1 - Y)T(Y)$ in the equation (**??**) turns out to be

$$K = \frac{q}{10p}$$

and expected solution of the Eq. (4.20) could be written in following form

$$\psi(\xi) = \frac{3}{2}\gamma \left[(1 - \tanh(\xi))(1 + \frac{1}{3}\tanh(\xi)\right] \tag{4.23}$$

with $\gamma = 24pk^2$.

4.2.1 Solution of Equation (4.20) for the Limiting Cases

In the absence of collisional term , dissipation coefficient tends to zero i.e., $q = 0$. So the Eq. (4.20) is reduced to the KdV(trnsformed) equation of following form

$$-\gamma\psi + \frac{1}{2}\psi^2 + pK^2\frac{d^2\psi}{d\xi^2} = 0 \tag{4.24}$$

the above equation illustrates the solitary wave solution (using the Tanh-method) of the following shape

$$\psi(\xi) = 3\gamma[1 - \tanh(\xi)][[1 + \tanh(\xi)], \tag{4.25}$$

With $\gamma = 4pK^2$. If dispersion coefficient tends to zero $p = 0$, then it represents that dissipation through the system is prevailing over the dispersive effects , then Eq. (4.20) is reduced to the transformed Burger's equation of the following form

$$-\gamma\psi + \frac{1}{2}\psi^2 - qK\frac{d\psi}{d\xi} = 0, \tag{4.26}$$

With the solution (using the Tanh-method) which represents the monotonic shock as under ,

$$\psi(\xi) = \gamma\left[1 - \tanh(\xi)\right], \tag{4.27}$$

With $\gamma = 2qK$.

4.3 Results and Discussion

In the current section, Eqs. (4.23), (4.25) along with (4.27) are analyzed numerically, these describe solutions of KdVBurger, KdV and Burger's equations(transformed) respectively. We would also like investigate that how nonlinear profiles of the obliquely propagating coupled drift waves are modified by density of protons and nonthermal distributions of the leptons . For the numerical analysis, we define the corresponding parameters are defind as $\mu_{\mathsf{p}} = 0.14, \frac{\mathsf{T}_e}{\mathsf{T}_P} = 3.33$, $\mu_+ = 1.43$, $\mu_- = 0.57$, $\theta = 0.9$, and $u = 0.4$ (where u being incontrast with C_{s}) compatible with parameter as in Ref. 4.18. In the figures contains, electrostatic potential $\psi(\xi)$ is being plotted as the function of ξ. Further more we also investigate the effects of various parameters on both width and amplitude of the electrostatic potential.

First of all in Fig.4.1 wave solution (shock) of the Eq. (4.23) is diagramed. In this solution we also consider superthermal effects of the electrons . We also observe that sign of the amplitude γ (or the quantity p which is directly affected by γ) inverted for the high values of κ_{e} , so there fore both the compressive along with the rarefactive shocks could exist. Amplitude of compressive (rarefactive) shock waves is decreasing (increasing) by increasing(decreasing) the value of κ_{e}. It could further be concluded from this figure that for defined parameters of plasma, only rarefactive shock waves may exist in the presence of huge amount of superthermal electrons in confinement. For $\kappa_{\mathsf{e}} \to \infty$ that only the compressive shocks could exist, having Maxwellian distribution for the electrons .

Fig.4.2 illustrates the shocks under the effects of the positron superthermality, it further illustrates that only compressive shocks exist for this case. For compressive shock waves, this trend of amplitude variation is totally opposte as in Fig.4. 1. There fore for a ambiplasma (magnetised) which have the nonthermal distribution function associated with the positron and electrons, the density of highly energetic electrons ought to be very larger while on the other hand popolation of the laptones need to be comparatively lesser in order to maintain and support the coupled drift acoustic shocks, and lower (higher) the percentage of fast positrons (electrons), the more will be the amplitude of shock waves. Backround of this scenario can be narrated by using the well defined plasma parameters. The number of negative ions is kept small as compared to that of positive ions ($\mu_+ > \mu_-$) which ultimately results in higher number of electrons compared to that of positrons. The electrons also are assumed to be at higher

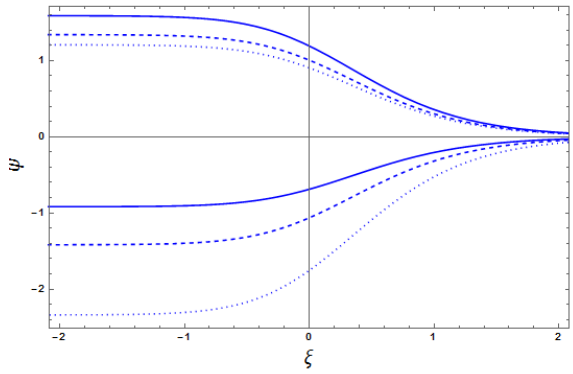

Figure 4-1: $\psi(\xi)$ vs. ξ for different values of κ_{e} , $\kappa_{\mathsf{p}} = 2$. while the other parameters are as that given in chapter.

temperature as compared to that of the positrons and their effects are more dominant especially when the amplitude of wave is changed from the rarefactive form to that of compressed one.

In fig.4.3 effects of concentration of positrons (μ_{p}) are explored when coupled drift acoustic shock mode propagate . We observe that when we increase the concentration of positron then shock strength is mitigated in terms of its magnitude. It is also noted that when we we increase the value of p , then it implies either concentration of positive ion (μ_+) is decreased or that of negative ion (μ_-) is increased , thus it is emphasized that an enhancing role is played by the positive ions, while negative ions are acting to reduce speed of the generation of drift acoustic coupled shocks.

In order to examine effects of various parameters of plasma on the kinds of solitary waves, Eq. (4.25) in Figs.**??** are analysed numerically. Further more in fig 4.4 we explore variation of width and amplitude of soliton with respect to nonthermally distributed electrons , thus the existance of compressive along with rarafactive solitons is varified. The width along with the amplitude of co rarefactive (compressive) soliton are decreasing (increasing) when we increase density of the superthermal particles (i.e. decreasingκ_{e}). It could further be concluded from the Fig.4.4, that width and amplitude of solitons in compressive mode vary significantly for

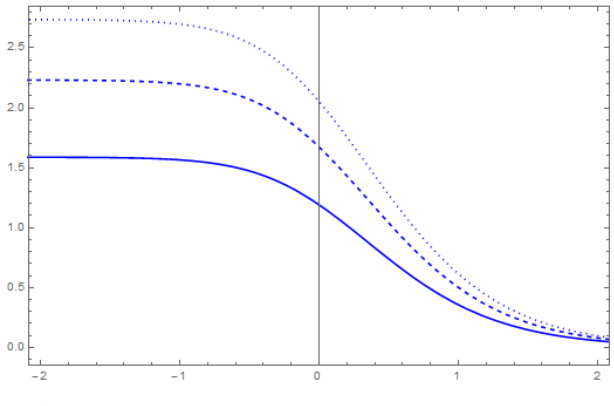

Figure 4-2: (Color online) Plot of $\psi(\xi)$ vs ξ for (4.23) by keeping the value of $\kappa_{\mathsf{p}} = 2$ fixed and varying κ_{p} such that $\kappa_{\mathsf{p}} = 2$ (solid blue line), $\kappa_{\mathsf{p}} = 2.2$ (dashed blue line) and $\kappa_{\mathsf{p}} = 2.4$ (dotted blue line) while all other parameters are the same as in Fig. 4.1

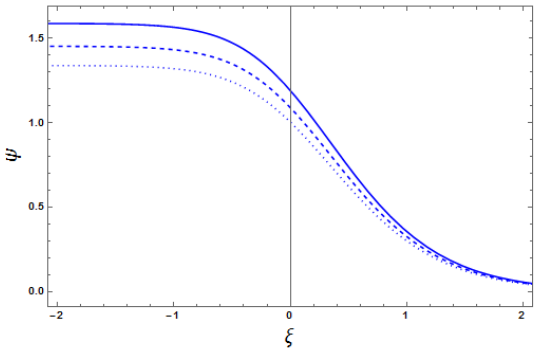

Figure 4-3: (Color online) $\psi(\xi)$ is plotted against ξ from Eq. (4.23) for different values of μ_{p} and fixed values of $\kappa_{\mathsf{e}} = \kappa_{\mathsf{p}} = 2$. The solid, dashed and dotted blue lines represent $\mu_{\mathsf{p}} = 0.14$, $\mu_{\mathsf{p}} = 0.16$ and $\mu_{\mathsf{p}} = 0.18$ respectively. All other parameters are the same as mentioned in Fig. 4.1

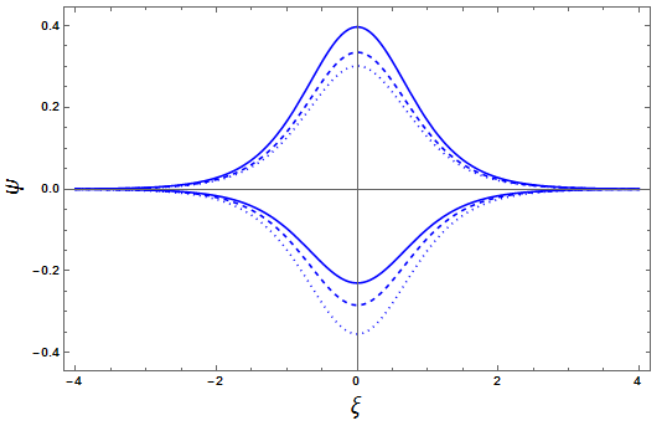

Figure 4-4: (Color online) The solitary wave potential $\psi(\xi)$ is plotted as a function of ξ from Eq. (4.25)for different values of κ_e and fixed value of $\kappa_p = 2$ such that $\kappa_e = 2$ (solid blue line), $\kappa_e = 2.2$ (dashed blue line) and $\kappa_e = 3.2$ (dotted blue line) for positive and $\kappa_e = 1.66$ (solid blue line), $\kappa_e = 1.67$ (dashed blue line) and $\kappa_e = 1.68$ (dotted blue line) for negative potentials.

smaller values of κ_e (i.e $\kappa_e \rightarrow 2 - 2.2$) . Literally speaking in the above case , soliton tends to be compressive in nature and electrons are showing the Maxwellian distribution function.

In Fig.4. 5 we are exploring the fact that how influential superthermal electrons are , on the soliton amplitude and width variation. Although the amplitude of the soliton is not inverted by positron superthermal population, yet its larger amount enhances (depletes) the height and width of soliton. Amplitude and the corresponding width of the soliton reduces significantly. If we increase the concentration of the positron, then this significantly reduce both the width and amplitude associated with the solitary wave, this sinario is depicted in Fig.4.6. For both the Figs.**??** the mechanism of wave-particle exchange is responsible for depeletion in the soliton potential. These kind of calculations could be possible through the use of kinetic theory , But this would be beyond the limitation and scope covered by this present work.

The counterbalance that exist between nonlinearity and the dissipation with in system can give rise to monotonic shocks. In Eq. (4.27) we have derived the solution of monotonic shocks , and in Figs.**??** we probe into the effects of various parameters of the concerned ambi

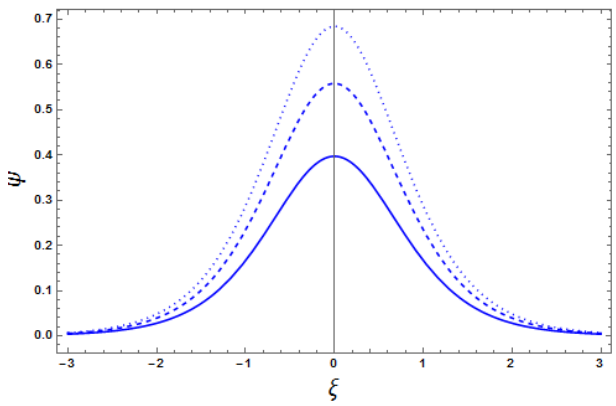

Figure 4-5: (Color online) Plot of $\psi(\xi)$ vs ξ for Eq. (4.25) by keeping the value of $\kappa_{\mathsf{p}} = 2$ fixed and varying κ_{p} such that $\kappa_{\mathsf{p}} = 2$ (solid blue line), $\kappa_{\mathsf{p}} = 2.2$ (dashed blue line) and $\kappa_{\mathsf{p}} = 2.4$ (dotted blue line) while all other parameters are the same as in Fig. 4.4.

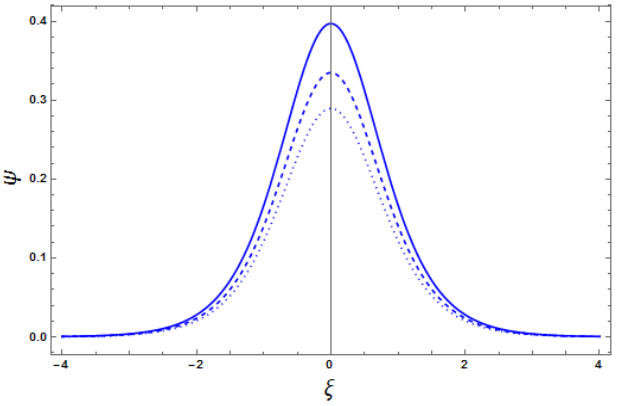

Figure 4-6: (Color online) $\psi(\xi)$ is plotted against ξ from (4.23) for different values of μ_{p} and fixed values of $\kappa_{\mathsf{e}} = \kappa_{\mathsf{p}} = 2$. The solid, dashed and dotted blue lines represent $\mu_{\mathsf{p}} = 0.14$, $\mu_{\mathsf{p}} = 0.18$ and $\mu_{\mathsf{p}} = 0.22$ respectively. All other parameters are the same as mentioned in Fig.4.4.

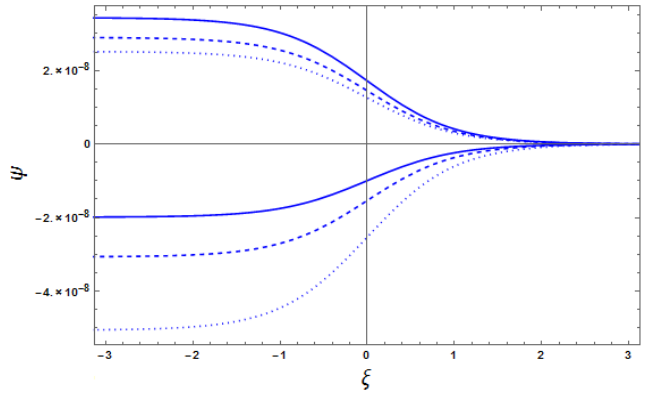

Figure 4-7: (Color online) The electrostatic potential $\psi(\xi)$ is plotted as a function of ξ from Eq. (4.27)for different values of κ_e and fixed value of $\kappa_p = 2$ such that $\kappa_e = 2$ (solid blue line), $\kappa_e = 2.2$ (dashed blue line) and $\kappa_e = 3$ (dotted blue line) for positive and $\kappa_e = 1.66$ (solid blue line), $\kappa_e = 1.68$ (dashed blue line) and $\kappa_e = 1.70$ (dotted blue line) for negative potentials, while all other parameters are the same as mentioned in chapter.

plasma on the formation of relevent shocks. The tendencey which these shocks are following under the influence of the superthermality of the electrons (Fig.4.7), superthermal positrons (Fig.4.8) and the variations in the density of positrons (Fig.4.9) is analogus to the solution of the transformed KdVBurger shocks (Figs.**??**), however the contrast emerges in the amplitude. In current case, amplitude that depends upon the dissipation coefficient q is small is due to the reason that dissipation in occuring with in system is more dominant over the dispersing effect.

.

.

4.4 Summary

In current chapter, we accorded a thorough theoretical analysis for transmission of the coupled drift acoustic in the ambiplasma that consist of negative/positive ions, along with the nonthermal electrons along with the positrons which obeys kappa distributions. For linear regime, we have derived dispersion relation, while in nonlinear sinario we have obtained non linear solutions

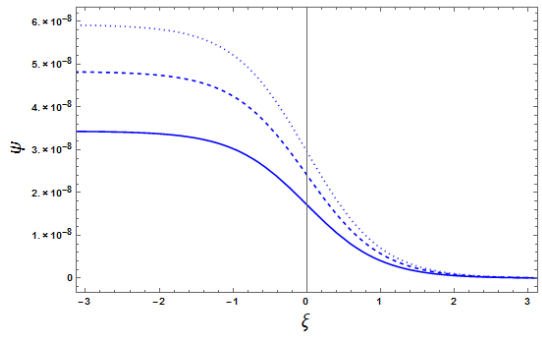

Figure 4-8: (Color online) Plot of $\psi(\xi)$ vs ξ for Eq. (4.27) by keeping the value of $\kappa_{\mathsf{p}} = 2$ fixed and varying κ_{p} such that $\kappa_{\mathsf{p}} = 2$ (solid blue line), $\kappa_{\mathsf{p}} = 2.2$ (dashed blue line) and $\kappa_{\mathsf{p}} = 2.4$ (dotted blue line) while all other parameters are the same as in Fig.4.7.

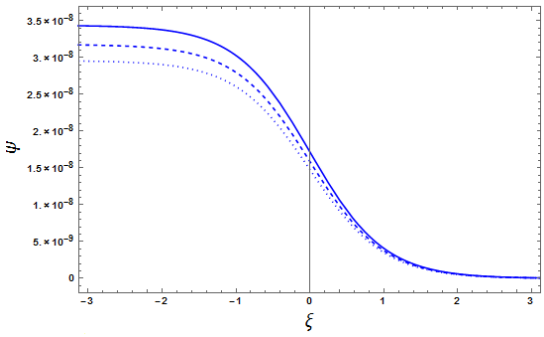

Figure 4-9: (Color online) $\psi(\xi)$ is plotted against ξ from Eq. (4.27) for different values of μ_{p} and fixed values of $\kappa_{\mathsf{e}} = \kappa_{\mathsf{p}} = 2$. The solid, dashed and dotted blue lines represent $\mu_{\mathsf{p}} = 0.14$, $\mu_{\mathsf{p}} = 0.18$ and $\mu_{\mathsf{p}} = 0.22$ respectively.

in the shape of the transformed KdVBurger type equation. In to further evaluate the solution of shock wave we have used Tanh-method. Further more , solutions of monotonic shock and solitary wave are also restored for limiting case of KdVBurger type equation. The nonlinear profiles i.e., shocks and solitons are investigated considering the effect of parameters of plasma i,e the positron superthermality and the electrons and the positron density variations. In the case of superthermal electrons positive/negative potentials (compressive, rarefactive) for shock and soliton, while positive potentials are observed for superthermal positrons. The greater density of superthermally distributed electrons suppresses amplitude of the compressive shocks and solitons while those of the positrons enhance it. The effect of variations (positrons) in density are also examined and it is deduced that when we increase the positron concentration then it reduces amplitudes of the nonlinear profiles, which indicates that positive accompanied by the negative ions actually enhances and reduces the propagation of shock waves and the solitary waves.

Chapter 5

Concluding Remarks

This chapter basically outlines the concluding remarks of our theses work.

In this thesis we have focused on the investigation of various linear and non linear structures that arises in multicomponent plasma. Our area of interest simply revolved around various instabilities. Such as rayleigh leigh Taylor instabilities and drift instabilities etc. Multi component plasma which was investigated was pair ion plasma, dense quantum magneto plasma and four component AMBI plasma Fluid model was used for this Purpose. Dispersion relation was derived for all the cases in linear regime , Followed by solitons and shocks. Results of these structures are further plotted in mathematica. The thesis begins with chapter first where we have discussed various topics relating directly or indirectly to our thesis.

In 2nd chapter we studied the R T mode in EPI quantum magneto plasma that consisted of the electron, positron and ion particles. Our calculations were based on both the analytical and numerical bases. We then used well known quantum hydrodynamic model and deduced a Generalized dispersion relation for the RT mode , under the approximation of drift wave scenario. The presence of the positron turns this algebraic equation into a cubic one. In clarified form the real and growth rate of RT mode was discussed with the positron concentration effect .We then used the Cardano's method to solve the cubic equation, for the real and imaginary roots of RT mode. It was also unveiled on us that the growth rates, was increasing with increase in density of electron while it is decreased with the increase of magnetic field (Bo) along with positron concentration.

In 3rd chapter we studied growth rates of various Rayleigh–Taylor mode in the nonuniform Pair Ion quantum magnetoplasma which consisted of the positive and negative ions with just a hint of electrons. The quantum hydrodynamic equations have been engaged. We then obtained an optimized dispersion relation for the RT mode, under the drift approximation. With the presumption that, both ions have same drift velocity, the growth rate (3.23) was derived with effects of both the classical and quantum phenomenons. The existence of negative ions with their different drift velocities turn the dispersion relation into a cubic equation. With the use of Cardano method we then obtained roots for both the real and imaginary modes of the wave associated with RT mode. We also then explored The growth rate of RT instability in detail with the density variation and the magnetic field. It is deduced that quantum speed and density gradient are improving due to density variation and hence RT mode is modified significantly. It was shown that growth rate of R–T mode in a nonuniform multi-ions quantum plasma increases (decreases) with density (magnetic field B_0). Our findings are general and could be helpful in understanding the RT imode in the celestial objects or future laboratory experiments. It is anticipated that in future a dense and highly magnetized multicomponent plasmas will be produced at laboratory. Thus the present investigations could be helpful in studying dense magneto plasmas on both astrophysical and laboratory level.

In 4th Chapter we presented a detail theoretical sketch for transmission of the coupled drift acoustic modes with in the four component ambi plasma, and non thermal electrons and positrons in non thermal regime of kappa distributions. In the linear regime, we have derived a dispersion relation , while in non linear sinario we have obtained an equation in form of the transformed KdV(b) type equation. After that we used Tanh-method for the pupose to deduce the exact shock wave solution for nonlinear equation. The solitary wave and monotonic shock solutions are also retrieved in the limiting cases of the KdV(b) type equation. The nonlinear profiles i.e., shocks and solitons are explored with the effect of plasma parameters such as the super thermality of electrons and positrons and variations in the density of positrons. In the case of superthermal electrons positive/negative potentials (compressive/rarefractive) for shock and soliton while for superthermal positrons only positive potentials are observed. The large number of superthermal electrons suppresses and that of positrons enhances the amplitude of the compressive shocks and solitons. The effect of variations (positrons) in density are also

studied and it is found that increasing the concentration of positron reduces the amplitudes of nonlinear profiles indicating positive and negative ions as an enhancing and reducing characters respectively for the propagation of shocks and solitons.

Bibliography

[1] F. Richard, *Plasma Physics An introduction*, The University of Texas.

[2] D. R. Nicholson, *Introduction to plasm physics*, John Willy and Sons.

[3] D. Gurnett, *Introduction to plasm physics ,with laboratory and space application*,Cambridge University, Press(2005).

[4] S. O. Dean, Application of plasma and fusion research. *Journal of fussion energy,* **14**, 2,1995.

[5] G. Chabrier, F. Douchin and A. Y. Potekhin, Dense astrophysical plasmas. *J. Phys. Condens. Matter* **14**, 9133 (2002).

[6] M. Marklund and P. K. Shukla, Nonlinear collective effects in photon-photon and photon-plasma interactions. *Review of Modern Physics* **78**, 591 (2006).

[7] N. Crouseilles, P. A. Hervieux, G. Manfredi, Quantum hydrodynamic model for the nonlinear electron dynamics in thin metal films. *Phys. Rev. B* **78**, 155412 (2008)

[8] K. Wiesemann, *A Short Introduction to Plasma Physics*, Ruhr-Universität Bochum, Germany(1994).

[9] C. K. Goertz, Dusty plasma in solar system. *Rev. Geophysics* **27**, 271 (1989).

[10] H. Thomas, G. E. Morfill, V. Demmel, J. Goree, B, Feuer-bacher, and D. Mohlmann, Plasma Crystal: Coulomb Crystallization in a Dusty Plasma. *Phys Rev Lett.* **73**, 652 (1994).

[11] A. Gondhalekar, P. C. Stangeby and J. D. Elder, *Nuclear Fusion* **34**,247 (1994).

[12] H. Saleem, Linear and nonlinear drift waves in collisionless and collisional electron-positron-ion plasmas. *Phys. of. Plasmas* **13**, 034503 (2006).

[13] A. Mushtaq *et al.*, Linear and nonlinear coupled drift and ion acoustic waves in collisional pair ion–electron magnetoplasma. *Physics Of Plasma,* **18**, 042305 (2011).

[14] A. Mushtaq *et al.*, Ion acoustic solitary waves in magnetised pair ion-electron plasma. *Phys. Of. Plasm*, **16**, 084501 (2009).

[15] A. E. Dubinov *et al.,* Nonlinear Theory of Electrostatic Baryonic Waves in Ambiplasma. *Journal of Experimental and Theoretical Physics*, **6**, 1051(2011).

[16] H. alfven, Antimatter and the Development of the Metagalaxy. *Review of Modern Physics*, **37,** 4 (1965).

[17] P. K Shukla *et al.,* Introduction to duty plasma, *Iop* (2002).

[18] R. l. Marino, *A dusty plasma primer*, university of lowa , lowa city(2001).

[19] A. Pahl, Electron Energy Distribution Function. *phys. of. plasm.* **35,** 4 (2014).

[20] P. A. Muñoz *et al.*, Non-Maxwellian electron distribution functions due to self-generated turbulence in collisionless guide-field reconnection. *Physics of Plasmas* **23**, 102103 (2016).

[21] T. Francesco *et al.,* Non-equilibrium in low-temperature plasmas. *Giorgio Dilecce,Eur. Phys.* **70**, 251 (2016).

[22] A. A. Abid *et al.,* Vasyliunas–Cairns distribution function for space plasma species, *Physics Of Plasma*, **22**, 084507 (2015).

[23] Habumugisha *et al.,* Onset of Linear Instability in a Complex Plasma with Cairns Distributed Electrons. *International Journal of Astronomy and Astrophysics*, **6**, 1-7 (2016).

[24] *Kappa distributions*: theory and applications in space plasmas, White paper.

[25] K. Saharia., The role of q-distribution on Non-linear fluctuation modes in plasma. *Conference: PSSI, At SINP, Kolkata*(2010).

[26] R. J. Golston, *Introduction to plasma physics*, Iop Publishing(1995).

[27] Stephan Brunner, Waves and Instabilities in Inhomogeneous Plasmas. *Crpp-ppb, Ch-1015 Lausanne,Switzerland*(2012).

[28] F.F. Chen, *Introduction plasma physics and controlled fusion.* Plenum Press, New York USA (1974).

[29] D. T. Farley *et al.,* The equatorial E-region and its plasma instabilities. *Ann. Geophys,* **27**, 1509–1520(2009).

[30] A. Rudolf, *Advanced space plasma physics*, Revised Edition, Imperial College Press, London (2001).

[31] John *et al.,* R-T Instabilities in young supernova remnants undergoing efficient particle accellaration. *The Astro Phys Journal,* **560** , 244È253(2001).

[32] P. Helander, G. G. Plunk, The universal instability in general geometry*, Inddian journal of physics,* **45**, 238(2000*).*

[33] Y. H. Chikawa, S. Watanabe, Instabilities in multicomponent plasma. *Colloque C6, suppltment au*, **12**, Tome 38 (1977).

[34] A. Mushtaq *et al.*, Electrostatic Solitary Waves in Pair-ion Plasmas with Trapped Electrons. *Braz. Jour. Phys,* **44**,614 (2014).

[35] Dr. A. Sharma, *Ion acceleration in plasmas*,TÁMOP-4.1.1.C-12/1/KONV-0005 projekt(2012).

[36] H. K. Andersen, Experiments on Shock Formation in a Q-Device, *Phys. Rev. Lett.* **19**, 149 (1967).

[37] A. Rudolf *et al.,* Advanced Space Plasma Physics. *Imperial College Press, London*,**10**, 2235 (2001).

[38] Q. Haque *et al.,* Nonlinear electrostatic drift waves in dense electron-positron-ion plasmas. *Physics of Plasma.* 15, 082315 (2008).

[39] P. K Shukla, A .A. Mamun, Instabilities in homogenious plasma. *New Journal of Physics,* **5** 17.1–17.37(2003).

[40] H. Siddiqui *et al.,* Effect of Trapping on Vortices in Plasma. *Journal Fusion Energy,* **27**,216 (2008).

[41] R. Daniel *et al.,* Injection and Trapping of Plasma Vortex Structures. *Physics of Fluids*, **9**, 1010 (1966).

[42] J.G. Robert , *Introduction to plasma physics ,Plasma Physics Laboratory*, Princeton University (2001).

[43] T. Gllot *et al.,* Interiors of giant planets inside and out side the solar system. *science*, **286**, 72(1999) .

[44] K. D. Anderson *et al.*, Physics of white dwarf stars, *Reports on Progress in Physics* , **53**, 837(1990).

[45] H.M. Horn *et al.*, Dense Astrophysical Plasmas. *Science* , **252**, 384(1991).

[46] A. O. Benz *et al., Plasma Astrophysics: Kinetic Processes in Solar and Stellar Coronae*, Springer (2001).

[47] J. Lindl *et al.,* Development of the indirect-drive approach to inertial confinement fusion and the target physics basis for ignition and gain. *Physics of Plasma* , **2**, 3933(1995).

[48] V.E. Fortov *et al.*, Extreme states of matter on Earth and in space. *Physics -Uspekhi* , **52**, 615 (2009).

[49] P. Shukla *et al.*, Nonlinear collective interactions in quantum plasmas with degenerate electron fluids. *Reviews of Modern Physics*, **83**,885(2011).

[50] G. Barak *et al.,* Quantum hydrodynamic model for the nonlinear electron dynamics in thin metal films, *Nature Physics* , **6**, 489 (2010).

[51] N. Crouseilles *et al.,* Quantum hydrodynamic model for the nonlinear electron dynamics in thin metal films. *Physical Review,* B, **21**, 78(2008.

[52] L. Ang *et al.,* New Scaling of Child-Langmuir Law in the Quantum Regime. *Physical Review Letter* ,**8**, 91(2003).

[53] W. Barnes *et al., Surface plasmon subwavelength optics,* Nature , **424**, 824(2003).

[54] E. Ozbay *et al.,* Plasmonics: Merging Photonics and Electronics at Nanoscale Dimensions. *Science* , **311**, 189(2006).

[55] A. Serbeto, Quantum plasma fluid model for high-gain free-electron lasers. *Plasma Physics and Controlled Fusion*, **8**, 51(2009).

[56] R. M„ Abolfath *et al.,* Piezomagnetic Quantum Dots. *Physical Review Letter* ,**5**, 101(2008).

[57] G. Manfredi, Fields Institute Communications, Physics Of Plasmas, **46**, 263(2005)

[58] F. Haas, *Quantum Plasmas: A Hydrodynamic Approach*, Springer, NewYork(2011).

[59] F. Haas, Manfredi, G. and Feix, M.R. Physical Review E, **62**, 2763(2000).

[60] F. Haas, Magnetohydrodynamic model for quantum plasmas. *Physics of Plasmas* , **12**, 01365(2005).

[61] A. Mushtaq *et al.,* Ion acoustic solitary wave with weakly transverse perturbations in quantum electron-positron-ion plasma. *Physics of Plasmas* , **14**,648 (2007) .

[62] M. Marklund *et al.,* Dynamics of Spin-12 Quantum Plasmas. *Physical Review Letter* , 98 (2007).

[63] G. Brodin *et al.,* Spin magneto hydro dynamics. *New Journal of Physics* , **9**, 277(2007).

[64] P. K. Shukla *et al.,* Formation and Dynamics of Dark Solitons and Vortices in Quantum Electron Plasmas. *Physical Review Letter* , 96(2006).

[65] A. Mushtaq *et al.,* Arbitrary magnetosonic solitary waves in spin 1/2 degenerate quantum plasma. *The European Physical Journal,* D , **64**, 419(2011).

[66] R. Maroof *et al.,* Magnetohydrodynamic waves with relativistic electrons and positrons in degenerate spin-1/2 astrophysical plasmas. *Physics of Plasmas* , **22**, 0124 (2015).

[67] R. Maroof *et al.*, Quantum dust magnetosonic waves with spin and exchange correlation effects. *Physics of Plasmas* , **23**, 124(2016).

[68] L. Rayleigh, *Proceedings of the London Mathematical Society* , 14, 170(1882).

[69] G. I. Taylor, Instability of liquid surfaces when accelerated in a direction perpendicular to their planes. *Proceedings of the Royal Society of London A* , **201**, 192(1950).

[70] S. Bodner, Rayleigh-Taylor Instability and Laser-Pellet Fusion. *Physical Review Letter* , **33**, 761(1974).

[71] S.Chandrasekhar *et al.,* Hydrodynamic and Hydromagnetic Stability. *Dover,* NewYork(1961).

[72] A. Mushtaq., Linear and nonlinear studies of two-stream instabilities in electron–positron–ion plasmas with quantum corrections. *Physica Scripta* , 78(2008).

[73] I. Zeba, J. Yahia, M. E. Shukla, P.K. and Moslem, W.M. *Physics Letter A*, **376**,2309(2012).

[74] B. Vitaly, M. Marklund, Modestov, The Rayleigh-Taylor Instability and Internal Waves in Quantum Plasmas. *Physics Letter A* , **372**, 3042(2008).

[75] J. Cao, Quantum effects on Rayleigh–Taylor instability in magnetized plasma. *Physics of Plasmas* ,15(2008) .

[76] G. A. Hoshoudy, Quantum Effects on the Rayleigh-Taylor Instability of Viscoelastic Plasma Model through a Porous Medium. *Journal of Modern Physics* , **2**, 1146(2011).

[77] G. A. Hoshoudy, effects on Rayleigh–Taylor instability in a vertical inhomogeneous rotating plasma. *Physics of Plasmas* , **16**, (2009).

[78] G. A. Hoshoudy, New Interpretation of Extragalactic Radio Sources. *Physics Letters A* , **373**, 2560 (2009).

[79] S. Ali, S. Ahmed, Z. Mirza, A. M. Ahmad, Rayleigh–Taylor/gravitational instability in dense magnetoplasmas. *Physics letters A* , **373**, 2940(2009).

[80] M. J. Rees, New Interpretation of Extragalactic Radio Sources. *Nature* , **229**, 312 (1971).

[81] M. J. Rees, M. J, *What the Astrophysicist Wants from the Very Early Universe,* In(1983)

[82] G. W. Gibbons et al, *The Very Early Universe* , Cambridge, University Press, Cambridge, **29** (1977).

[83] F. C. Michel, Theory of pulsar magnetospheres, *Reviews of Modern Physics* , **54**, 1(1982).

[84] H. R. Miller *et al., Active Galactic Nuclei*, Springer-Verlag, Berlin(1987).

[85] F. B. Rizzato, Weak nonlinear electromagnetic waves and low-frequency magnetic-field generation in electron-positron-ion plasmas. *Journal of Plasmas Physics* , **40**, 289(1981).

[86] C. M. Surko, Use of the positron as a plasma particle. *Physics of Fluids B* , **2**, 1372(1990)

[87] T. Murphay, Positron trapping in an electrostatic well by inelastic collisions with nitrogen molecules. *Physical Review A*, **46**, 5696(1992).

[88] V. I. Berezhiani, large relativistic density pulses in electron-positron-ion plasmas, *Physical Review E* , **52**, 1968(1995).

[89] M. Hoshino, Preferential positron heating and acceleration by synchrotron maser instabilities in relativistic positron–electron–proton plasmas. *Physics of Fluids B* , **3**, 818(1991).

[90] M. Hoshino, J. Arons,Y. Gallant, A. B. Langdon, The Astrophysical Journal , **390**, 454(1992).

[91] V. I. Berezhiani, Pair production in a strong wake field driven by an intense short laser pulse. *Physical Review A*, 46(1992).

[92] R. Greaves, An Electron-Positron Beam-Plasma Experiment. *Physical Review Letter* , **75**, 3847(1995).

[93] J. Zhao, Coalescence of two parallel current loops in a nonrelativistic electron–positron plasma. *Physics of Plasmas* , **3**, 844(1996).

[94] F. F. Chen, *Introduction to Plasma Physics and Controlled Fusion.* Plenum,New York (1984).

[95] S. Ali e*t al.,* Linear and nonlinear ion-acoustic waves in an unmagnetized electron-positron-ion quantum plasma. *Physics of Plasmas* ,**14**, 325(2007).

[96] W. M. Moslem, S. Ali, P. K. Shukla *et al., Drift waves in Magnitised plasma*, *Physics of Plasma* , **45**,1232(2007).

[97] M. Opher, Nuclear Reaction Rates and Energy in Stellar Plasmas: The Effect of Highly Damped Modes. *Phys. Plasmas* 8, 2454 (2001).

[98] M. Marklund, Nonlinear collective effects in photon-photon and photon-plasma interaction. *Rev. Mod. Phy.* **78** 591 (2006).

[99] M. Leontovich, Izv. Akad. Nauk Uzb. SSR, Ser. Fiz.-Mat. Nauk, *Ion acoustic waves*, **8**, 16 (1994).

[100] G. Agrawal, Nonlinear Fibre Optics, inroduction to non linear physics. *Academic Press,* San Diego(1995).

[101] A. Markowich, C. Ringhofer and C. Schmeiser, *Semiconductor Equations*, Springer, Vienna(1990).

[102] M. Bonitz, A. Filinov, J. Boning and J. W. Dufty, *Introduction to Quantum Plasmas*, Springer Series, Berlin (2009).

[103] G. Manfredi, How to model quantum plasmas. *Fields. Inst. Commun.* **46**, 263 (2005).

[104] C. Gardner, The Quantum Hydrodynamic Model for Semiconductor Devices. *SIAM. J. Appl. Math.* **54**, 409 (1994).

[105] F. Haas, Multistream model for quantum plasmas. *Phys. Rev. E.* **62**, 2763 (2000).

[106] D. Anderson, Statistical effects in the multistream model for quantum plasmas. *Phys. Rev. E.* **65**, 046417(2002) .

[107] F. Haas, Stability analysis of a three-stream quantum-plasma equilibrium. *Braz. J. Phys.* **33**, 128 (2003).

[108] M. Marklund, Magnetosonic solitons in a fermionic quantum plasma. *Phys. Rev. E*, **76**, 067401 (2007).

[109] G. Brodin, Spin solitons in magnetized pair plasmas. *Phys. Plasmas* **14**, 112107 (2007).

[110] P. K. Shukla, and L. Steno, Nonlinear aspects of quantum plasma physics. *J. Plasma Physics.* **74**, 719 (2008).

[111] A. Mushtaq, Magnetohydrodynamic spin waves in degenerate electron-positron-ion plasmas. *Phys. Plasmas* , **19**, 052101 (2012).

[112] W. Oohara, Pair-Ion Plasma Generation using Fullerenes. *Phys. Rev. Lett.* 91, 205005 (2003).

[113] W. Oohara, D. Date and R. Hatakeyama, Electrostatic Waves in a Paired Fullerene-Ion Plasma. *Phys. Rev. Lett.* **95**, 175003 (2005).

[114] M. S. Zobaer, Nonlinear Propagation of Dust-Ion-Acoustic Waves in a Degenerate Dense Plasma. *J. Mod. Phys.* **3**, 755 (2012).

[115] M. Akbari, Quantum Electrostatic Shock-Waves in Symmetric Pair-Plasma. *Op J. Aco* **2**, 72 (2012).

[116] U. M. Abde *et al.,* Ion-acoustic waves in a degenerate multicomponent magnetoplasma, *J. Plasma Physics,* **79**, 163 (2013).

[117] U. M. Ab, Dust-ion-acoustic solitary waves in a dense pair-ion plasma. *Physica B.* **405**, 3914 (2010).

[118] L. D. Landau, E.M. Lifshitz, *Fluid Mechanics,* Pergamon Press, Oxford(1989).

[119] D. Sharp, An Over View of Rayleigh Tayler Instability. *Physica. B.* **12,** 3 (1984).

[120] R. J. Goldston, P. H. Rutherford, *Introduction to Plasma Physics*, Institute of Physics Publishing, Bristol (1995).

[121] Z. W. Wu, W. L. Zhang, D. Li, W. H. Yang, Chin. Phys. Lett. **21**, 200 (2004).

[122] K. Bhatia, A. Sharma, *Proc. Natl. Acad. Sci. India*, A. **6,** 239 (1998).

[123] M. Mikhail *et al.,* The Rayleigh–Taylor instability in quantum magnetized plasma with para- and ferromagnetic properties. *Phys. Plasmas.* **16** 032106 (2009).

[124] C. Jintao, R. Huijun, W. Zhengwei and K. C. Paul, Instabilities in quantum plasmas. *Phys. Plasmas*, **15,** 012110 (2008).

[125] S. Ali, Rayleigh–Taylor/gravitational instability in dense magneto plasmas. *Phys. Lett. A.* **373** 2940 (2009).

[126] S. E. Woosley, The collapse of white dwarfs to neutron stars. *Astrophys. Journal.* **391**, 228 (1992).

[127] K. Kashiyama, White dwarf pulsars as possible cosmic ray electron-positron factories. *Phys. Rev. D,* **83**, 023002 (2011).

[128] Y. Fujita, K. Kohri, R. Yamazaki and K. Ioka, Is pamila anamely caused by the supernova explosions near... *Phys. Rev. D,* **80**, 063003 (2009).

[129] G. Giesen, M. Boudaud, Y. Genolini, V. Poulin, M. Cirelli, P. Salati and P. D. Serpico, Secondary astrophysical component and immediate implications for DM,JCAP , 1509 **09**, 023(2015) .

[130] M. Kachelriess, New Calculation Of Anti Proton Production By Cosmic Ray Protons And Nuclie. *Astrophys. J.* **803**, 54 (2015).

[131] K. Koi, Unlocking the secrets of cosmos. *Prog. Theor. Exp. Phys.* 021E01 (2016)

[132] L. D. Landau and E. M. Lifshitz, *Statistical Physics*, Part 1, Pargamon Press Inc. USA, (1980).

[133] F. Haas, Quantum ion acoustic waves. *Phys. Plasmas,* **10**, 3858(2003).

[134] M. Nasir, Ion Streaming Instabilities in Pair Ion Plasma and Localized Structure with Non-Thermal. Electrons. *Braz. J. Phys.* **45**, 633 (2015).

[135] S. Ali, Linear and nonlinear ion-acoustic waves in an unmagnetized electron-positron-ion quantum plasma. *Phys. Plasmas,* **14**, 082307 (2007).

[136] W. M. Moslem, Solitary, explosive, and periodic solutions of the quantum Zakharov-Kuznetsov equation and its transverse instability. *Phys. Plasmas,* **14**, 082308 (2007).

[137] M. Bonitz, V. S. Filinov, V. E. Fortov, P. R. Levashov, and H. Fehske, Crystallization in Two-Component Coulomb Systems, *Phys. Rev. Lett.* **95**,235006 (2005).

[138] V. M. Zhdanov, *Transport Processes in Multicomponent Plasma* (Taylor & Francis, New York, 2002).

[139] Alexandr Chertkov *et al.,* Analysis of Theories of Fully Ionized Space Plasma, *Space Sci. Rev.* **95**, 25(2001).

[140] Yu.v.kovtun *et al.,* Pasama and gases. Ukr. J. Phys. **55**, 1269(2010).

[141] H. Alfvrn, Antimatter and the Development of the Metagalaxy. *Rev. Modern Phys.* **37**, 652(1965).

[142] B. Lehnert, Problems of matter-antimatter boundary layers. *Astrophys. Space Sci.* **46**, 61(1977).

[143] G. L. Klara, B. Singh, *Astrophys and Space Sciences*, **103**, 321(1984).

[144] V. Pierrard and M. Lazar, Kappa Distributions: Theory and Applications in Space Plasmas. *Solar Phys.* **267**, 153(2010)

[145] V. M. Vasyliunas, Low-energy electrons on the day side of the magnetosphere, *J. Geophys. Res.* **73**, 2839(1968)

[146] G. Livadiotis, *Kappa Distributions: Theory and Applications in Plasmas* (Elsevier, 2017).

[147] D. Summers, R. M. Thorne, The modified plasma dispersion function. *Phys. Plasmas.* **3**, 1835 (1991).

[148] D. Summers, R. M. Thorne, Calculation of the dielectric tensor for a generalized Lorentzian , *J Geophys. Res.* **97**, 16827(1992).

[149] D. Summers *et al., J. Geophys. Res.* **103**, 487(1998).

[150] M. A. Hellberg, R. L. Mace, Generalized plasma dispersion function for a plasma with a kappa-Maxwellian velocity distribution. *Phys. Plasmas* **9**, 1495(2002)

[151] M. A. Hellberg, R. L. Mace, A new formulation and simplified derivation of the dispersion function for a plasma with a kappa velocity distribution. *Phys. Plasmas,* **16**, 072113(2009)

[152] S. Zaheer and G. Murtaza, Weibel instability with semirelativistic Maxwellian distribution function. *Phys. Plasmas* **14**, 022108(2007)

[153] L. I. Rudakov and R. Z. Sagdeev, Dokl. Akad. Nauk SSSR **138**, 581(1961).

[154] N. D. Angelo and R. W. Motley, Electrostatic oscillation near ion cyclotron frequencey. *Phys. Fluids*, **5**, 633(1962).

[155] M. Adnan, S. Mehmood, A.Qamar, Coupled ion acoustic and drift waves in magnetized superthermal electron-positron-ion plasmas. *Phys. Plasmas.* **21,** 092119(2014)

[156] M. Lazar et al, *Monthly Notices Royal Astron.* Soc. **401**, 362(2009)

[157] A.Mushtaq *et al.,* Spatially limited ion acoustic drift soliton in electron-positron-ion magneto plasma. *Phys. Plasmas,* **15**,082313(2008)

[158] W. Masood and A. M. Mirza, Non linear vortex structures with perpendicular shear flow. *Astrophys. Space Sci.* **350**, 517(2014).

[159] A. B. Mikhailovskii *et al.,* Matter anti matter theory, *Phys. Lett.* 105A, 45(1984).

[160] S. V. Antipov, M. V. Nezlin, E. N. Snezhkin, A. S. Trubnikov, chaos Zh. Eksp, Rossby soliton in laboratory. *Teor. Fiz.* **82**, 145(1982).

[161] A. Marcowith, A. Bret , A. Bykov *et al.,* The micro physics of collissional shock waves, *Rep. Prog. Phys.* **79**, 046901(2016).

[162] A. Mushtaq, R. Saeed, Q. Haque, Coupled electrostatic drift and ion acoustic waves in pair ion–electron plasma. *Phys. Plasmas*, **18**, 042305(2011).

[163] M. N. Khattak, A. Mushtaq, Z. Ehsan, Electrostatic baryonic solitary waves in ambiplasma with nonextensive leptons. *Chinese J. Phys.* **54**, 503(2016).